

**Rational Design and Preliminary Validation
of Novel BU10119 Analogs
for the Management of
SSRI Refractory Depression**

*Submitted in partial fulfilment
of the requirements of the
Degree of Master of Pharmacy*

Matthew Grech

Department of Pharmacy

University of Malta

2021



L-Università
ta' Malta

University of Malta Library – Electronic Thesis & Dissertations (ETD) Repository

The copyright of this thesis/dissertation belongs to the author. The author's rights in respect of this work are as defined by the Copyright Act (Chapter 415) of the Laws of Malta or as modified by any successive legislation.

Users may access this full-text thesis/dissertation and can make use of the information contained in accordance with the Copyright Act provided that the author must be properly acknowledged. Further distribution or reproduction in any format is prohibited without the prior permission of the copyright holder.

**Dedicated to my family and friends
for their continuous support**

Abstract

Kappa Opioid Receptor and Mu Opioid Receptor Antagonism has been shown to be useful in the treatment of SSRI Refractory Depression.

BU10119 is a dual Kappa Opioid Receptor and Mu Opioid Receptor antagonist that is used in this study as a lead. The crystallographic structures of both the opioid receptors were obtained from Protein Data Banks 4DJH and 4DKL.

The Virtual Screening Approach and the *de novo* Design Approach are performed in this study. Virtual Screening Approach involves a Ligand Based Drug Design, while the *de novo* Design Approach involves a Structure Based Drug Design.

During the Virtual Screening Approach, BU10119 was superimposed onto antagonists for both receptors to identify the optimal conformers. Consensus Pharmacophores were created for each antagonist using LigandScout®.

During the *de novo* Approach, different seed structures were created derived from the optimal BU10119 spatial arrangement and allowed to grow within the ligand binding pocket of the respective receptor. This approach resulted in a total of six molecular seed structures of high affinity to the Kappa Opioid Receptor, and limited activity to the Mu Opioid Receptor. These six molecular seed structures had diverse structures from the novel BU10119 molecule.

This study proved valuable in exploring the maximum ligand binding pocket area through the creation of a pharmacophore during the Virtual Screening Approach. The *de novo* Approach was used as further validation to this study in as a more innovative approach.

Acknowledgements

First and foremost, I would like to express my sincerest gratitude to Doctor Claire Shoemake of the Department of Pharmacy for her constant guidance, support and most of all patience throughout these past five years.

I would also like to extend my gratitude to Professor Lillian Azzopardi, Head of the Department of Pharmacy, and Professor Anthony Serracino Inglott, for their continuous encouragement and help throughout this course.

I would also like to thank all the lecturers and staff at the Department of Pharmacy for all of their help.

Finally, I would like to thank my family and my girlfriend for all of their patience and support, as well as my colleagues and friends for making these past five years an unforgettable experience.

Table of Contents

Dedication	ii
Abstract.....	iii
Acknowledgements.....	iv
List of Tables	ix
List of Figures	x
List of Appendices	xiii
List of Abbreviations	xiv
Chapter 1: Introduction	1
1.1 Depression and SSRI Refractory Depression.....	1
1.2 New Targets for the Kappa opioid receptor	3
1.3 Kappa Opioid Receptors.....	7
1.3.1 Kappa Opioid Receptor Agonists.....	8
1.3.2 Reward Complex and Stress.....	8
1.3.3 Kappa Opioid Receptor and Neuronal Circuits	9
1.3.4 Conditioned Place Aversion and Conditioned Place Preference	10
1.3.5 Physiological Effects of the Kappa Opioid Receptor	12
1.4 Kappa Opioid Receptor Antagonists	14
1.4.1 The cAMP Response Element Binding and Behavioural Studies.....	14
1.4.2 Evidence Showing the Effect of κ OR Antagonists	15
1.4.3 The κ OR Antagonists: Nor-Binaltorphimine, 5'-Guanidinonaltrindole, 5'- Acetamidinoethylnaltrindole & JD1c	17
1.4.4 Buprenorphine in combination with Samidorphan	21
1.4.5 The Continuous Research for new κ OR Antagonists.....	22

1.5 Combined therapy	24
1.5.1 Buprenorphine	25
1.5.2 Naltrexone.....	26
1.5.3 Buprenorphine/Naltrexone Combination.....	27
1.5.4 Previous Buprenorphine/Samidorphan Combination Therapy	27
1.5.5 Limitations to the Buprenorphine/Naltrexone Combined Therapy	28
1.6 BU10119	29
1.7 Drug Design	30
1.7.1 Rational Drug Design.....	30
1.7.2 Computational Aided Drug Discovery	30
1.7.2.1 Pharmacophore Based Drug Design (Ligand Based Drug Design).....	32
1.7.2.2 Receptor Based Drug Design (Structure Based Drug Design)	32
1.7.3 X-Ray Crystallography in Structure Determination.....	33
1.7.4 Lead Molecules	34
1.7.5 Protein Data Bank	34
1.8 Computational Tools and Software.	35
1.8.1 SYBYL [®] -X Version 2.0 ⁶	35
1.8.2 PoseView [®]	35
1.8.3 X-Score Version 1.2 ⁸	36
1.8.4 LigBuilder [®] Version 2.1 ⁹	36
1.8.5 Accelrys BIOVIA [®] Draw Version 18.1 ¹⁰	36
1.8.6 BIOVIA [®] Discovery Studio Visualizer.....	37
1.8.7 UCSF Chimera [®] Version	37

1.8.8 ChemSketch [®] Version 11	37
1.8.9 LigandScout [®] 3.12.....	38
1.8.10 ZINCPharmer [®] 14	38
1.9 Aim	39
Chapter 2: Methodology	41
2.1 Selection of Protein Data Bank Crystallographic Depositions.....	41
2.2 Extraction of Ligands.....	43
2.3 Conformational Analysis	45
2.3.1 Generation of BU10119 conformers.....	45
2.3.2 Calculation of the Ligand Binding Energy (kcal mol ⁻¹).....	46
2.3.3 Calculation of the Ligand Binding Affinity (pKd)	46
2.3.4 Choosing the Optimal Conformer	47
2.4 Virtual Screening.....	49
2.4.1 Generating pharmacophores	49
2.4.2 Hit Molecule Screening using ZincPharmer [®]	52
2.4.3 Filtration of hits using Mona [®]	53
2.4.4 Generation of Protomols using Sybyl-X [®]	54
2.5 de novo – Structure Based Drug Design	56
2.5.1 2-Dimensional Topology Map Generation	56
2.5.2 Generation of Seed Molecules	56
2.5.3 de novo Design	57
2.5.4 Sorting and Filtering Ligands Obtained	58

Chapter 3: Results	60
3.1 Results obtained from Virtual Screening	60
3.1.1 Creation of Consensus Pharmacophores	60
3.1.2 Calculation of Ligand Affinity to Ligand Binding Pocket.....	61
3.2 Results obtained from <i>de novo</i> modelling	63
3.2.1 Structure Activity Relationship.....	63
3.2.2 Seeds generated using <i>de novo</i> design	65
Chapter 4: Discussion	91
Conclusion	101
References	102
List of Publications	113
Appendices	114
Appendix A: FREC Ethics Approval	114
Addendum	115

List of Tables

Table 3.1: The two optimal ligands obtained through the Virtual Screening Approach for the κ OR.....	61
Table 3.2: The two optimal ligands obtained through the Virtual Screening Approach for the μ OR.....	62
Table 3.3: Table showing the 2-Dimensional and 3-Dimensional structures of the seeds created from 011_BU10119.mol2 as the optimal conformer for the κ OR	66
Table 3.4: Table showing the top five molecules with the highest affinity and two molecules with the lowest affinity to the ligand binding pocket of the κ OR for each seed and their properties.....	71
Table 4.1: Table comparing the Virtual Screening Approach and <i>de novo</i> Approach.....	93
Table 4.2: Table showing the number of molecular cohorts obtained through the <i>de novo</i> Design.....	95
Table 4.3: Table comparing the P2 molecules with the highest and lowest affinity to the ligand binding pocket for each seed structure.....	96

List of Figures

Figure 1.1: The PDB- Crystallographic Deposition file 2N2F	4
Figure 1.2: Molecular Structure of Nor-Binaltorphimine.....	5
Figure 1.3: A simplified scheme representing the interactions between DYNs and the κ OR at the neuronal circuits.	9
Figure 1.4: Highly simplified scheme by which KORs are thought to regulate mood.....	10
Figure 1.5: 2D Structure of Morphine.....	12
Figure 1.6: The PDB-Crystallographic Deposition file 4DKL	13
Figure 1.7: Simplified Model to explain how Stress, CREB, DYN and Kappa Opioid Receptors regulate mood and DA release.	17
Figure 1.8: 2D Structure of GNTI.....	18
Figure 1.9: 2D Structure of ANTI.	18
Figure 1.10: 2D Structure of JDtic.....	19
Figure 1.11: The PDB-Crystallographic Deposition file 4DJH	20
Figure 1.12: 2D Structure of Samidorphan.	22
Figure 1.13: 2D Buprenorphine Structure.....	25
Figure 1.14: 2D Naltrexone Structure.	26
Figure 1.15: Simplified Figure explaining the processes involved in Computational Aided Drug Discovery (CADD).	31
Figure 2.1: The structure of BU10119 modelled through the de novo approach.....	42
Figure 2.2: Structure of the morphinan antagonist BF0601 extracted from the μ OR.....	43
Figure 2.3: Structure of the kappa opioid receptor antagonist JDC1300 (also known as JDtic) extracted from the κ OR.....	44
Figure 2.4: Structure of the human kappa opioid receptor bound to the kappa opioid receptor antagonist JDC1300.....	50

Figure 2.5: Structure of the kappa opioid receptor antagonist JDC1300 together with its pharmacophore and surrounding amino acids within the receptor site.....	51
Figure 2.6: Structure of the mu opioid receptor bound to the morphinan antagonist BF0601..	51
Figure 2.7: Structure of the mu opioid receptor BF0601 together with its pharmacophore and surrounding amino acids within the receptor site.....	52
Figure 2.8: Structure of the kappa opioid receptor showing the protomol which represents the virtual ligand binding pocket	55
Figure 2.9: Structure of the mu opioid receptor showing the protomol which represents the virtual ligand binding pocket	55
Figure 2.10: Outline of the Structure Based Drug Design Process.....	56
Figure 3.1: Structure of the consensus pharmacophore for the JDC1300 with the optimal BU10119 conformers for the kappa opioid receptor.....	60
Figure 3.2: Structure of the consensus pharmacophore for BF0601 with the optimal BU10119 conformers for the mu opioid receptor.....	61
Figure 3.3: Figure showing ZINC00118327, the optimal conformer for the κ OR.....	62
Figure 3.4: Figure showing ZINC93209494, the optimal conformer for the μ OR.....	62
Figure 3.5: 2-Dimensional Topology Map created using the optimal conformer for the κ OR (011_BU10119.mol2) and the κ OR Ligand Binding Pocket.....	63
Figure 3.6: 2-Dimensional Topology Map created using the optimal conformer for the κ OR (006_BU10119.mol2) and the μ OR Ligand Binding Pocket.....	64

Figure 4.1: Figure showing the critical ligand interactions between the P2 molecule 39
obtained from Seed 2 after docking into the Kappa Opioid Receptor.....100

List of Appendices

Appendix A: FREC Ethics Approval.....	114
----------------------------------------------	------------

List of Abbreviations

3D – Three - Dimensional

AMG - Amygdala

ANTI – 5'-Acetamidinoethylaltrindole

cAMP – cyclic Adenosine Monophosphate

CBT – Cognitive Behavioural Therapy

CCBT – Computerised Cognitive Behavioural Therapy

CPA – Conditioned Place Aversion

CPP – Conditioned Place Preference

CREB – cAMP Response Element Binding

DA - Dopamine

δOR – Delta (δ) Opioid Receptor

DSM-V – Diagnostic and Statistical Manual, 5th Edition

DYN – Dynorphin

EMP – Elevated-Plus Maze

GNTI - 5'-Guanidinonaltrindole

GPCR – G-Protein Coupled Receptor

HBA – Hydrogen Bond Affinity

HBD – Hydrogen Bond Donor

ICD-10 – International Classification of Disease, 10th Edition

JNK – c-Jun N-terminal Kinase

κOR – Kappa (κ) Opioid Receptor

LBA – Ligand Binding Affinity (pKd)

LBE – Ligand Binding Energy (kcalmol⁻¹)

LDB – Light Dark Box

LT – Light Therapy

MAOIs – Mono-Amine Oxidase Inhibitors

μOR – Mu (μ) Opioid Receptor

NAc – Nucleus Accumbens

NICE CG90 – National Institute for Clinical Excellence – Clinical Guideline 90

NIH - Novelty-Induced Hypophagia

NMR – Nuclear Magnetic Resonance

NOR - Nociception/Orphanin FQ Receptor

Nor-BNI - Nor-Binaltorphimine

PDB – The RCSB Protein Data Bank

PDYN – Prodynorphin

PFC – Prefrontal Cortex

PTSD – Post-Traumatic Stress Disorder

RDD – Rational Drug Design

RMSD - Root Mean Squared Deviation

SD – Sprague-Dawley

SNRIs – Selective Norepinephrine Reuptake Inhibitors

SSRIs – Selective Serotonin Reuptake Inhibitors

TBI – Traumatic Brain Injury

TCAs – Tricyclic Antidepressants

VTA – Ventral Tegmental Area

WKY – Wistar Kyoto

WHO – World Health Organisation

Chapter 1

Introduction

Chapter 1: Introduction

1.1 Depression and SSRI Refractory Depression

Depression is a vast diagnosis. A depressed mood and/or a loss of interest in activities usually of pleasure to the person is indicative to the diagnosis of depression as explained in the National Institute for Clinical Excellence Clinical Guideline 90 (NICE CG90, Oct 2009). For depression to be diagnosed, both the Diagnostic and Statistical Manual of Mental Disorders – 5th edition (DSM-V) and the International Classification of Disease 10th edition (ICD-10) require the symptoms to be experienced for at least a couple of weeks and symptoms need to be present for most of every day.

Depression has been ranked as the fourth most common cause of disability worldwide by the The World Health Organization (WHO, 2015)¹ (Murray & Lopez, 1996a). Lifetime incidence estimates of major depressive disorders ranged from 1.0% (Czech Republic) to 16.9% (US) (Andrade *et. al.*, 2003)

More than three hundred million people are affected with depression according to the WHO (2015). Depression is a serious disease and at its worst it can lead to suicide. Around eight hundred thousand suicides are reported per annum. Suicide is the second commonest cause of death in fifteen to twenty-nine year olds. (WHO, 2015)¹. The WHO¹

¹ World Health Organisation [Internet]. Depression Factsheet. 2018. Available from: <http://www.who.int/en/news-room/fact-sheets/detail/depression>. [Accessed online 29.04.2018.]

has stated that the burden of depression is rising globally and has called for a coordinated, comprehensive response to mental disorders at country level.

A number of treatment options exist when treating depression. These can be divided into pharmacological and non-pharmacological therapies. Pharmacological options would include treatment using tricyclic antidepressants (TCAs), mono-amine oxidase inhibitors (MAOIs), selective serotonin reuptake inhibitors (SSRIs) and serotonin-norepinephrine reuptake inhibitors (SNRIs). Non-pharmacological therapies would include light therapy (LT), cognitive behaviour therapy (CBT), computerised cognitive behavioural therapy (CCBT) and structured group physical activity programmes (NICE CG90).

Depression has been subdivided into several different types and grades. It can be mild, moderate or severe. One of the latter is SSRI Refractory Depression, where is no response or only partial response after at least four weeks of treatment. (DSM-V, 2013).

Effective management of the clinical condition is critically dependent on patient adherence with antidepressant therapy. However, it is well known that 50 to 75 percent of patients with major depression prematurely discontinue antidepressant therapy leading to a lack of adherence to treatment (Keller *et. al.*, 2002; Trivedi *et. al.*, 2007). This could be due to a number of factors, including patient factors such as concerns about adverse events, as well as factors stemming from healthcare workers such as poor patient education and inadequate follow-up (Sansone & Sansone, 2012).

This long duration of treatment, side-effect profile of the medication used to treat depression and the poor adherence to treatment in patients with depression obviate the need for further and continuing research aimed at the discovery of novel treatment that leads to better disease management while reducing the side effect burden of medication.

1.2 New Targets for the Kappa opioid receptor

Opioid radioligand binding assays were the method by which opioid receptors were discovered in brain homogenates (Pert & Snyder, 1973). Some decades later, cloning studies differentiated three receptors: μ , δ and κ (Evans *et. al.*, 1992)(Kieffer *et. al.*, 1992)(Chen *et. al.*, 1993). The kappa opioid receptor (κ OR) belongs to the G-protein-coupled class of receptors (GPCRs). These are expressed in brain area with activity in cognitive function, reward pathways and mood states. (Carroll & Carlezon, 2013).

Prodynorphin is the most common precursor for opioid peptides that act as agonists at the κ OR. Dynorphin A, despite binding also to μ and δ opioid receptors, has a much higher affinity for κ receptors (Law *et. al.*, 2000). This leads to inhibition of adenylate cyclase, increasing the potassium conductance, decreasing the calcium conductance and results in mobilisation of intracellular calcium (Piros *et. al.*, 1996).

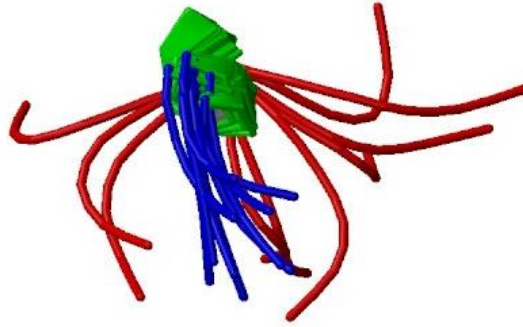


Figure 1.1: The PDB- Crystallographic Deposition file 2N2F (O'Connor C *et. al.*, 2015) showing the bound coordinates of the Human Kappa Opioid Receptor to Dynorphin 1-13. Rendered in BIOVIA Discovery Studio Visualizer.²

Pfeiffer *et. al.* (1986) had described how the activation of the μ receptors elevates mood, while KOR activation results in melancholy and psychomimetic effects in humans. Bals-Kubik *et. al.* (1993) further associated KOR activation with anhedonia-dysphoria and anxiety-like side effects in rodents. These studies lead to theory that opposite endogenous opioid systems could control perceptual experiences and emotions (Pfeiffer *et. al.*, 1986).

McLaughlin *et. al.* (2003) tested the hypothesis that endogenous dynorphin released through stressful experiences may result in stressful behavioural responses and block the reward pathway of cocaine. As explained by Can *et. al.* (2012), one of the behavioural tests that can be used to evaluate antidepressant drugs is the Forced Swim

² BIOVIA Discovery Studio Visualizer[®]. Available from: <http://accelrys.com/products/collaborative-science/biovia-discovery-studio/visualization.html>

Test (FST). In this test, mice are placed in a transparent tank. The tank is filled with water, making it virtually inescapable. Their escape related mobility was then measured. This test is considered to be highly reliable, also due to the fact that it requires no specialised equipment. The principal findings of McLaughlin *et. al.* (2003) were that a Repeated FST resulted in numbness, rigidity, and an increase in conditioned place preference for cocaine, usually inhibited by nor-binaltorphimine (nor-BNI), a κ OR antagonist, and prodynorphin disturbance. The FST is a widely used predictive animal model for the study of depression, where the extent of depression is exhibited through the time taken for immobility to set in (McLaughlin *et. al.*, 2003).

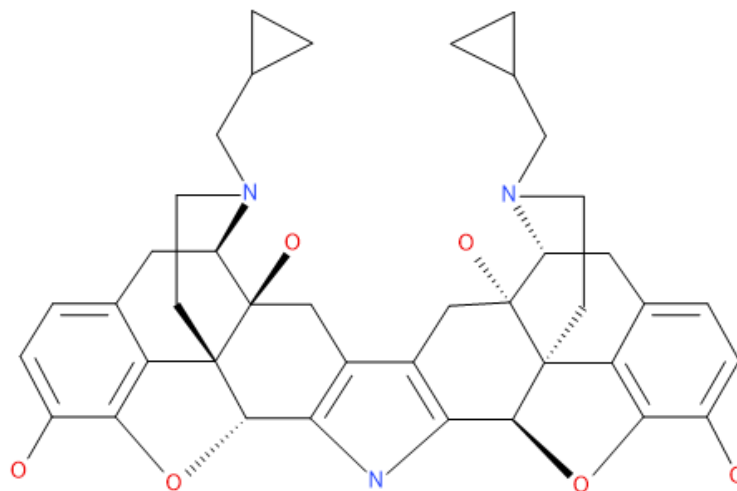


Figure 1.2: 2D Molecular Structure of Nor-Binaltorphimine. Rendered using Accelrys BIOVIA[®] Draw.³

Knoll *et. al.* (2010) effectively summarised the effects of activation of the κ OR. Acute stress facilitates the stimuli such as homeostasis that aid in escape. Chronic stress situations on the other hand showed signs of increased risk of depression and an

³ Accelrys Biovia Draw[®]. Available from: <http://accelrys.com/products/collaborative-science/biovia-draw/draw-no-fee.php>

increased drug craving that stems from a higher chance of participation in drug-seeking behaviour. Such stress and stimuli lead to an elevation of cyclic Adenosine Monophosphate (cAMP) response element binding protein (CREB) in the nucleus accumbens (NAc). This then leads to elevated levels of dynorphin which are thought to result in negative mood states. Pliakas *et. al.* (2001) have established that this relationship in the NAc elicits the signs of major depression in rodents whereas disruption of CREB function in the NAc had antidepressant-like effects very similar to those of standard antidepressants.

In a previous study, Pliakas *et. al.* (2001) had described that nor-BNI prevented immobility due to the FST. They hypothesised that κ OR antagonists also play a role in the treatment of depression through blocking of the endogenous function of dynorphin. The fact that disruption of the dynorphin gene also results in reduction in immobility also suggests that κ OR antagonism may play a role as a new target in the management of depression. Through the hypotheses above regarding κ OR involvement in reward complexes and the potential drug-seeking behaviour of drugs of abuse, the potential κ OR antagonism has potential to create new treatment targets for depression and withdrawal from drugs of abuse.

In another study, Mague *et. al.* (2003) have studied the effect of intracerebroventricular administration of nor-BNI on the decreased the immobility in the FST. They further reported that treatment with two κ -antagonists resulted in comparable results. 5'-acetamidinoethylnaltrindole (ANTI) was potent and effective after systemic administration while 5'-guanidinoaltrindole (GNTI) was only effective after intracerebroventricular treatment and showed no clinical efficacy with systemic

administration. The behavioural effects of the κ -antagonists were reported to resemble those of TCAs (desipramine) and SSRIs (fluoxetine and citalopram) (Mague *et. al.*, 2003).

Carr *et al.* (2010) performed a study in Wistar Kyoto (WKY) rats which are considered a recognised genetic model of comorbid depression and anxiety. Carr *et. al.* (2010) reported that despite WKY rats are known to exhibit more immobility when compared to Sprague-Dawley (SD) rat strains, administration of κ OR antagonists in the WKY rats provided more visible antidepressant action. The antidepressant desipramine on the other hand reduced immobility in the FST in both rat strains.

1.3 Kappa Opioid Receptors

The opioid system is a neuromodulatory system that is made up of three GPCRs: mu (μ OR), delta (δ OR) and kappa (κ OR). These receptors are found through the central and peripheral nervous systems. These receptors' effects are initiated under physiological conditions resulting in the inhibition of neuronal activity (Lalanne *et. al.*, 2014).

George *et. al.* (1994) have used northern blot techniques to map out the areas where opioid receptors are present in rat brain. Kappa receptor mRNA is located in the hippocampus, hypothalamic nuclei and cortex, NAC, as well as other areas of interest such as the Olfactory tubercle, dentate gyrus and caudate putamen.

1.3.1 Kappa Opioid Receptor Agonists

Dynorphin (DYN) is an opioid peptide with its precursor being the Prodynorphin (PDYN) gene that activates the κ OR while having a low affinity for μ OR and δ OR. Other opioid agonists such as endorphins and enkephalins have a poor affinity to the κ OR. This makes the dynorphin/ κ OR signalling pathway unique within the opioid system (Chavkin *et. al.*, 1982).

1.3.2 Reward Complex and Stress

The important role of opioid receptors in psychiatric disorders that are characterised by changes in the reward system stems from the fact that opioid receptors are highly involved reward pathways. (Le Merrer *et. al.*, 2009). κ OR progressively emerged as an anti-reward system that limits the use of potentially addictive drugs (Lalanne *et. al.*, 2014). The fact that κ OR is activated during both acute and chronic stressful situations, explains the role of the κ OR in the development of depressive states (Lutz & Kiefler, 2013)(Lalanne *et. al.*, 2014).

1.3.3 Kappa Opioid Receptor and Neuronal Circuits

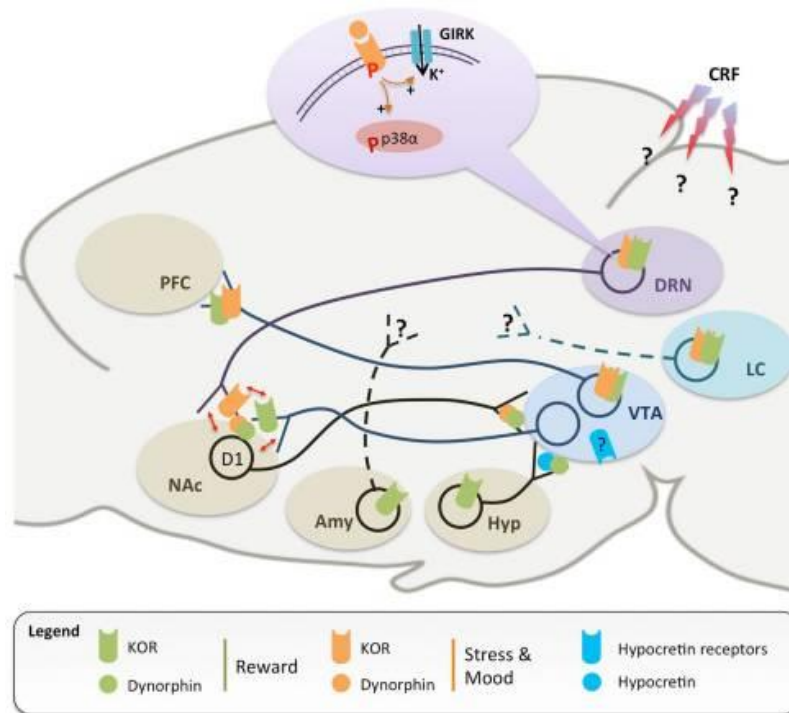


Figure 1.3: A simplified scheme representing the interactions between DYNs and the KOR at the neuronal circuits. The reward pathways are marked in green, while the stress-induced pathways are marked in orange. Both the reward and stress pathways are regulated by the DYN at the KOR. Adopted from: Lalanne L, Ayranci G, Kieffer BL & Lutz PE. The kappa opioid receptor: from addiction to depression, and back. *Frontiers in Psychiatry*. 2014; 5(170): 1-17.

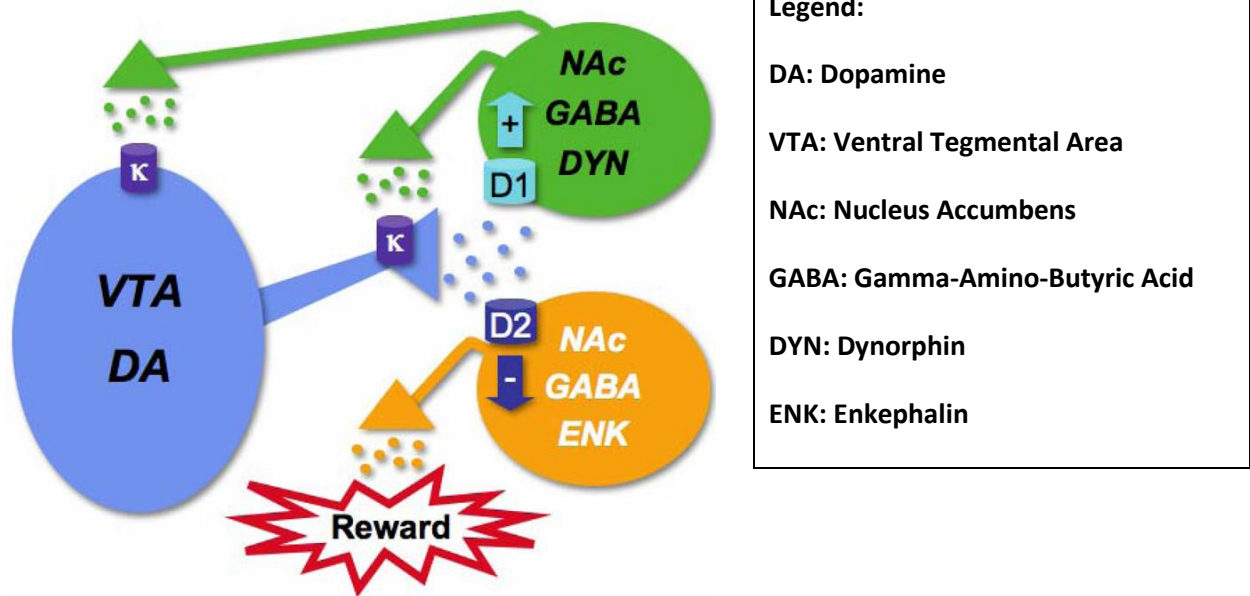


Figure 1.4: Highly simplified scheme by which κ ORs are thought to regulate mood. DA neurones (in blue) in the VTA have projections reaching the NAc. Here, DA acts on two types of GABAergic neurones. The D2 GABAergic neuron, marked in orange, acts through the activation of inhibitory G-Proteins (G_i) resulting in the inhibition of reward complexes. The other type of neurones (green) express Dopamine 1 and DYN. DA binding to Dopamine1 activates stimulatory G-Proteins (G_s), thus increasing the activity of both GABAergic neurones. Stimulation of G_i Coupled κ ORs by DYN decreases Dopamine 2 function, thus increased inhibition of reward. Adopted from: Carlezon WA Jr, Beguin C, Knoll A & Cohen BM. Kappa-opioid ligands in the study and treatment of mood disorders. *Pharmacology & Therapeutics*. 2009; 123: 334-343.

1.3.4 Conditioned Place Aversion and Conditioned Place Preference

Studies using various methods such as Conditioned Place Aversion (CPA) (Bals-Kubik *et al.*, 1993)(Lalanne *et al.*, 2014), microdialysis (Spanagel *et al.*, 1992)(Lalanne *et al.*, 2014) and immunohistochemistry (Margolis *et al.*, 2006)(Lalanne *et al.*, 2014) have suggested a pathway whereby NAc dopamine effects are independent of VTA κ ORs but rather control dopamine release resulting in CPA. Lalanne *et al.*, (2014) maintain that these results provide robust indications that κ OR antagonism is affects the reward

complexes experienced with social interactions and drugs of abuse. Studies have also identified the κ OR in the pre-synaptic terminals of dopamine neurones expressing the NAc (Spanagel *et. al.*, 1993)(Lalanne *et. al.*, 2014) while dopamine neurons including the PFC expressed the κ OR in both the pre- and post-synaptic terminals (Lalanne *et. al.*, 2014).

Morphine is known to be a potent μ OR agonist. μ OR activation produces euphoria in both animal and human models. Shippenberg and Hertz (1986) & Lalanne *et. al.*, (2014), in their seminal rat studies have publicised that Morphine as a κ OR agonist resulted in opposite effects, producing CPP (resulting in positive motivational properties) and CPA (resulting in negative motivational properties). CPP and CPA are forms of conditioning that were hypothesised by Pavlov to prove experience learned behaviour. It has been postulated that κ OR-induced CPA might be a mechanism that contrasts the reward complex system that contributes to the degree of pleasantness or unpleasantness related to the circumstance in question (Lalanne *et. al.*, 2014).

There is ample evidence that κ OR agonists induce a CPA response in rodents (Suzuki *et. al.*, 1992)(Bruijnzeel, 2009). CPA can be inhibited by pre-administration of nor-BNI (Zhang *et. al.*, 2004). κ OR agonists have been shown to increase the brain reward complexes in rats (Todtehkopf *et. al.*, 2004). This indicates that the κ OR agonists results in anhedonia which is one of the main symptoms of depression.

1.3.5 Physiological Effects of the Kappa Opioid Receptor

kOR agonists decrease swimming in the FST due to an increase in immobility. (Mague *et al.*, 2003)(Bruijnzeel, 2009). This points to the fact that kOR agonists induce a behavioural response in the FST as seen in amphetamine withdrawal. This is in contrast to what is seen during antidepressant treatment.

The acute effects of kOR agonists in humans have been the subject of studies that suggest that kOR agonists induce signs of melancholy in rodents and humans (Pfeffer *et al.*, 1986)(Rimoy *et al.*, 1994)(Walsh *et al.*, 2001)(Bruijnzeel, 2009). Braida *et al.*, (2008) & Bruijnzeel *et al.*, (2009) suggested that sub-therapeutic doses of kOR agonists result in a positive mood state while supra-therapeutic doses of kOR agonists will result in depressed mood states.

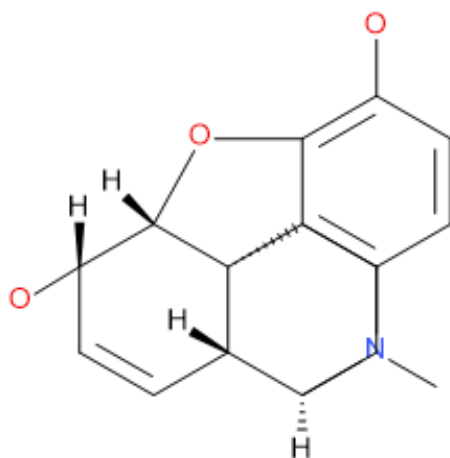


Figure 1.5: 2D Structure of Morphine. Rendered Using Accelrys Biovia Draw[®].³

³ Accelrys Biovia Draw[®]. Available from: <http://accelrys.com/products/collaborative-science/biovia-draw/draw-no-fee.php>

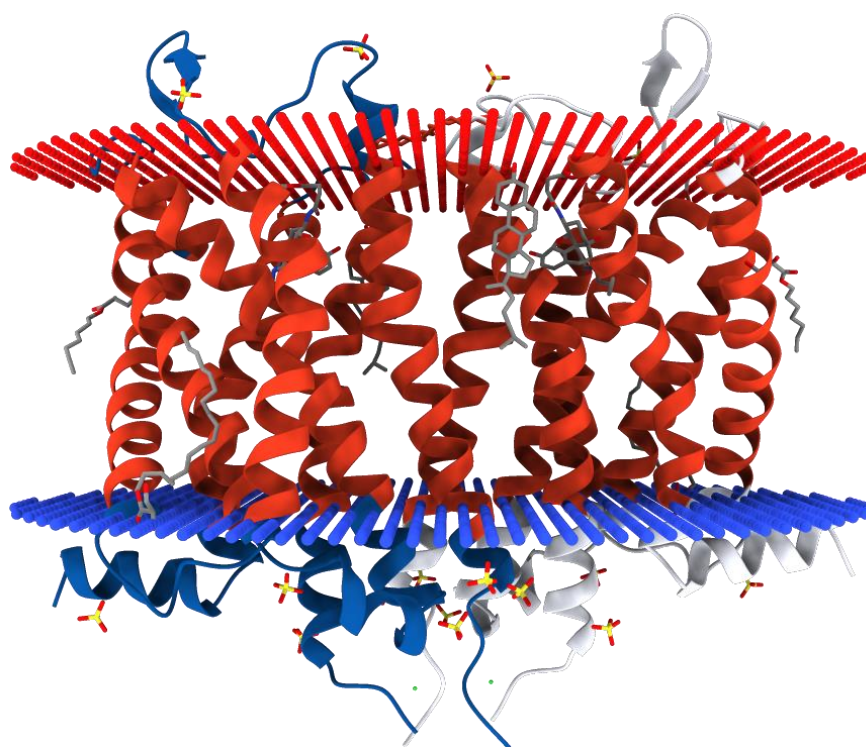


Figure 1.6: The PDB-Crystallographic Deposition file 4DKL (Manglik A *et. al.*, 2012) showing the bound coordinates of the Mu-Opioid Receptor to a Morphinan Antagonist. Rendered in Biovia Discovery Studio Visualiser 4.5.²

² BIOVIA Discovery Studio Visualizer[®]. Available from: <http://accelrys.com/products/collaborative-science/biovia-discovery-studio/visualization.html>

1.4 Kappa Opioid Receptor Antagonists

The potential role of κ OR antagonists in the treatment of a host of psychiatric nervous system disorders including anxiety, depression and substance abuse is currently being extensively researched. It is known that stress can trigger or exacerbate these conditions. κ OR antagonists are able to oppose stress, and this can explain their potential efficacy in this wide range of conditions. (Carlezon & Krystal, 2016)

1.4.1 The cAMP Response Element Binding and Behavioural Studies

The role of the NAc, as part of the mesolimbic system, in motivation and in the pathophysiology of psychiatric illness is well established (Nestler & Carlezon, 2006). DYN acts on κ ORs. These depressive signs are mitigated by κ OR antagonists. This has been shown in pre-clinical screening procedures commonly used in the identification of the common antidepressant medication classes. (Knoll & Carlezon, 2009).

There is evidence that CREB produces antidepressant-like effects in preclinical models due to its involvement in neuroplastic events (Dranovsky & Hen, 2006). Increased CREB function leads to an increased therapeutic effect of antidepressant agents. Carlezon *et al.* (1998) have demonstrated that elevated CREB function showed a reduction in the reward complex effects and CPAs associated with high doses and intermediate doses of cocaine respectively. These effects are strong indicators of anhedonia and dysphoria.

1.4.2 Evidence Showing the Effect of kOR Antagonists

Extensive evidence suggests that elevated DYN plays a pivotal role in the depressive-like effects of elevated CREB function in the NAc (Bals-Kubik *et. al.*, 1993). These include:

- i. Administration of kOR agonists results in depressive effects (Pfeiffer *et. al.*, 1986)
- ii. Microinjection of kOR agonists into the NAc resulted in CPAs similar to doses of cocaine in rats overexpressing CREB (Bals-Kubik *et. al.*, 1993).
- iii. Nor-BNI blocked the depressant-like effects of CREB and produced antidepressant-like of its own, thus producing similar effects to CREB dysfunction (Pliakas *et. al.*, 2001). This finding strongly implicated DYN and kORs in the presence of depressive-like symptoms.

Knoll *et. al.*, (2007) have demonstrated that acute administration of nor-BNI and JDTic produced anxiolytic-like effects in two other tests robustly used to measure antidepressant effects. The Elevated-Plus Maze (EPM) Test is a test used to measure anxiety in laboratory animals such as rodents. Thus, EPM is useful as a screening test for the function of drugs known to either cause, or relieve, anxiety, known as anxiogenic or anxiolytic respectively. The Open-Field test on the other hand is a model used to evaluate anxiety-like behaviour in animals. The test involves subjecting the test animal to an unknown environment such as a glass box that is inescapable. kOR antagonists are currently the only class of agents that produce both antidepressant and anxiolytic effects together. This is important because although currently available treatment, such as SSRIs, are known to ultimately produce both antidepressant and anxiolytic effects in people, these effects usually take a couple of weeks to be seen, and patient adherence

and patient education are very important in these circumstances. Moreover, initial anxiogenic effects with SSRIs may adversely affect adherence to treatment. Thus the use of κ OR antagonists in the future may result in improvement in treatment as people may discontinue their treatment. (Carlezon & Krystal, 2016)

Carlezon & Krystal (2016) have postulated that increased DYN expression promotes activation of κ ORs, which decreases dopamine function and triggers depressive and anxious behaviours. This kind of behaviour is consistent with the evidence that dopamine modulates anxiety in animal models (Reis *et. al.* 2004). κ OR antagonists block DYN actions, thereby restoring dopamine function (Van't Veer & Carlezon, 2013). This function adds complexity in the drug development phase as almost all medications used for mood disorders currently facilitate brain dopamine function (Wise & Bozarth, 1987). This is shown in Figure 1.7 on the following page.

However, studies by Carlezon & Chartoff (2007) have shown that although κ OR antagonists can increase DA concentrations caused by increased κ OR expression, the enhancement of DA function is limited to the point where this makes the drug work through the reward complexes and thus increase its potential addictive properties. On the other hand, mania-like states that are sometimes seen through the administration of the commonly used antidepressants and stimulants is not likely to be seen with κ OR antagonists.

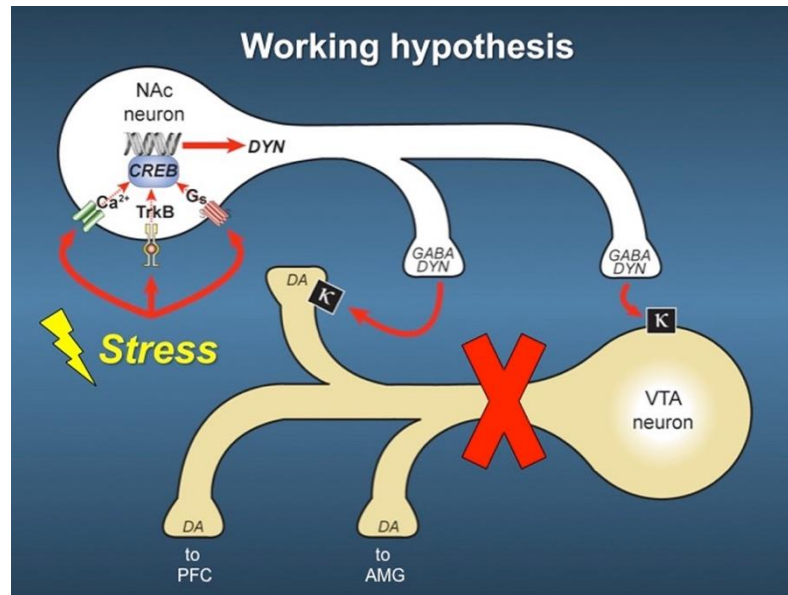


Figure 1.7: Simplified Model to explain how Stress, CREB, DYN and Kappa Opioid Receptors regulate mood and DA release. Adopted from: Carlezon WA Jr & Krystal A. Kappa-Opioid Antagonists for Psychiatric Disorders: from bench to clinical trials. *Depression and Anxiety*. 2016; 33: 895-906.

1.4.3 The κOR Antagonists: Nor-Binaltorphimine, 5'-Guanidinonaltrindole, 5'-Acetamidinoethylnaltrindole & JDtic

One of the major downfalls in animal studies, both rodents and primates, as well as humans, is that the currently available κOR antagonists have extended durations of action. Together with its long acting KOR antagonist properties, nor-BNI induced a short and immediate μOR antagonist action (Broadbear *et. al.*, 1994). Second generation novel molecules such as ANTI and GNTI have been shown to be more selective to the κOR due to their simplified structure, while JDtic was identified as a selective κOR antagonist with high efficacy (Thomas *et. al.*, 2001)(Wang *et. al.*, 2007).

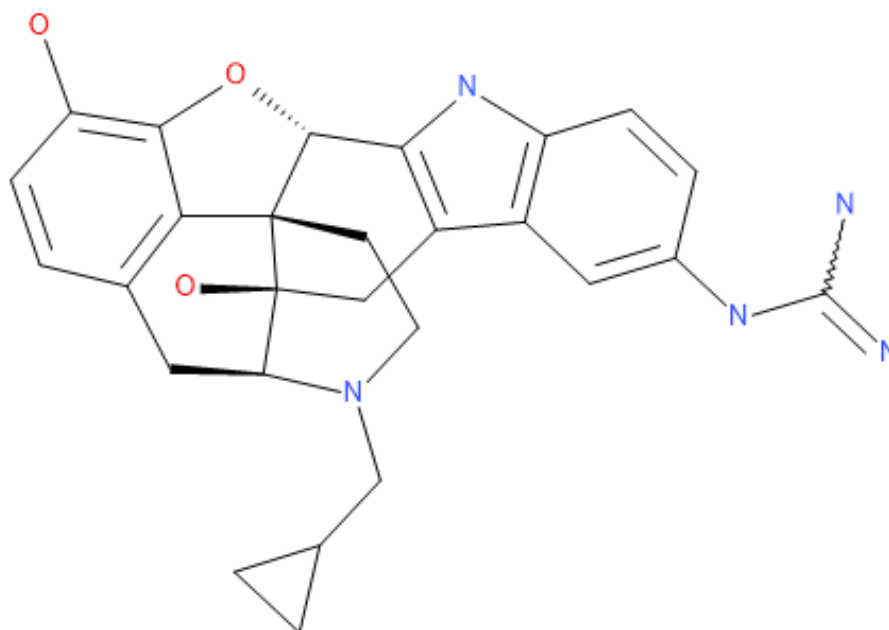


Figure 1.8: 2D Structure of GNTI. Rendered using Accelrys Biovia[®] Draw.³

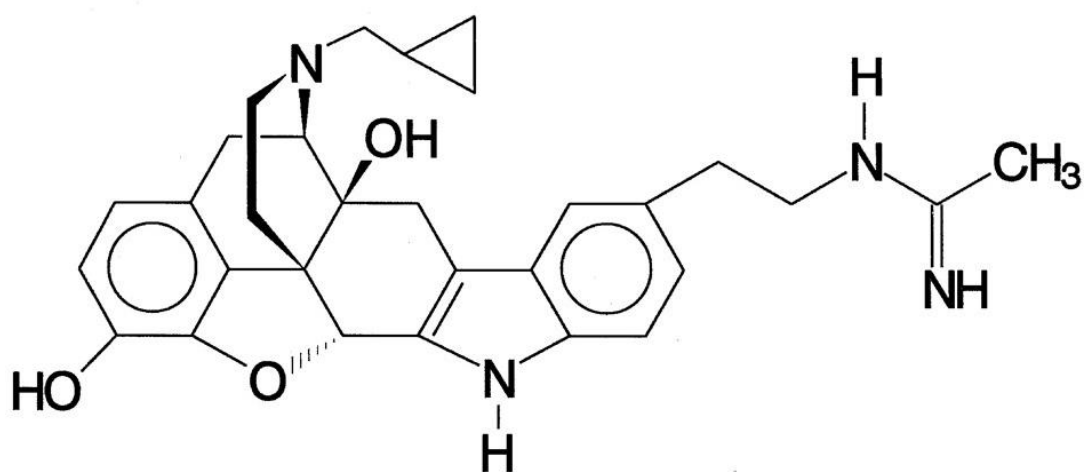


Figure 1.9: 2D Structure of ANTI. Adopted from: Carlezon WA Jr *et al.*, 2009. Structure was unable to be rendered using Accelrys BIOVIA Draw.³

³ Accelrys Biovia[®] Draw. Available from: <http://accelrys.com/products/collaborative-science/biovia-draw/draw-no-fee.php>

Nor-BNI and GNTI are both morphine analogues, with norBNI being created as a bivalent derivative of Naltrexone, itself a derivative of morphine (Portuguese *et. al.*, 1987).

JDTic is a trans-3,4-dimethyl(3-hydroxyphenyl)piperidine analogue, a non-selective opioid agonist. It is a high efficacy, orally-active selective κ OR antagonist with an extended duration of action (Li *et. al.*, 2016). JDTic however showed signs of clinical toxicity during human trials, that were not observed during the *in vivo* and *in vitro* studies on the molecule (Chavkin & Martinez 2015).

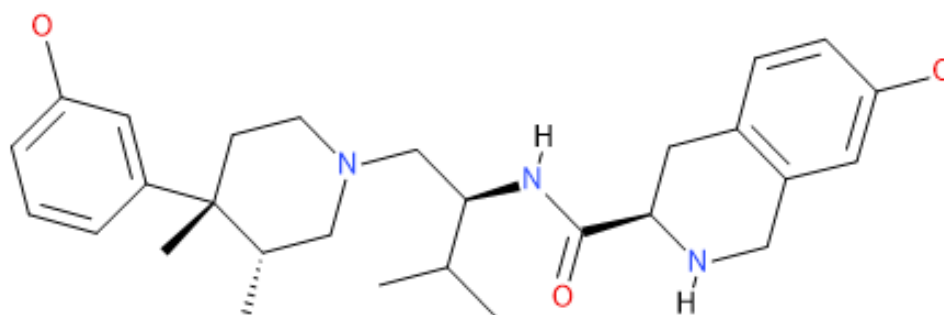


Figure 1.10: 2D Structure of JDTic. Rendered using Accelrys Biovia Draw.³

³ Accelrys Biovia® Draw. Available from: <http://accelrys.com/products/collaborative-science/biovia-draw/draw-no-fee.php>

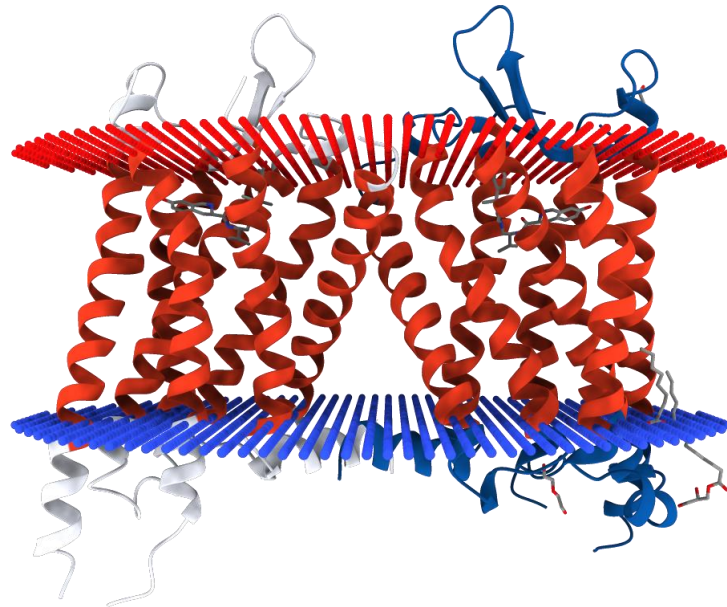


Figure 1.11: The PDB-Crystallographic Deposition file 4DJH (Wu H *et al.*, 2012) showing the ribboned structure of the bound coordinates for the human kappa opioid receptor, in complex with JD1c. Rendered in Biovia Discovery Studio Visualiser 4.5.²

A number of studies (Endoh *et al.*, 1992)(Spanagel & Shippenberg, 1993)(Beardsley *et al.*, 2005)(Metcalf & Coop, 2005) have shown that despite the few similarities in structure, all kOR antagonists have a delayed onset of its kOR antagonist action (24-48hours) and extended effects *in vivo* that may last up to several weeks. Nor-BNI, for example, has been pharmacodynamically shown to have an extremely long-acting mechanism through inhibiting the analgesic effect induced by buprenorphine for up to three weeks *in vivo* (Horan *et al.*, 2013).

² BIOVIA Discovery Studio Visualizer[®]. Available from: <http://accelrys.com/products/collaborative-science/biovia-discovery-studio/visualization.html>

³ Accelrys Biovia Draw[®]. Available from: <http://accelrys.com/products/collaborative-science/biovia-draw/draw-no-fee.php>

This creates significant concerns regarding drug accumulation for the use of nor-BNI as a clinical drug. GNTI is orally inactive due to its poor blood-brain barrier penetration due to the presence of a fully ionized guanidinium group in its structure. (Munro *et. al.*, 2012).

1.4.4 Buprenorphine in combination with Samidorphan

Buprenorphine is synthesised from thebaine. It was initially designed as an analgesic with a long duration of action with targeted action against opioid addiction. (Li *et. al.*, 2016) The antidepressant effect of buprenorphine has been investigated in view of the unique κ OR antagonist and μ OR partial agonist properties for the treatment of refractory depression (Bodkin *et. al.*, 1995). However, its use is restricted by mu-like side effects such as nausea, constipation and dyspnoea (Ray *et. al.*, 2004)

A fixed combination of buprenorphine and ALKS33 (known as Samidorphan or ALKS 5461) is being developed for the sublingual administration in people with major depressive disorder. Samidorphan is a full μ OR antagonist, aimed at reversing the side effects resulting from the Mu-like moieties in buprenorphine. However, there was insufficient evidence of overall effectiveness in major depressive disorder upon its preliminary review.

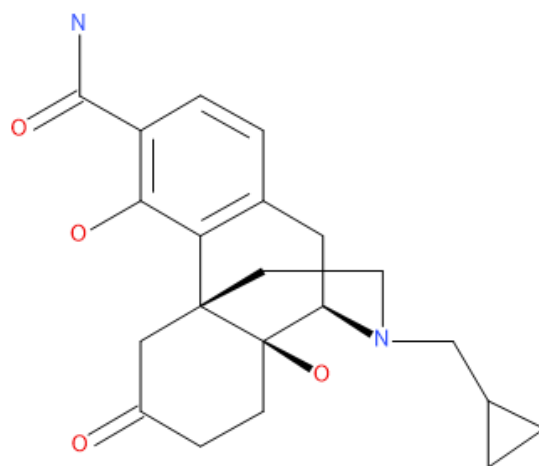


Figure 1.12: 2D Structure of Samidorphan. Rendered using Accelrys Biovia Draw.³

1.4.5 The Continuous Research for new κ OR Antagonists

Bruchas *et. al.* (2007) have shown that κ OR antagonists result in a vast number of changes in the c-Jun N-terminal kinase (JNK) function. This is thought to be the reason for the long-lasting *in vivo* effects. The long-lasting effects of nor-BNI could be counteracted through the pre-treatment administration of Naloxone, an opioid receptor antagonist (Bruchas *et. al.*, 2007). It would be interesting to optimise shorter-lasting selective κ OR antagonists with high efficacy, which will help to determine the importance of the long-lasting effects of these antagonists (Carlezon *et. al.*, 2009).

Buprenorphine has shown promising antidepressant results in clinical experiments (Bodkin *et. al.*, 1995). It is a mixed μ OR agonist/ κ OR antagonist, although most evidence points at it being a κ OR partial-agonist. On the other hand, true antagonists (e.g., nor-BNI) provide no results. (Zhu *et. al.*, 1997). Similarly, the mixed μ OR/ κ OR antagonists

³ Accelrys Biovia Draw[®]. Available from: <http://accelrys.com/products/collaborative-science/biovia-draw/draw-no-fee.php>

Extensive studies have been performed on Naltrexone and Nalmephehene in substance abuse and compulsion disorder clinical trials, diseases in which comorbid depression is very common.

The continuous search for new kOR antagonists, despite the problems being encountered through both research phases and clinical trials, emphasises the importance and the need for the identification of new molecules with the possibility of an antagonistic effect on kORs.

1.5 Combined therapy

Both DYNs and kORs are vastly present in brain areas involved in the reward complex, as well as cognitive behaviour and the response to stress. These areas include the hippocampus, amygdala (AMG), locus coeruleus, hypothalamus, ventral tegmental area (VTA) and NAc (Kitchen *et al.*, 1997).

When rodents are exposed to stress during the FST, they exhibited increased immobility, in keeping with pro-depressive-like behaviour (McLaughlin *et al.*, 2003; Carlezon *et al.*, 2006). This happens when DYN is released or when kOR agonists are administered. Conversely, removal of the k-receptor gene or PDYN gene blocking results in a stress-induced pro-depressive-like effect (McLaughlin *et al.*, 2003).

Currently available k-antagonists' use *in vivo* is limited by their pharmacological properties – long-lasting antagonist effects and slow onset of action (Beguin & Cohen, 2009). For example, nor-BNI's k-antagonist effect starts after 24 hours, continues at high levels for more than a week and returns to control levels not before at least 1 month has passed, and can last for even a few months. Thus their effect is not easily reversed. In a thesis presented by Almatroudi *et al.* (2015), Buprenorphine and Naltrexone were used as an alternative approach. This approach involved the use of medications already licensed and marketed for other indications.

1.5.1 Buprenorphine

Buprenorphine is a semi-synthetic opioid that acts as a partial μ OR agonist and a k OR antagonist. Buprenorphine also has partial agonist activity at the nociception/orphanin FQ receptor (NOR). It is clinically licensed as a strong analgesic, as a substitute in opioid addiction treatment and has also shown potential in the management of refractory depression. Emrich *et al.* (1983) have reported that buprenorphine induced strong antidepressant effect in patients. Bodkin *et al.* (1995) purport buprenorphine to also be effective in patients with SSRI-refractory depression. The biggest barrier to its clinical use is that, like other μ -agonists, there is a risk of abuse and dependence.

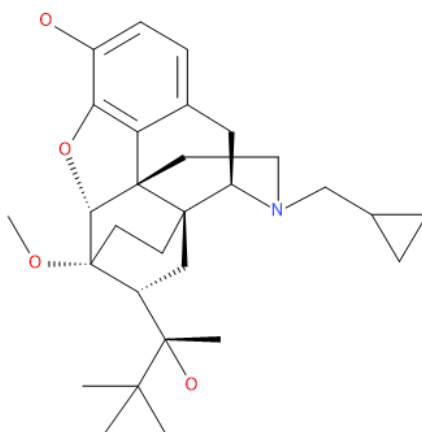


Figure 1.13: 2D Buprenorphine Structure. Rendered using Accelrys BIOVIA Draw.³

³ Accelrys Biovia Draw[®]. Available from: <http://accelrys.com/products/collaborative-science/biovia-draw/draw-no-fee.php>

1.5.2 Naltrexone

Naltrexone, a partially selective to non-selective opioid receptor antagonist. Studies have shown a higher affinity for μ OR than κ OR and is licensed as treatment in alcohol addiction abstinence (Rosner *et al.*, 2010). Grienko *et al.* (2003) demonstrated naltrexone's use in heroin addicts to reduce the chances of relapse. However, naltrexone had no valuable effect on the depressed mood resulting in reduced patient adherence. Grienko *et al.* (2003) tried to counteract this by combining naltrexone with SSRI antidepressants.

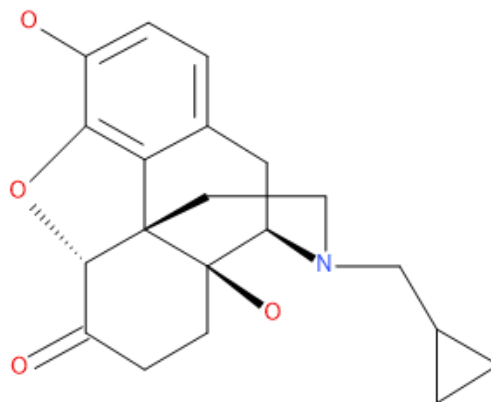


Figure 1.14: 2D Naltrexone Structure. Rendered using Accelrys BIOVIA Draw.³

³ Accelrys Biovia Draw[®]. Available from: <http://accelrys.com/products/collaborative-science/biovia-draw/draw-no-fee.php>

1.5.3 Buprenorphine/Naltrexone Combination

It is therefore understandable that some authors hypothesised that combining naltrexone with buprenorphine would reduce anhedonia, reduce dysphoria and the subsequent relapse risk during maintenance treatment. Rothman *et al.*, (2000) posed a thesis that showed a positive response with a combination of Buprenorphine and Naltrexone that exceeded that from naltrexone alone.

Rothman *et al.*, (1991) had postulated that combining the buprenorphine with naltrexone would result in a κ OR “overdrive”. Thus in a Buprenorphine and Naltrexone combination, the naltrexone would almost totally block the μ OR agonist effects of buprenorphine, allowing its κ OR antagonist action to prevail thereby improving anhedonia as well as Naltrexone compliance itself (Gerra *et al.*, 2006).

1.5.4 Previous Buprenorphine/Samidorphan Combination Therapy

Ehrich *et al.* (2015) have reported that a buprenorphine/samidorphan combination had adequate clinical action in major depressive disorder patients without potential of addiction. Samidorphan is a μ OR antagonist. The safety and tolerability profile of the buprenorphine and samidorphan combination was favourable with the most commonly reported adverse effects were the commonly associated side effects associated with opioids such as nausea and vomiting.

1.5.5 Limitations to the Buprenorphine/Naltrexone Combined Therapy

Almatroudi *et al.* (2015) have demonstrated that a buprenorphine (1mg/kg) in combination with naltrexone (1mg/kg) showed short acting κ -antagonist results in rodent clinical trials. They also showed that this dose combination causes neither CPA or CPP, and does not result in any significant locomotor effects. The authors acknowledge that one important caution is that these findings are based on mouse behaviour paradigms (Cryan *et al.*, 2002)

Administration of this combination at the correct doses was not easily achievable due to the fact that Naltrexone is orally administered, while Buprenorphine is administered sublingually (Almatroudi *et al.*, 2015). This is because the oral bioavailability of buprenorphine is very poor and the use of higher doses of naltrexone will need careful titration to prevent adverse effects (Bouza *et al.*, 2004). Cicero *et al.* (2014) have described how the abuse potential of buprenorphine has had risen dramatically in the five years preceding their study, particularly in those who also use heroin. For these reasons, Buprenorphine is rarely used for its antidepressant properties, but is more commonly used as a methadone substitute as medication for withdrawal, or to wean patients off opioids.

The challenge present is to fulfil the need for a shorter-acting and safe κ OR antagonist with high clinical efficacy to provide acceptable antidepressant results through an alternative route (Almatroudi *et al.*, 2015). The addiction potential and adherence problems that arise from the separate administration of these two drugs make the combination undesirable.

1.6 BU10119

It has already been established that the combination of buprenorphine and naltrexone provides effective antidepressant effect without addictive or other adverse, for example sedating effects. In order to overcome the dosing difficulties presented in having to administer two drugs through two different routes, researchers have come up with a single compound combination of buprenorphine/naltrexone, BU10119. This also eliminates the abuse potential (Cueva *et al.*, 2015). In a thesis presented by Almatroudi *et al.* (2015), they concluded that:

“In vitro pharmacology shows that BU10119 is a κ OR antagonist with little efficacy at the μ -opioid receptor. Here we have shown that BU10119 has antidepressant-like activity in the FST and NIH. These effects are equipotent with the combination of buprenorphine/naltrexone and consistent with its κ OR antagonist potential.”

Almatroudi (2015), in his thesis, also remarked that the Buprenorphine/Naltrexone combination and BU10119 had no clinical effect in the EPM and light-dark box (LDB) tests. The latter tests are aimed to assess anxiety-related behaviours.

Cueva *et al.* (2015) have studied further the potential in the development of compounds with similar pharmacological profiles to that of Buprenorphine, but with lower efficacy at μ OR. Cueva *et al.* (2015) report on a series of orvinol analogues with differing methyl group positions which then resulted in a more robust κ OR antagonism with limited to non-existent μ OR antagonist effect. Others are seen to have analgesic potential with lesser side-effects (Cueva *et al.*, 2015).

1.7 Drug Design

1.7.1 Rational Drug Design

The process of discovering new drugs is a very challenging one, that is also highly time consuming and expensive. A multidisciplinary approach, as described by Mandal *et al.*, (2009), is necessary for the drug development process. Rational Drug Design (RDD) is used to decrease the costs and increase the speed of discovery of possible drug molecules. X-Ray Crystallography, Nuclear Magnetic Resonance (NMR) and Computer Technology allow predictions to be made at much higher accuracy regarding the ligands that have the potential to further proceed in the drug design process. The ultimate aim, of course, is to have molecules that become medicinal products (Parenti & Rastelli, 2012).

1.7.2 Computational Aided Drug Discovery

RDD procedures rely on the functioning 3-Dimensional structures of either the ligand or the ligand receptor complexes being studied. This knowledge is required in the search for novel structures, which are generated using the computational molecular modelling. Due to these processes being modelled via computers, this process can also be known as Computational Aided Drug Discovery (CADD).

CADD can be split into two general classifications:

- i. Pharmacophore Based Drug Design (also known as Ligand Based), and
- ii. Receptor Based Drug Design (also known as Structure Based)

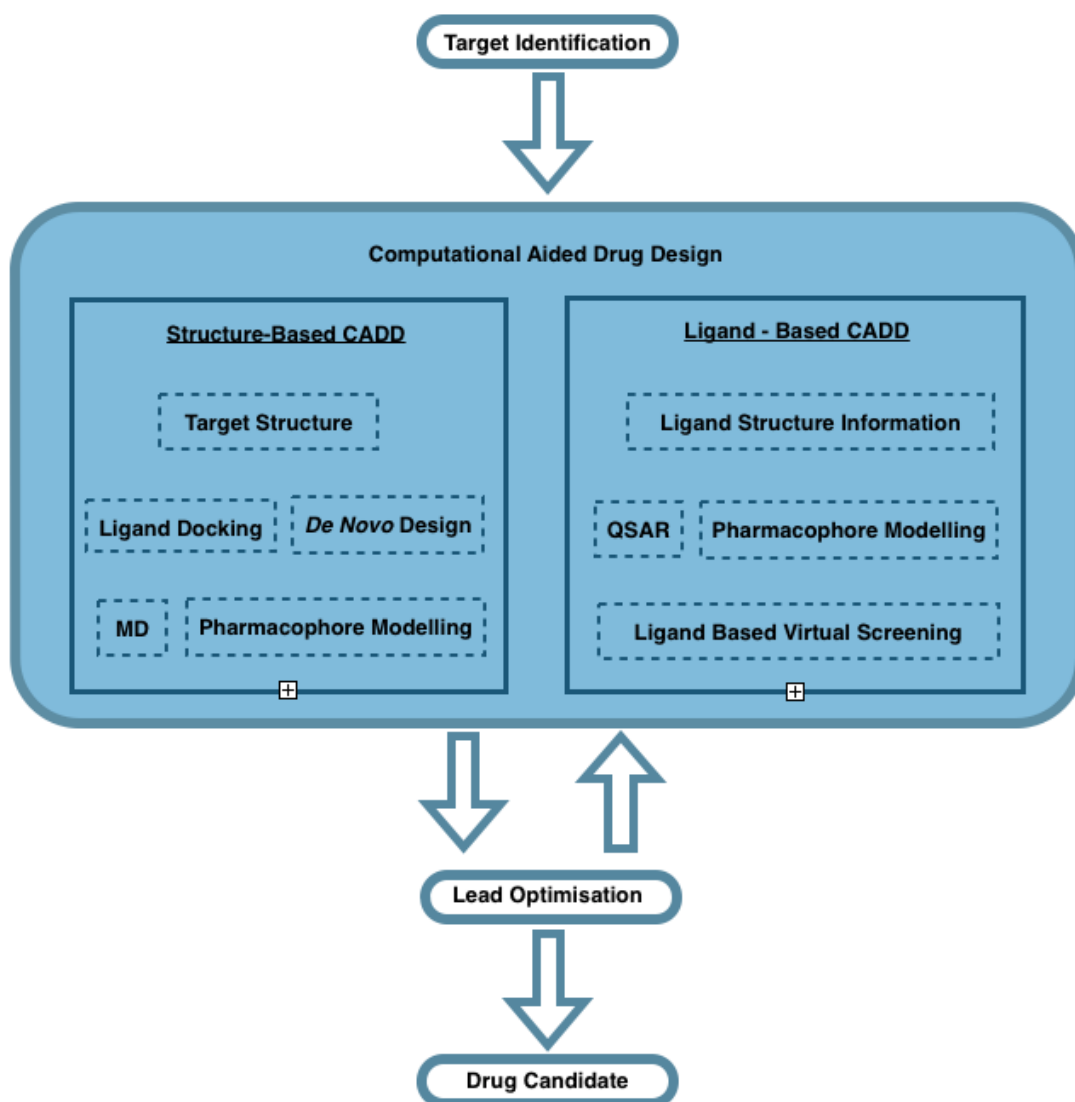


Figure 1.15: Simplified Figure explaining the processes involved in Computational Aided Drug Discovery (CADD). The aim is that these Design Processes lead to the identification of multiple lead compounds. Adapted from: Sliwoski G *et al.*, 2014.

1.7.2.1 Pharmacophore Based Drug Design (Ligand Based Drug Design)

Pharmacophore Drug Design is applied when the three dimensional structure of the ligand is known, but the structure of the receptor is not. The pharmacophore of the molecule is that part of the molecular structure that allows the molecule to perform its pharmacological or biological interaction at its target site. The pharmacophore of the ligand is obtained through the use of computational software.

1.7.2.2 Receptor Based Drug Design (Structure Based Drug Design)

In receptor based drug design, the receptor is considered to be the target for which the drug molecule is designed. The 3D structure of the receptor bound to its endogenous ligand (or drug) is known. X-Ray Crystallography and NMR are important crystallographic methods for obtaining the structure of the receptor. This type of drug design is preferred in RDD as the information available about the receptor allows the molecular design process to be more efficient, making the process of the identification of a molecule that fits into the receptors' active site easier to design (Hughes *et al.*, 2011). After the structure of the ligand receptor complex is known, this structure is screened against a large library of chemical compounds for the identification of any hit molecules. This process is known as high-throughput screening. The molecules that are expected to succeed, eventually forming lead molecules, are selected by conducting further studies on the hit molecules, and modifying the pharmacophore of these hit molecules and lead molecules.

Receptor Based Drug Design can also be divided into two methods:

- i. Virtual Screening
- ii. Building Ligands

Virtual screening involves a process that searches for viable ligands that are capable of interacting with the ligand binding pocket of the receptor in question. A search through a database of molecules is conducted to identify molecules suitable for interactions.

Building Ligands on the other hand is a process which, unlike in Virtual Screening, the ligand is built from scratch. This is known as *De Novo* Design. The main disadvantage with this method is that it is more time consuming than Virtual Screening.

1.7.3 X-Ray Crystallography in Structure Determination

According to Vijayakrishnan (2009), X-Ray Crystallography is the most reliable method to define the 3D structure. This method of determination gives information on both the structural information of the crystallographic deposition being used in the drug design process, as well as the coordinates needed in the *in silico* design methods.

1.7.4 Lead Molecules

A lead molecule is a molecule that is considered to be drug like, but is never said to be a drug. Tests on lead compounds are performed *in vivo* to allow the identification of drug candidates. A lead molecule shows sub-optimal affinity to the target and sub-optimal drug-like properties, for example shows a good bioavailability. There is however enough evidence to support the fact that the lead molecule could become a clinically useful molecule by optimisation.

1.7.5 Protein Data Bank

The RCSB Protein Data Bank (PDB)⁵ is one of the largest online repositories. It contains the crystallographic deposits of proteins, nucleic acids and other large biological compounds isolated using X-Ray Crystallography or NMR (Berman, *et al.*, 2000). The advance in computational technologies and methods for collection of crystallographic deposits of macromolecular crystal structures aided highly in the growth of the PDB. The interactions between many receptors and small molecules can be found via the PDB.

⁵ [rcsb.org/pdb/](https://www.rcsb.org/pdb/) [Internet]. University College of San Diego & Rutgers University New Jersey: Structural Bioinformatics; c1971. [cited 2018 May 10]. Available from: <https://www.rcsb.org>

1.8 Computational Tools and Software.

Computational Tools have made the process of determining the 3D structure of the proteins and ligands in questions, as well as the protein ligand complex, a much more simplified and less economically consuming process.

According to Parenti & Rastelli (2012), the relationship between *in silico* and experimental results obtained should be in agreement when the computational methods and protocols being implemented are validated. The list of software used for the purpose of this project have been listed below.

1.8.1 SYBYL[®]-X Version 2.0⁶

SYBYL-X (Tripos) is a computational tool that, through lead optimisation, allows molecular modelling from a known sequence. This computational tool allows the modelling and simulation of small molecules and macromolecules, as well as cheminformatics and lead identification. (Ash *et. al*, 2010)

1.8.2 PoseView[®]⁷

PoseView (Stierand & Rarey, 2007; Stierand & Rarey, 2010) enables the medicinal chemist to view PDB files in a 3D format, but generated into a 2D diagram via direct input (i.e. through crystal structures) or through a docking program.

⁶ SYBYL[®]-X. Available from: <http://sybyl-x.software.informer.com/2.0>

⁷ PoseView[®]. Available from: <https://www.biosolveit.de/download/index.html>

1.8.3 X-Score Version 1.2⁸

X-Score is a free-to-download computational tool that calculates the binding affinity of a ligand to its target protein. The receptor structure should be obtained in the PDB file format and the ligand in the 'mol2' file format for the program to be able to calculate the binding affinity. X-Score[®] (Wang *et al*, 2002) is only used when the ligand is already docked in the Ligand Binding Pocket, a function that is done by the computational tool SYBYL[®]-X.

1.8.4 LigBuilder[®] Version 2.1⁹

LigBuilder is able to build ligand molecules bound to the binding pocket and screen them. This program is used for Structure Based *de novo* Drug Design and Lead Optimisation. (Wang *et al*, 2000). The three main features incorporated into this program, and are required to be used sequentially are Cavity, Build and Fragment Database (Yuan *et. al.*, 2011).

1.8.5 Accelrys BIOVIA[®] Draw Version 18.1¹⁰

BIOVIA Draw (Accelrys Software Inc., 2001) allows the medicinal chemist to obtain a high definition two-dimensional structure of the structure required, as well as any biological sequences or reactions required. The program a free-to-download after a short registration for all students and academic staff.

⁸X-Score Version 1.2. Available from: <http://sw16.im.med.umich.edu/software/xtool/>

⁹LigBuilder[®] Version 2.1. Available from:
<ftp://162.105.160.5/pub/incoming/yxyuan/Web/ligbuilder/index.html>

¹⁰Accelrys BIOVIA Draw[®]. Available from: <http://accelrys.com/products/collaborative-science/biovia-draw/draw-no-fee.php>

1.8.6 BIOVIA[®] Discovery Studio Visualizer¹¹

BIOVIA Discovery Studio Visualizer (Dassault Systèmes BIOVIA, 2015) is a program that allows the visualisation of PDB files in 3D. This makes the process of *in silico* investigation simpler through the modelling of structures and biological processes. Discovery Studio can provide the required details about the interactions formed by the ligand/receptor complex in both 2D and 3D formats.

1.8.7 UCSF Chimera[®] Version 1.12¹²

UCSF Chimera (Pettersen *et al.*, 2004) enables the visualisation and rendering of PDB files in a 3D format. UCSF Chimera is able to analyse molecules and receptors, as well as creating animations and high quality images of the required structures using complex functions.

1.8.8 ChemSketch[®] Version 11¹³

ChemSketch (ACD/ChemSketch, 2006) is a sketching application that allows the user to draw from scratch the chemical structures of the molecules needed. It also allows the calculation of molecular weight, 2D and 3D structure viewing, molar refractivity, prediction of LogP and density among others. It also contains a function that allows the user to find out the exact name of the structure being studied, as long as it has less than 3 rings and 50 atoms.

¹¹ BIOVIA Discovery Studio Visualizer[®]. Available from: <http://accelrys.com/products/collaborative-science/biovia-discovery-studio/visualization.html>

¹² UCSF Chimera[®] Version 1.12. Available from: <https://www.cgl.ucsf.edu/chimera/download.html>

¹³ ChemSketch[®] Version 11. Available from: <http://www.acdlabs.com/resources/freeware/chemsketch/>

1.8.9 LigandScout[®] 3.12

LigandScout is an application that creates the three dimensional pharmacophore models from data about the structures, affinities and energies of the molecule-ligand complexes. A pharmacophore describes the arrangement of the essential groups for the interaction of the molecules in space. (Wolber, 2005).

1.8.10 ZINCPharmer[®] 14

ZINCPharmer is an online domain that is used to obtain purchasable compounds using the pharmacophores produced using LigandScout[®] (Wolber, 2006). Any acceptable compounds are given as hits for each pharmacophore from separate databases embedded in the online interface. (Koes, 2012).

¹⁴ ZINCPharmer[®]. Available from: <http://zincpharmer.csb.pitt.edu/pharmer.html>

1.9 Aim

This literature review has been instrumental in highlighting depression as a condition that warrants further research if management is to be optimised and patient compliance increased. The identification of the κ OR as a novel target in the management of depression represents a step forward. Literature also evidences the synergistic anti-depressant effect of buprenorphine and naltrexone, but it is also indicative of administration limitations, and of the fact that buprenorphine has been linked to abuse. The paper of Almatroudi *et al.* (2015) has highlighted an innovative approach to the design of novel anti-depressant molecules through the combination of pharmacophoric moieties from buprenorphine and naltrexone which retain the synergistic effect of co-administration of these molecules and significantly limit their adverse effects and problems of administration.

This literature review consequently shows that there is a basis for the execution of this study which aims to use the BU10119 scaffold that combines the essential moieties of buprenorphine and naltrexone into a single molecule as a lead. This molecule will be docked into the κ OR and the critical interactions forged between it and the κ OR ligand binding pocket exploited in both *De novo* and Virtual Screening exercises for the identification of superior κ OR modulators. The optimal structures will be identified for further validation.

Chapter 2

Methodology

Chapter 2: Methodology

2.1 Selection of Protein Data Bank Crystallographic Depositions

BU10119 is a dual K/U antagonist and its use as a potential treatment for SSRI Refractory Depression is being studied in this *in silico* study. Since BU10119 is a dual antagonist, two PDB crystallographic depositions were used. *de novo* based and receptor-based drug-design approaches were adopted in this study.

The PDB crystallographic depositions chosen for this study were:

- 4DJH (Wu, 2012) describing the structure of the human kappa opioid receptor bound to the kappa opioid antagonist JDTC.
- 4DKL (Manglik, 2012) describing the crystal structure of the mu-opioid receptor bound to the morphinan antagonist BF0601.

Molecular modelling of the novel BU10119 molecule was carried out *de novo* using Sybyl-X®. (Ash *et. al.*, 2010)

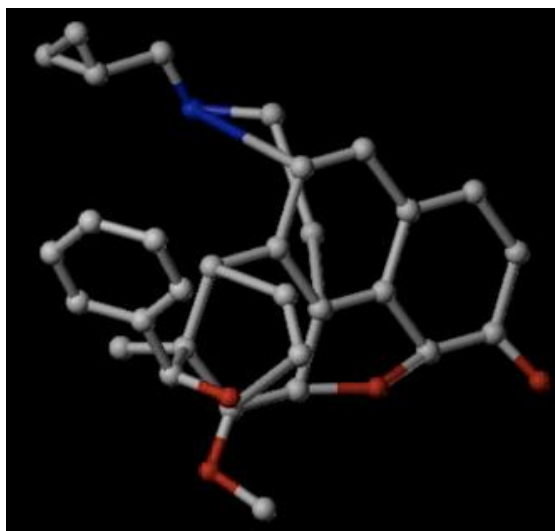


Figure 2.1: The structure of BU10119 modelled through the *de novo* approach using Sybyl-X (Ash *et. al*, 2010).

2.2 Extraction of Ligands

Sybyl-X[®] (Ash *et. al*, 2010) was used for molecular modelling and PDB visualisation.

The morphinan antagonist BF0601 was extracted from the μ OR obtained from the PDB crystallographic deposition 4DKL (Manglik, 2012). Similarly, the kappa antagonist JDTic (also labelled as JDC1300) was extracted from the κ OR obtained from the PDB crystallographic deposition 4DJH (Wu, 2012). The extraction of ligands was carried out using Sybyl-X[®] (Ash *et. al*, 2010).

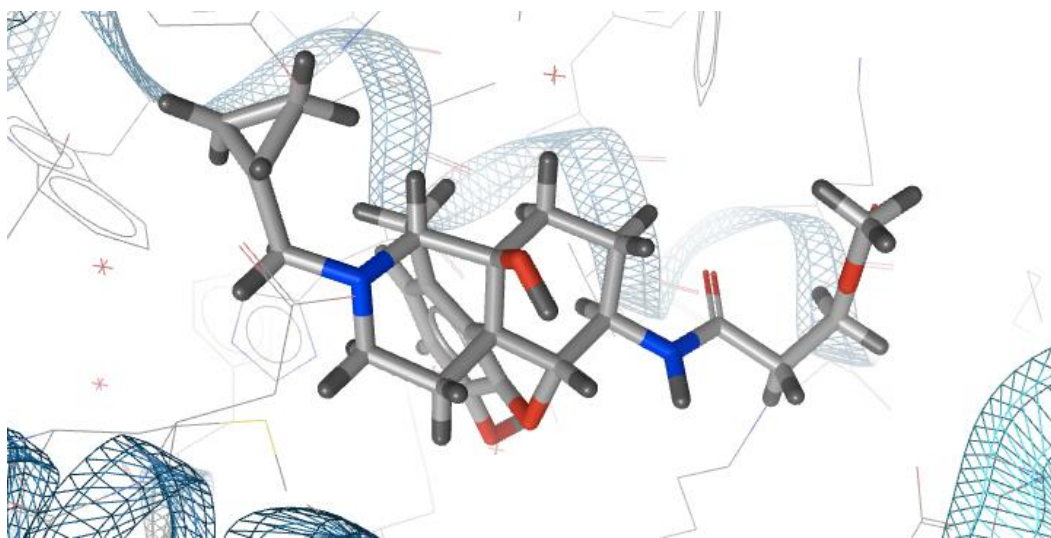


Figure 2.2: Structure of the morphinan antagonist BF0601 extracted from the μ OR using Sybyl-X (Ash *et. al*, 2010).

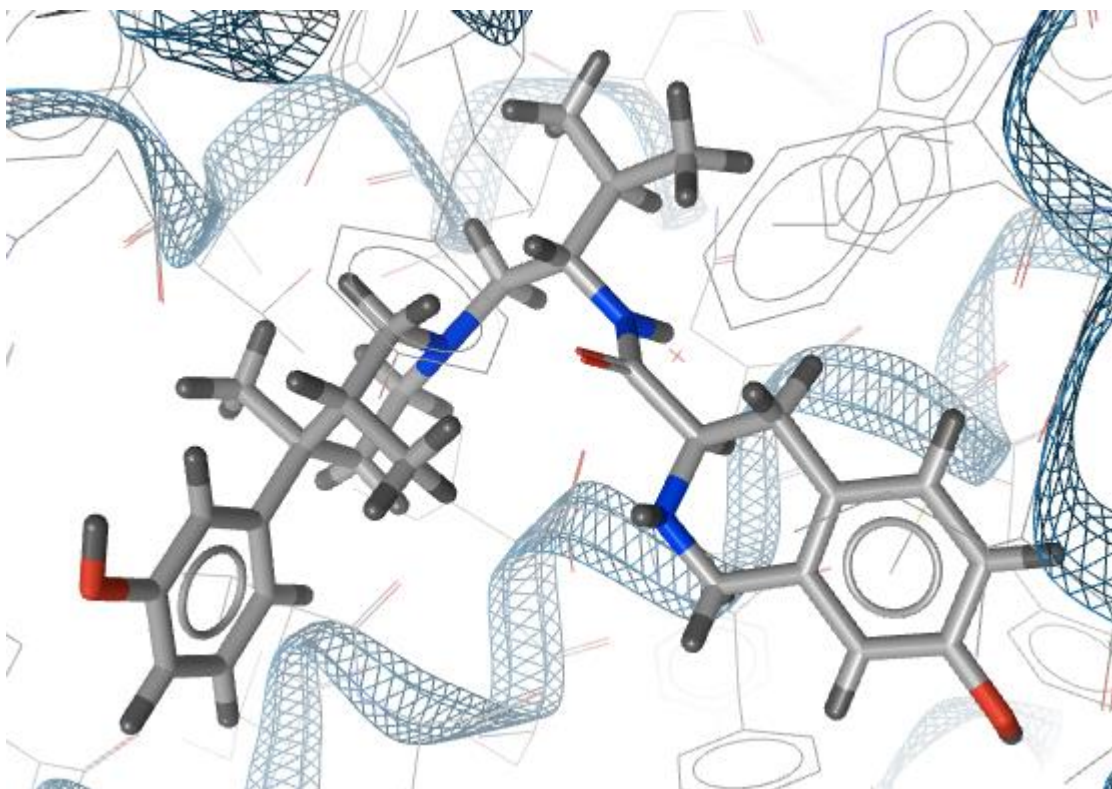


Figure 2.3: Structure of the kappa opioid receptor antagonist JDC1300 (also known as JD1c) extracted from the κ OR using Sybyl-X (Ash *et. al*, 2010).

Molecular simplification was also carried out using Sybyl-X[®] (Ash *et. al*, 2010). This involved the extraction of small molecules that are not critical to binding. These were the water molecules lying at a distance greater than 5Å from the ligand binding pocket and other molecules that did not affect ligand binding. The apo forms of both the κ OR and the μ OR were created using the processes above, and were saved in the PDB format.

2.3 Conformational Analysis

2.3.1 Generation of BU10119 conformers

The 'Similarity Suite' tool in Sybyl-X[®] (Ash *et. al*, 2010) was used to generate different conformers of BU10119. This tool is utilised to probe the conformational space of both the apo- κ OR ligand binding pocket and the apo- μ OR ligand binding pocket to identify the optimal BU10119 conformers for each receptor.

BU10119 was used as a lead in a Virtual Screening exercise to identify analogous structures. It was then docked into the apo- κ OR and conformational analysis was used to identify the optimal binding poses of this molecule. This Virtual Screening exercise was repeated to obtain the optimal binding conformations of BU10119 when docked in the apo- μ OR.

Conformational analysis was performed in order to identify the optimal conformation of BU10119 within the ligand binding pocket for each receptor. 20 BU10119 conformers for each receptor subtype were generated using Sybyl-X^{®6} and each conformer represented a conformation of BU10119 within the receptor subtype ligand binding pocket. This was done to allow the optimal exploitation of the available space of the ligand binding pocket. Each conformer was numbered so as to be easily identified. This created a total of 40 BU10119 conformers, 20 for the κ OR and 20 for the μ OR.

2.3.2 Calculation of the Ligand Binding Energy (kcal mol⁻¹)

The ligand binding energies (LBEs) for all the 40 conformers were calculated using Sybyl-X[®] (Ash *et. al*, 2010) and expressed in kcal/mol. The LBE is used as a prediction for molecular stability. This was calculated by adding up the sums of different energy values for each conformer which are:

- i. Van der Waals Energy
- ii. Torsional Energy
- iii. Angle Bending Energy
- iv. Bond Stretching Energy
- v. Out of Plane Bending Energy

2.3.3 Calculation of the Ligand Binding Affinity (pKd)

X-Score[®] (Wang *et al.*, 2002) is a computational programme that has been designed specifically to calculate the different binding affinities between different poses of BU10119 for both receptors. The apo forms of the kOR and μ OR, together with the respective BU10119 conformers for each receptor were entered and X-Score[®] (Wang *et al.*, 2002) was run to obtain the Ligand Binding Affinity (LBA).

LBA is the baseline affinity of the ligand previously extracted to the respective receptor.

This was calculated by using several functions such as:

- i. Van der Waals Interactions
- ii. Hydrophobicity
- iii. Hydrogen bonding

These values were used to measure the LBA, representing the average affinity, that is expressed in pKd. This was done for all the 40 BU10119 conformers at either the κ OR ligand binding pocket, or the μ OR ligand binding pocket.

2.3.4 Choosing the Optimal Conformer

The values obtained from X-Score[®] (Wang et al., 2002) which calculated the LBA (pKd) and the LBE (kcal mol⁻¹) which was calculated in Sybyl-X[®] (Ash *et. al*, 2010) of each BU10119 conformer were all inputted in a Microsoft[®] Excel sheet.

The conformers were viewed using Sybyl-X[®] (Ash *et. al*, 2010) and grouped according to their conformational shape in space. This was done for both the 20 best conformers for the κ OR as well as the 20 best conformers for the μ OR and resulted in 5 groups for the best conformers for the κ OR and 7 groups for the best conformers for the μ OR.

A graph was plotted comparing the conformers for each receptor subtype. This compared the LBE (kcalmol^{-1}) versus the LBA (pKd) values for each of the conformers according to the respective opioid receptor they bind to. The best BU10119 conformers for each receptor from each group were chosen taking into account the LBE (kcalmol^{-1}) and the LBA (pKd). The optimal conformers have a high affinity (LBA) and low energy (LBE) to the ligand binding pocket. The distance between these two on the graph determines the stability relative to the affinity of the Ligand Binding Pocket. This will yield conformers with high affinity and stability to the ligand binding pocket. Thus, this resulted in the choice of a total of 5 BU10119 structures that are dissimilar in space that fit into the κ OR, and 7 BU10119 dissimilar structures in space that fit into the μ OR. These structures were then kept for use in Virtual Screening.

2.4 Virtual Screening

2.4.1 Generating pharmacophores

Two separate consensus pharmacophores were modelled using LigandScout® (Wolber, 2005). These pharmacophores represent the 3D interactions showing hydrogen bond donors, hydrogen bond acceptors, lipophilic (hydrophobic) areas and positive ionisable areas between the molecule BU10119 and the extract obtained from the Ligand Binding Pocket of either the κ OR and μ OR. The consensus pharmacophores created represent:

- i. An average between the JDC1300 molecule (κ OR antagonist) and the 5 optimal BU10119 conformers for the ligand binding pocket of the κ OR found previously through Conformational Analysis.
- ii. An average between the BF0601 molecule (μ OR antagonist) and the 7 optimal BU10119 conformers for the ligand binding pocket of the μ OR found previously through Conformational Analysis.

An Overall Consensus Pharmacophore represents the common areas between two or more separate consensus pharmacophores. An Overall Consensus Pharmacophore could not be created between the two pharmacophores created above. This indicated that the two separate pharmacophores could not be superimposed.

The PDB 4DJH (Wu et al., 2012) crystallographic deposition was imported into LigandScout® (Wolber, 2005). A display of the κ OR and the coordinates of its bound ligands was shown in 'Macromolecular View'. The κ OR antagonist JDC1300 was chosen and viewed in 'Active View' in order to observe the amino acids of the ligand within the receptor site in more detail. The amino acids that create the critical interactions with the ligand can also be viewed. A pharmacophore was created for JDC1300. The 5 optimal BU10119 conformers for the ligand binding pocket of the κ OR found above were also inserted separately into LigandScout® (Wolber, 2005) and pharmacophores of each were created. A consensus pharmacophore representing an average of JDC1300 and the BU10110 scaffolds was modelled using the 'Alignment' tab. This process was repeated for the μ OR antagonist BF0601, and the 7 optimal BU10119 conformers for the ligand binding pocket of the μ OR.

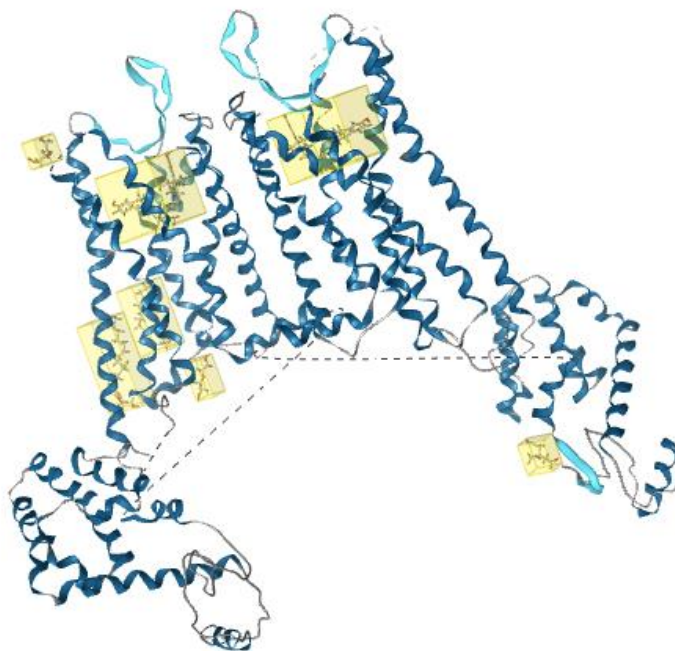


Figure 2.4: Structure of the human kappa opioid receptor bound to the kappa opioid receptor antagonist JDC1300 obtained using the 'Macromolecular View' in LigandScout® (Wolber, 2005).

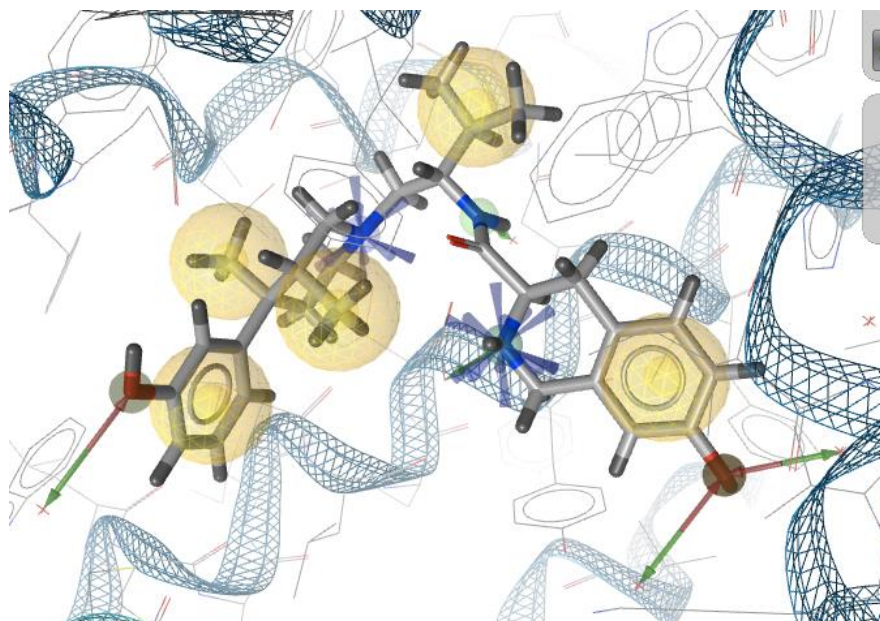


Figure 2.5: Structure of the kappa opioid receptor antagonist JDC1300 together with its pharmacophore and surrounding amino acids within the receptor site obtained using the 'Active View' in LigandScout® (Wolber, 2005).

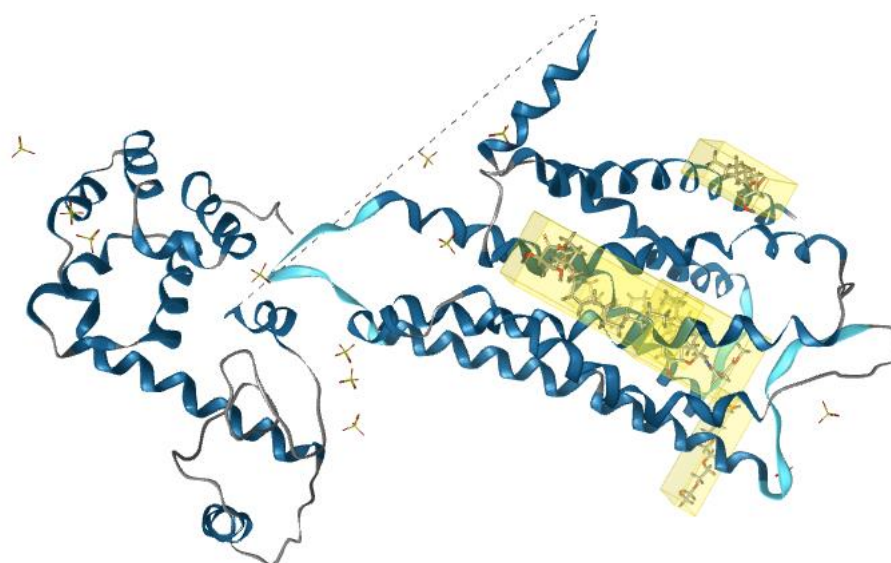


Figure 2.6: Structure of the mu opioid receptor bound to the morphinan antagonist BF0601 obtained using the 'Macromolecular View' in LigandScout® (Wolber, 2005).

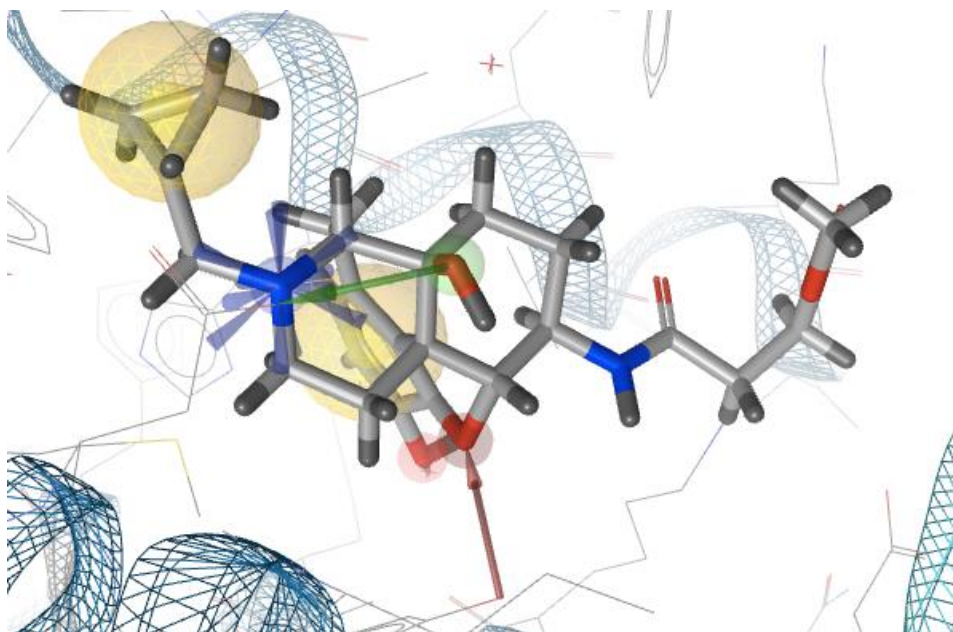


Figure 2.7: Structure of the mu opioid receptor BF0601 together with its pharmacophore and surrounding amino acids within the receptor site obtained using the 'Active View' in LigandScout® (Wolber, 2005).

2.4.2 Hit Molecule Screening using ZincPharmer®

ZincPharmer® (Koes, 2015) is an online software that was used to find compounds with electronic properties and spatial arrangement similar to the optimal conformer which was previously identified. Both consensus pharmacophores were read into this software.

The following filters were applied to the software to ensure that the molecules obtained would exhibit drug-like pharmacological, physicochemical and biological activity:

- i. Maximum Total Number of Hits: 300
- ii. Maximum Root Mean Squared Deviation (RMSD): 1
- iii. $1 \leq \text{Molecular Weight} \leq 300$
- iv. $1 \leq \text{Rotatable Bonds} \leq 5$

These filters were set to yield results from the three following databases:

- i. Zinc Purchasable (Last updated December 2014)
- ii. Zinc Drug Database (Last updated September 2014)
- iii. Zinc Natural Products (Last updated September 2014)

The JDC1300 / BU10119 consensus pharmacophore was read into ZincPharmer[®] (Koes, 2015). From all three databases listed above, a total of 641 hits were produced. The BF0601 / BU10119 consensus pharmacophore was also read into this online database and resulted in a total of 361 hits between all three databases. This resulted in a total of 1002 hits between both consensus pharmacophores.

2.4.3 Filtration of hits using Mona[®].

The hits obtained from ZincPharmer[®] (Koes, 2015) were then filtered using the programme MONA[®] (Hilbig & Rarey, 2015). This programme was used in order to filter the 1002 hits above into molecules that are in accordance to the Lipinski's Rule of 5 (Lipinski *et. al.*, 2015). When inputting the 1002 molecules, the programme automatically decreased these hits to 937, meaning that there were 65 molecules that were common for both consensus pharmacophores.

The limits used to filter the hit molecules are:

- i. $1 \leq \text{Hydrogen Donors} \leq 5$
- ii. $1 \leq \text{Hydrogen Acceptors} \leq 10$
- iii. $1 \leq \text{LogP} \leq 5$
- iv. $0 \leq \text{Molecular Weight} \leq 500$

The above filters produced a total of 371 Lipinski Compliant Molecules for the JDC1300 / BU10119 consensus pharmacophore, and 168 Lipinski Compliant Molecules for the BF0601 / BU10119 consensus pharmacophore. This means that there are a total of 539 Lipinski Compliant Molecules to be studied for their affinity to their respective protomols. The hit molecules were separately saved in *.mol2* format.

2.4.4 Generation of Protomols using Sybyl-X®

A protomol is the virtual Ligand Binding Pocket. The protomol represents the energetically unstable amino acids at the core of each receptor. A protomol was created for both the κ OR and the μ OR. This was done using the 'Surflex Simulation' function in Sybyl-X® (Ash *et. al*, 2010) based on the opioid receptor structures obtained from PDB 4DJH (Wu, 2012) and 4DKL (Manglik, 2012).

The 371 Lipinski Compliant Molecules obtained from the JDC1300 / BU10119 consensus pharmacophore were inputted into the protomol generated for the κ OR. Sybyl-X® (Ash *et. al*, 2010) then produced a table ranking these 371 molecules in order from highest affinity to lowest affinity to the protomol. This process was repeated for the 168 Lipinski Compliant Molecules obtained from the BF0601 / BU10119 consensus pharmacophore.

Through ranking the filtered molecules in order of affinity, the optimal conformers for each receptor could be identified. The optimal conformer showed the highest Ligand Binding Affinity to the protomols created. *006_BU10119.mol2* was identified as the optimal conformer for the μ OR (pdb 4DKL (Manglik, 2012)) while *011_BU10119.mol2* was identified as the optimal conformer for the κ OR (pdb 4DJH (Wu, 2012)).

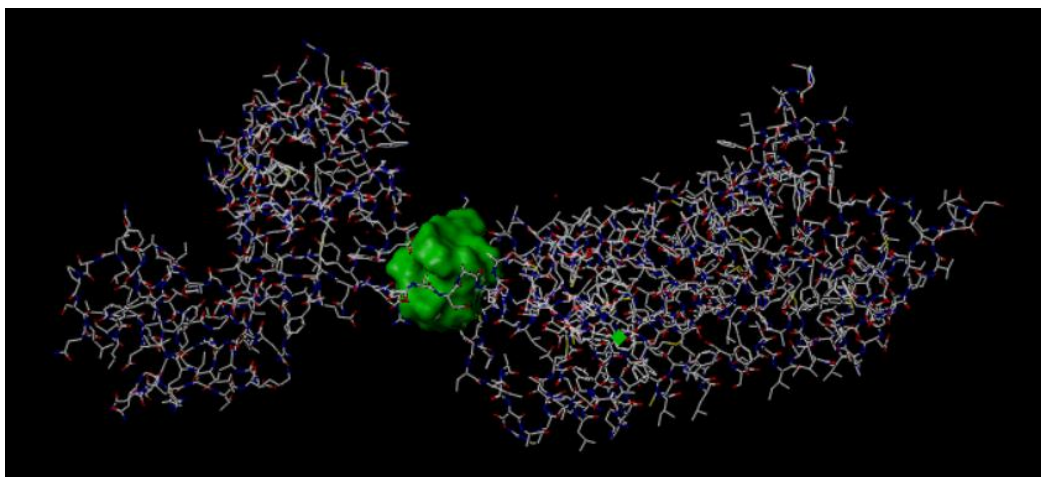


Figure 2.8: Structure of the kappa opioid receptor showing the protomol which represents the virtual ligand binding pocket created using the 'Surflex Simulation' function in Sybyl-X® (Ash *et. al*, 2010). The green area represents the protomol.

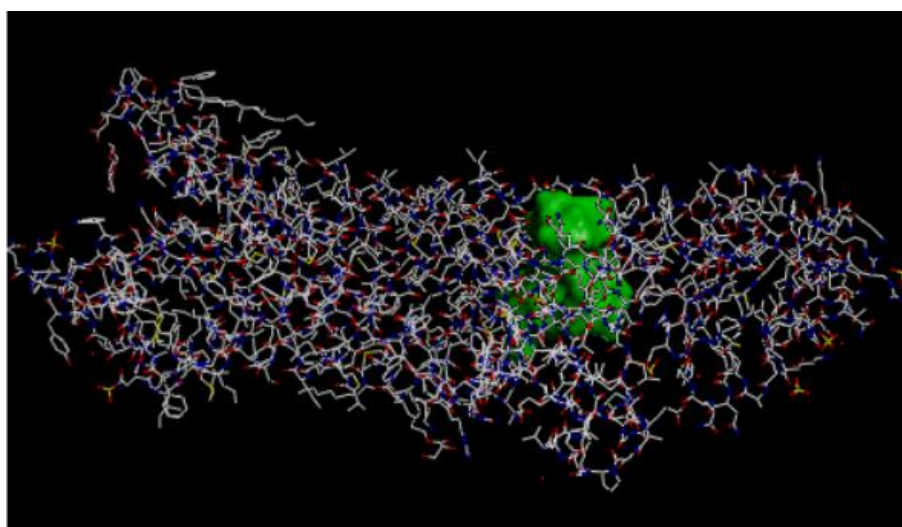


Figure 2.9: Structure of the mu opioid receptor showing the protomol which represents the virtual ligand binding pocket created using the 'Surflex Simulation' function in Sybyl-X® (Ash *et. al*, 2010). The green area represents the protomol.

2.5 *de novo* – Structure Based Drug Design

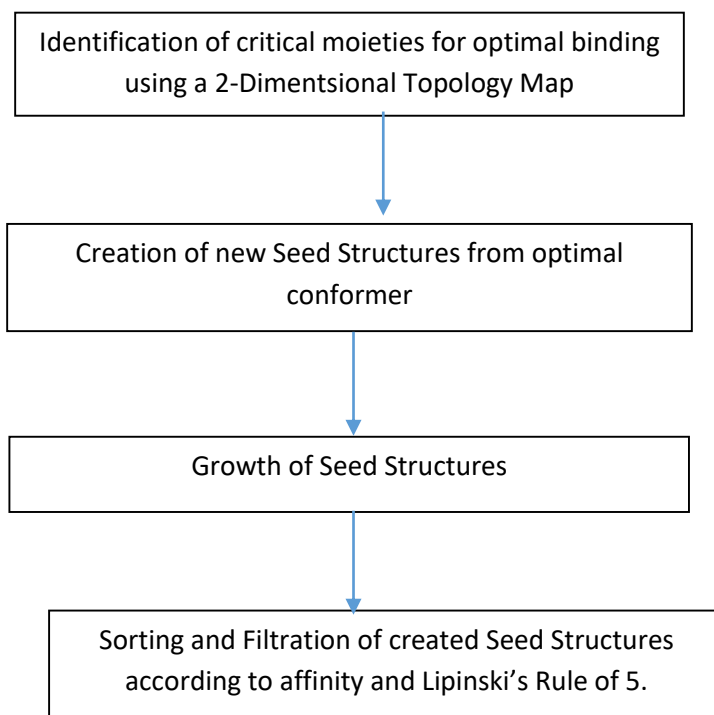


Figure 2.10: Outline of the Structure Based Drug Design Process

2.5.1 2-Dimensional Topology Map Generation

The molecules with the highest affinity obtained from the JDC1300 / BU10119 consensus pharmacophore docking were used to produce a 2-Dimensional Topology Map using PoseView® (Stierand & Rarey, 2010). These maps are used to view the critical interactions between the optimal conformer and its respective receptor. This step was repeated for both the κ OR and the μ OR.

2.5.2 Generation of Seed Molecules

The 2-Dimensional Topology Maps allowed for the identification of unfavourable atoms in the optimal conformer. Seed generation was primarily targeted at removing these unfavourable atoms, being instead replaced with an 'Special Hydrogen' atom (H.sp) that allows growth at that locus.

2.5.3 *de novo* Design

De Novo Design is a process which uses the receptor's three dimensional structure to model novel lead molecules by growing molecules into the 'POCKET' module of LigBuilder® (Yuan *et. al.*, 2011). This module was used to create a 3D map of the kOR Ligand Binding Pocket, together with a general pharmacophore. Both the Ligand Binding Pocket map and the general pharmacophore were coloured according to atom type with red sites denoting Hydrogen-bond donors, blue sites denoting Hydrogen-bond acceptors, and green sites denoting areas of hydrophobicity.

The 3D Ligand Binding Pocket map was recognised as the pharmacophore space within which molecular growth could be sustained. To this end, the previously modelled seed structures were docked into this modelled space and molecular growth was sustained using the previously designated H.spc as anchorage points. *De novo* molecular growth was carried out using 2 separate algorithms in LigBuilder® - 'GROW' and 'LINK' (Yuan *et. al.*, 2011). The grow algorithm allowed uni-directional growth, while the Link algorithm was used to join 2 separate seed fragments.

A total of 6 Seed Structures were created using *011_BU10119.mol2*- the optimal conformer for the kOR during Virtual Screening.

The Grow and Link algorithms produced *de novo* molecular cohorts which subsequently organised using the 'PROCESS' module of Ligbuilder® (Yuan *et. al.*, 2011). Here, the new structures were classified for each modelled seed structure, into families based on pharmacophoric similarity. Within each family, molecules were ranked according to affinity for the respective receptor. The process output also included allied molecular

information such as general formula, ClogP, molecular weight and synthetic feasibility. There was no information regarding the Hydrogen-bond donor and Hydrogen-bond acceptor count for the newly designed molecules.

2.5.4 Sorting and Filtering Ligands Obtained

The information as supplied by the 'PROCESS' module of LigBuilder® (Yuan *et. al.*, 2011) guided the methodology through which the de novo designed molecules were filtered for Lipinski rule compliance. The first filtration stage utilised the information given by the 'PROCESS' module of LigBuilder® (Yuan *et. al.*, 2011). This means that only molecules complying with Lipinski's Rules from a molecular weight and ClogP perspective were retained (Lipinski *et. al.*, 2015).

In a second filtration process the molecular cohort that survived the first filtration was read into Biovia® Draw (Dassault Systèmes BIOVIA, 2001), where they were subjected to a Hydrogen-bond donor and Hydrogen-bond acceptor count. The molecules complying with Lipinski's rules from this perspective formed the molecular cohort that was accepted for subsequent analysis (Lipinski *et. al.*, 2015).

Chapter 3

Results

Chapter 3: Results

3.1 Results obtained from Virtual Screening

3.1.1 Creation of Consensus Pharmacophores

A consensus pharmacophore is a three dimensional arrangement of structures showing the critical features of ligand molecules required to successfully interact with the target receptor at its Ligand Binding Site (Dror *et. al.*, 2010).



Figure 3.1: Structure of the consensus pharmacophore for JDC1300 with the optimal BU10119 conformers for the kappa opioid receptor obtained using the 'Alignment' tab in LigandScout® (Wolber, 2005). The yellow areas represent hydrophobic interactions.

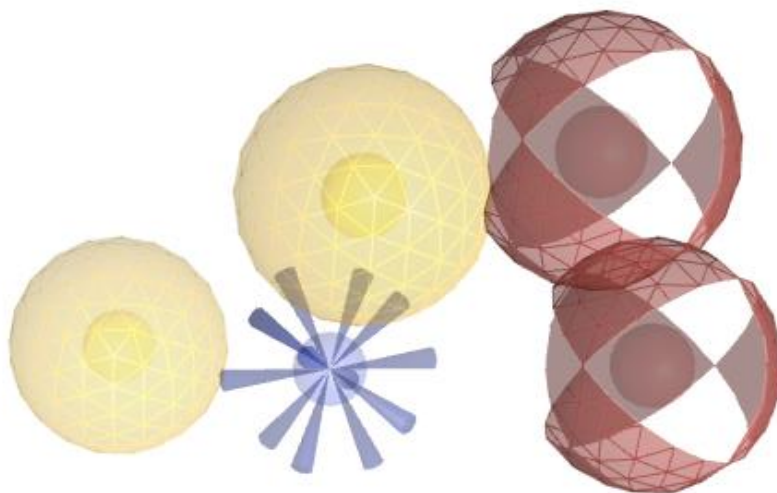


Figure 3.2: Structure of the consensus pharmacophore for BF0601 with the optimal BU10119 conformers for the mu opioid receptor obtained using the ‘Alignment’ tab in LigandScout® (Wolber, 2005). The yellow areas represent hydrophobic interactions, blue area representing a positive ionisable area while the red part represents hydrogen bond acceptors.

3.1.2 Calculation of Ligand Affinity to Ligand Binding Pocket

The Lipinski Rule compliant ligands obtained from ZINCPharmer® were successfully docked into the respective protomol created. Each ligand was ranked in order of affinity, as seen in Table 3.1 and Table 3.2 below, for the kOR and μ OR respectively (Lipinski *et. al.*, 2015).

Table 3.1: The two optimal ligands obtained through the Virtual Screening Approach for the kOR

ZINCPharmer® ligand ID	Total score
ZINC00118327	5.35
ZINC70666627	4.95

Table 3.2: The two optimal ligands obtained through the Virtual Screening Approach for the μ OR

ZINCPharmer® ligand ID	Total score
ZINC93209494	6.95
ZINC48253928	5.12

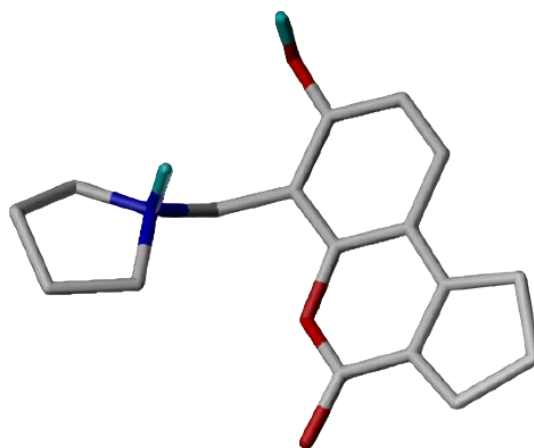


Figure 3.3: Figure showing ZINC00118327, the optimal conformer for the κ OR. Rendered using BIOVIA Discovery Studio (Dassault Systèmes BIOVIA, 2015).

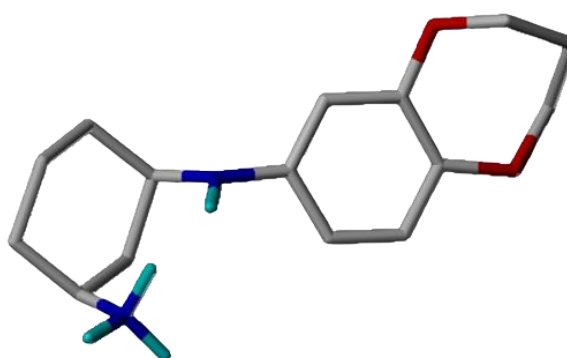


Figure 3.4: Figure showing ZINC93209494, the optimal conformer for the μ OR. Rendered using BIOVIA Discovery Studio (Dassault Systèmes BIOVIA, 2015).

3.2 Results obtained from *de novo* modelling

3.2.1 Structure Activity Relationship

Two-Dimensional Topology Maps were created to indicate the critical interactions between the optimal molecule and its respective ligand binding pocket. These maps were used as a guide in the seed creation process, removing the atoms resulting in unfavourable interactions, while keeping the atoms with critical interactions with the ligand binding pocket.

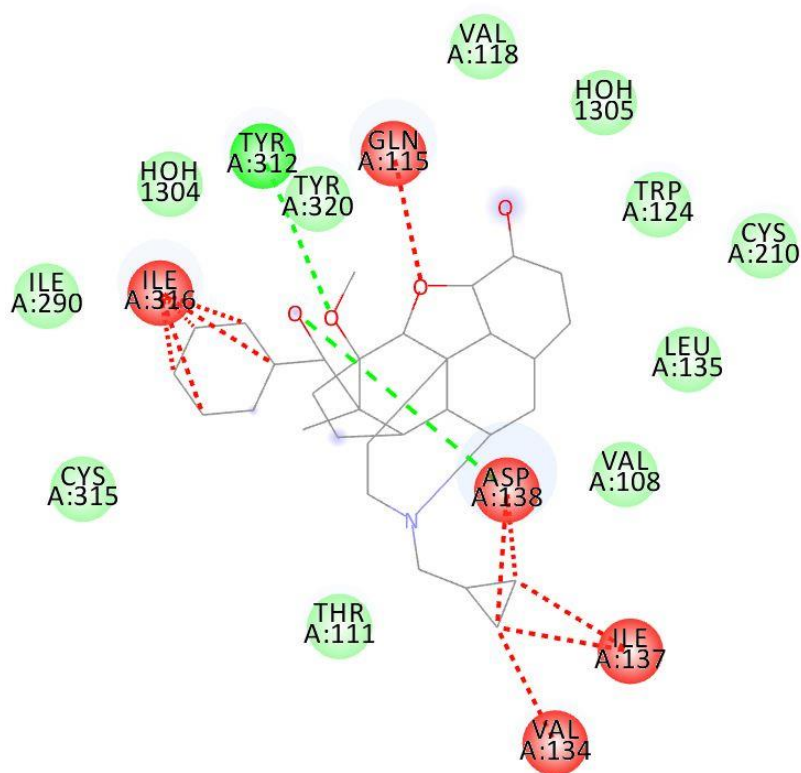


Figure 3.5: 2-Dimensional Topology Map created using the optimal conformer for the kOR (*011_BU10119.mol2*) and the kOR Ligand Binding Pocket. The red circles indicate unfavourable interactions, while the green circles indicate the critical interactions. Rendered using PoseView® (Steirand & Percy, 2010).

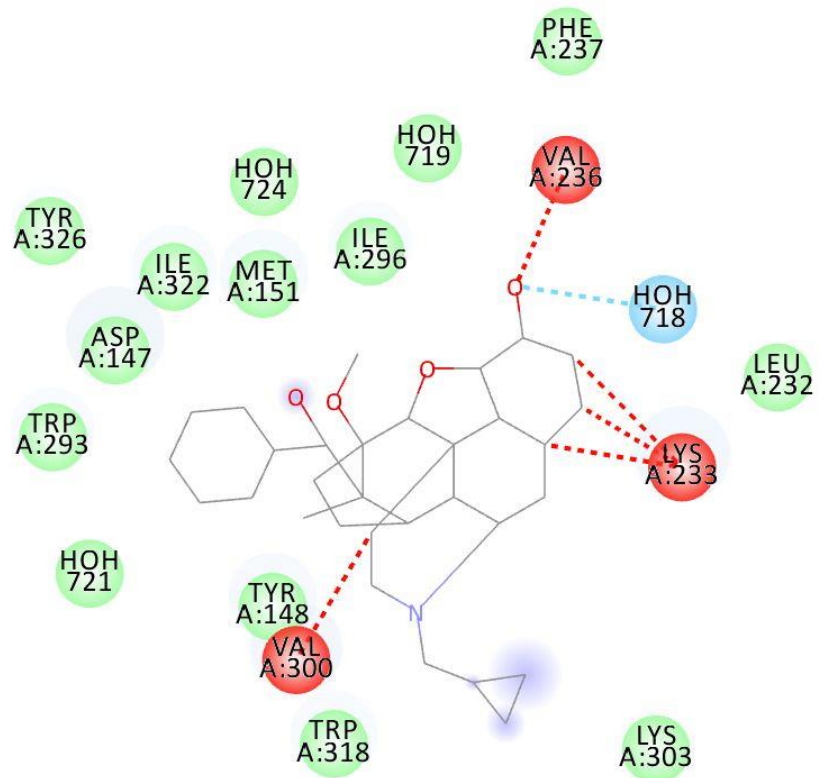


Figure 3.6: 2-Dimensional Topology Map created using the optimal conformer for the μ OR (*006_BU10119.mol2*) and the μ OR Ligand Binding Pocket. The red circles indicate unfavourable interactions, the green circles indicate the critical interactions while the blue circle indicates a hydrophobic interaction. Rendered using PoseView® (Stierand & Percy, 2010).

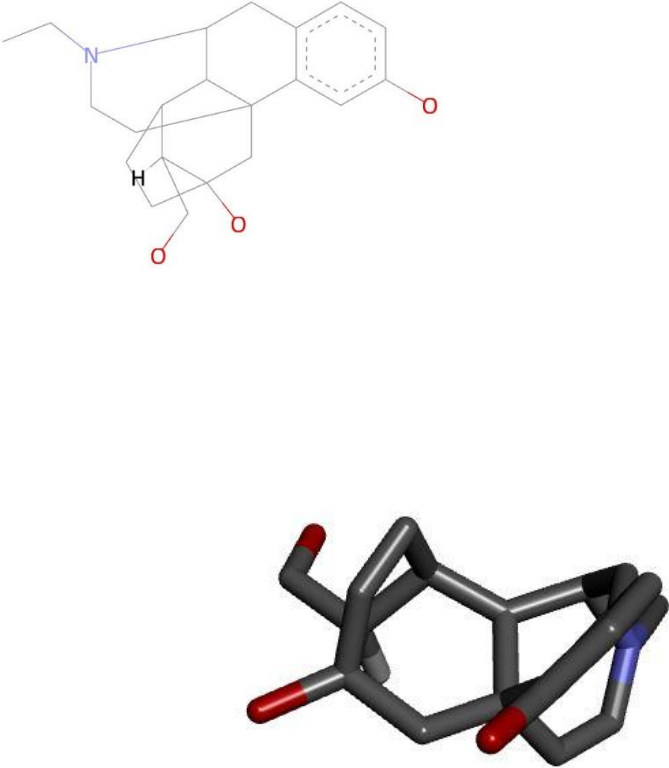
3.2.2 Seeds generated using *de novo* design

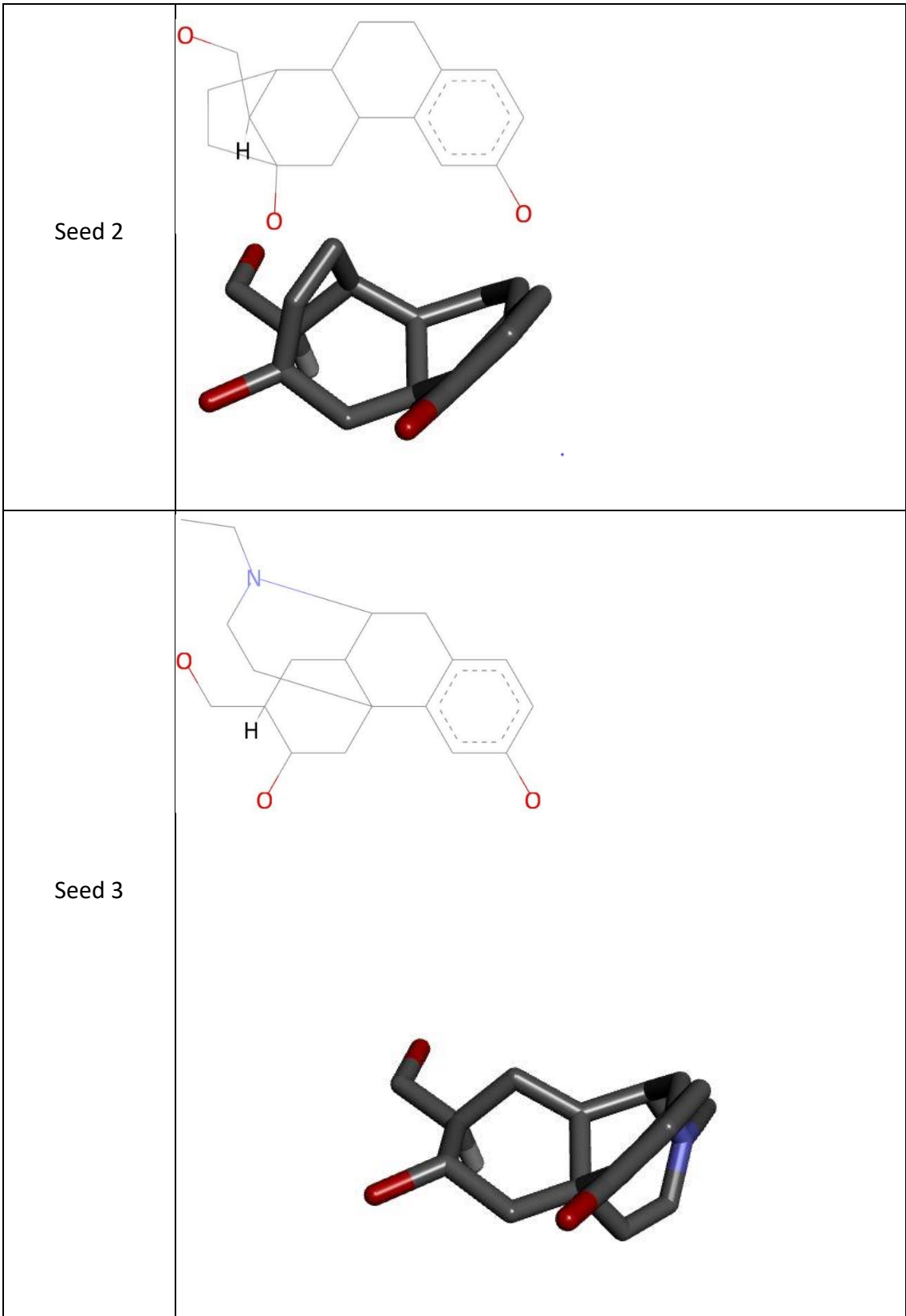
The advantages of the *de novo* Design Approach include the fact that the ligand binding pocket was shown to be bioactive and that the seed structures were modelled to incorporate the atoms that are most critical to binding, and thus will result in high affinity molecules. However, the set back of the *de novo* Approach is that these seed structures are user created, and thus there is less structural innovation when compared to the Virtual Screening Approach.

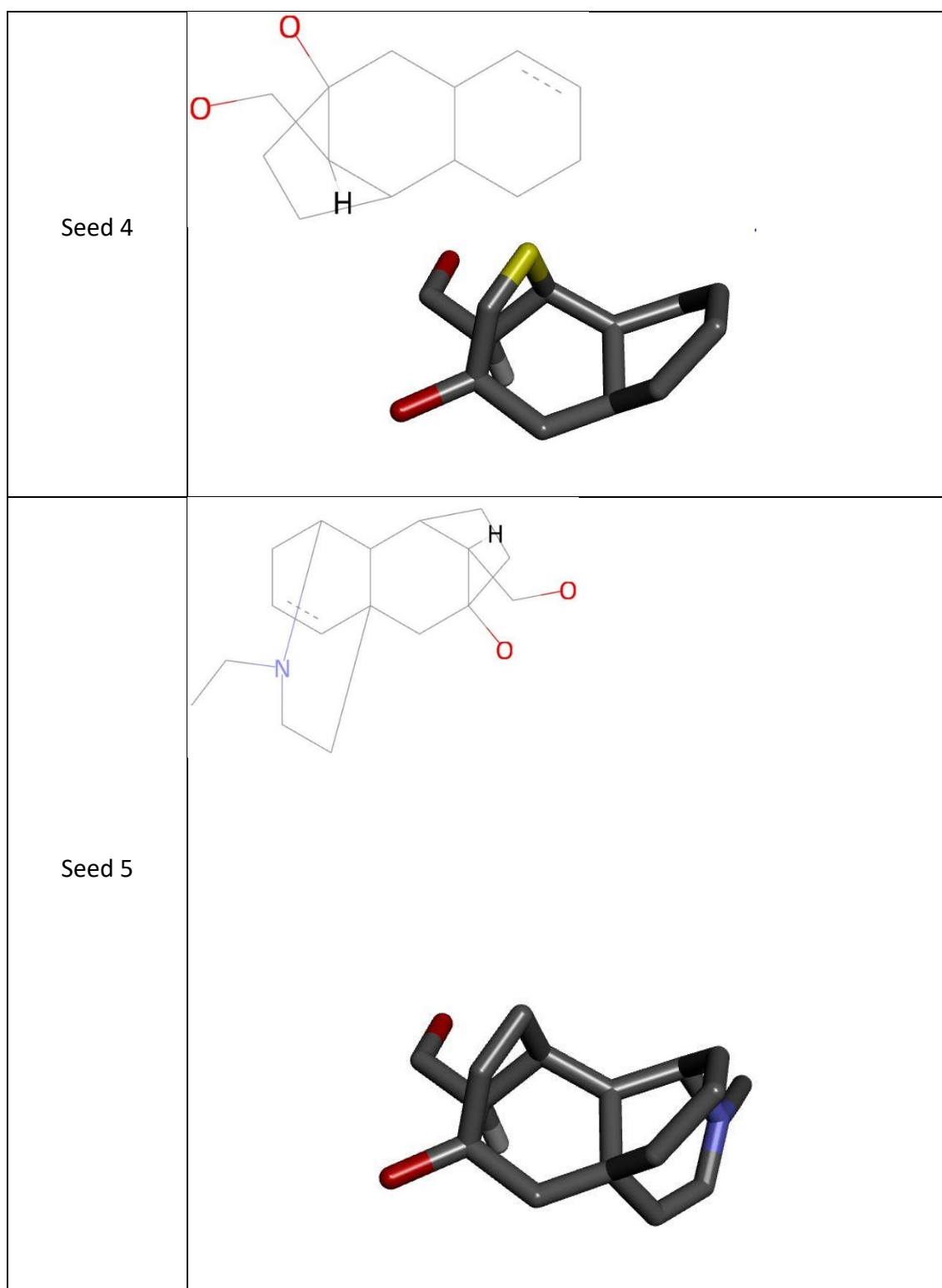
Through the *de novo* Approach, a total of 6 seeds were created for the kOR. The 6 seeds were created using SYBYL-X[®] (Ash *et. al*, 2010) through guidance of the Topology Map created earlier. Atoms resulting in unfavourable interactions were removed from the optimal conformer, inserting the '*H.spc*' atom as a locus for the 'GROW' and 'LINK' function. The 6 seeds created were described as 6 different pharmacophores (P1) that were eventually modified using the 'GROW' function.

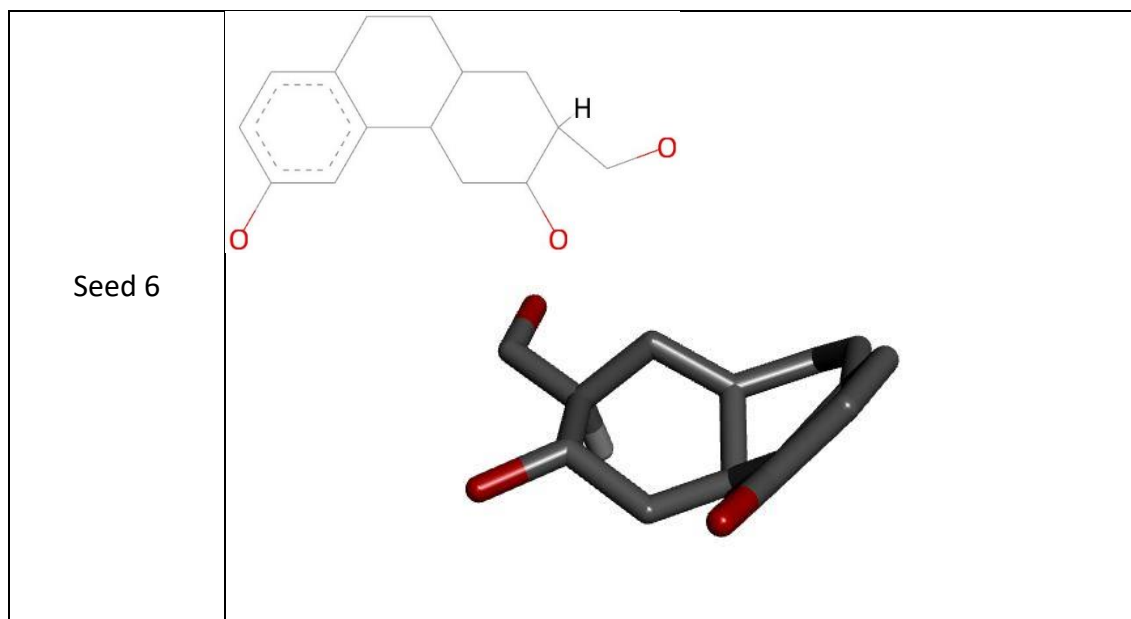
The differing structures of the seeds created can be viewed in Table 3.3 on the next page.

Table 3.3: Table showing the 2-Dimensional and 3-Dimensional structures of the seeds created from 011_BU10119.mol2 as the optimal conformer for the κ OR. Rendered using BIOVIA Discovery Studio (Dassault Systèmes BIOVIA, 2015).

Seed Number	Structure
Seed 1	 <p>The image displays two representations of the chemical structure for Seed 1. The upper representation is a 2D skeletal structure showing a complex polycyclic system. It features a central bicyclic core with a nitrogen atom (blue) and a hydrogen atom (white) attached. A phenyl ring is fused to the system, with a carbonyl group (red oxygen) at the para position. Another carbonyl group is attached to the bicyclic core. The lower representation is a 3D ball-and-stick model of the same molecule, with carbon atoms in grey, oxygen atoms in red, and the nitrogen atom in blue.</p>







These 200 molecules were readily split into families, and through a filtering process, only Lipinski Compliant Molecules were kept (Lipinski *et. al.*, 2015). These molecules were then described as Pharmacophores 2 (P2). Unlike the creation of P1, where this was user driven using the programme SYBYL-X[®] (Ash *et. al.*, 2010), the creation of P2 was computer generated. The Lipinski Rule Compliant Molecules (Lipinski *et. al.*, 2015) were then sorted in order of descending affinity to the Ligand Binding Pocket.

For Seed 1, a total of 5 families were created, with molecule 7 from family 2 having the highest affinity and molecule 33 from family 4 having the lowest affinity.

For Seed 2, a total of 4 families were created, with molecule 29 from family 2 having the highest affinity and molecule 78 from family 2 having the lowest affinity.

For Seed 3, 1 family was created, with molecule 20 being the only resulting molecule after filtering.

For Seed 4, a total of 9 families were created, with molecule 34 from family 2 having the highest affinity and molecule 153 from family 5 having the lowest affinity.

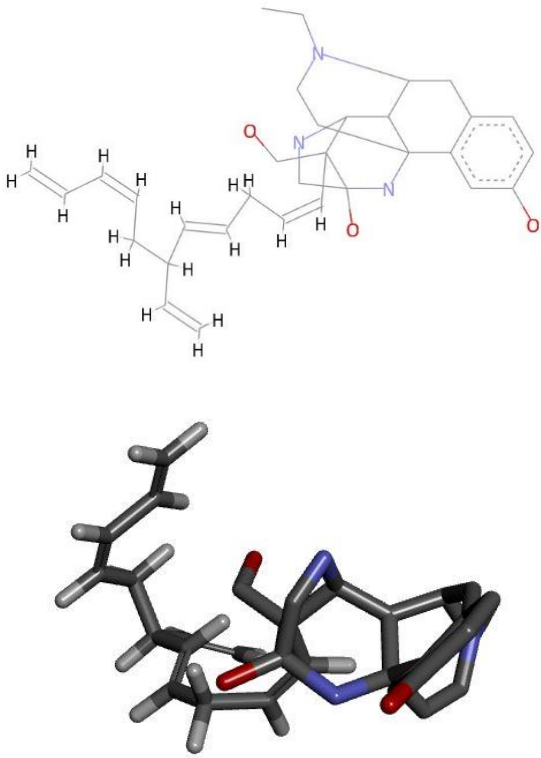
For Seed 5, a total of 6 families were created, with molecule 39 from family 4 having the highest affinity and molecule 53 from family 4 having the lowest affinity.

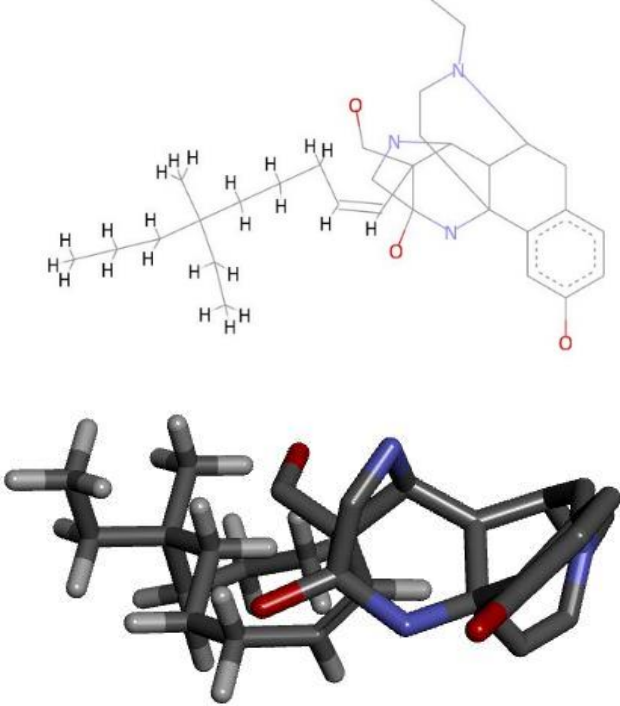
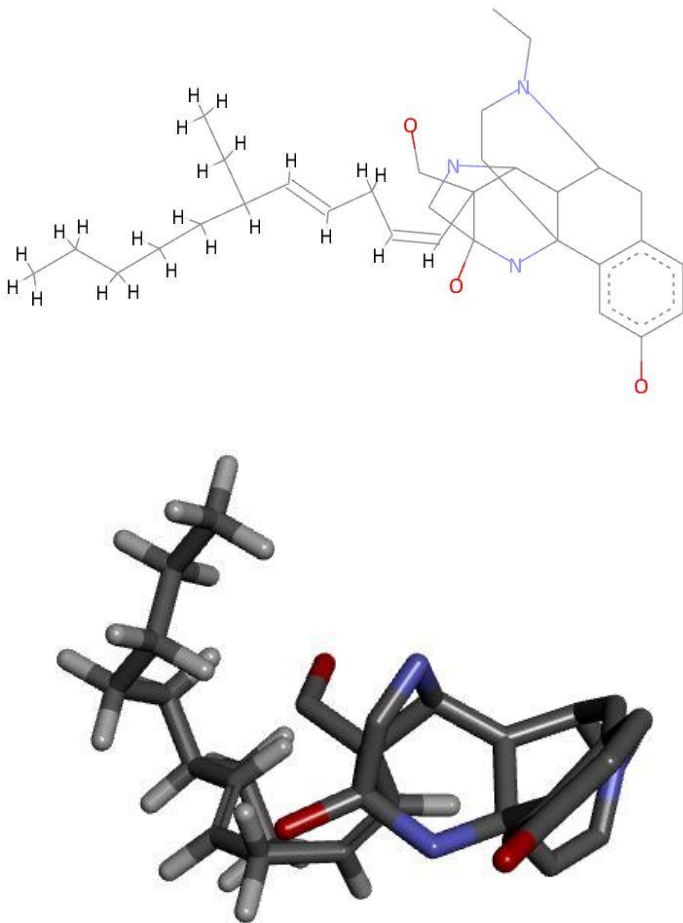
For Seed 6, a total of 9 families were created, with molecule 3 from family 1 having the highest affinity and molecule 86 from family 9 having the lowest affinity.

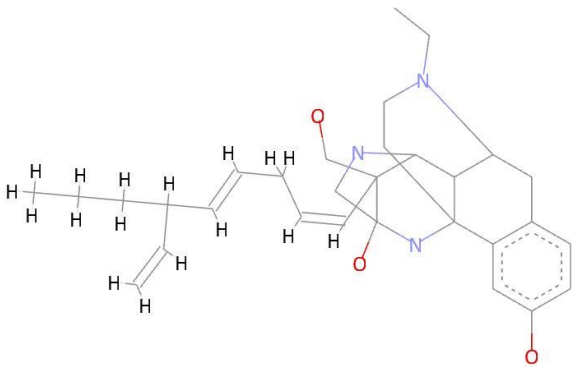
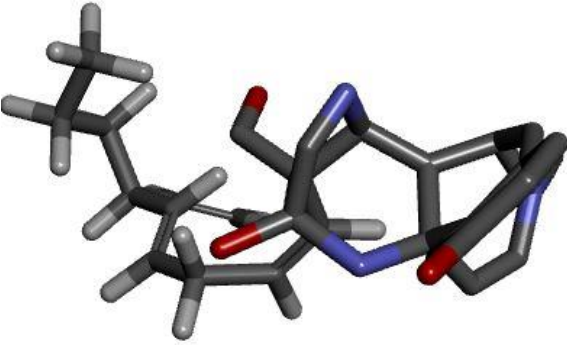
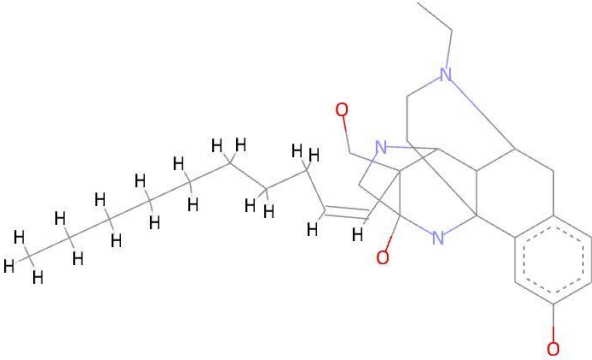
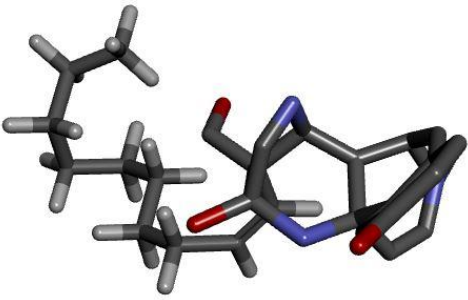
The filtered results obtained for Seeds 1 through 6 from the *de novo* Approach are presented in Appendix A to Appendix F.

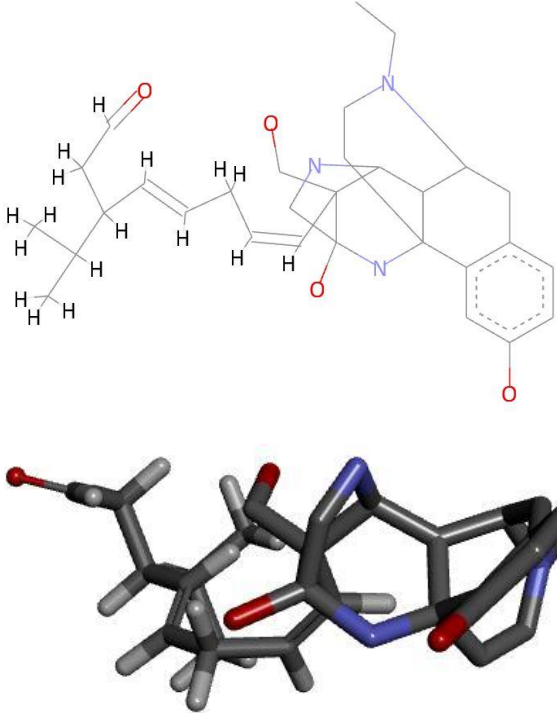
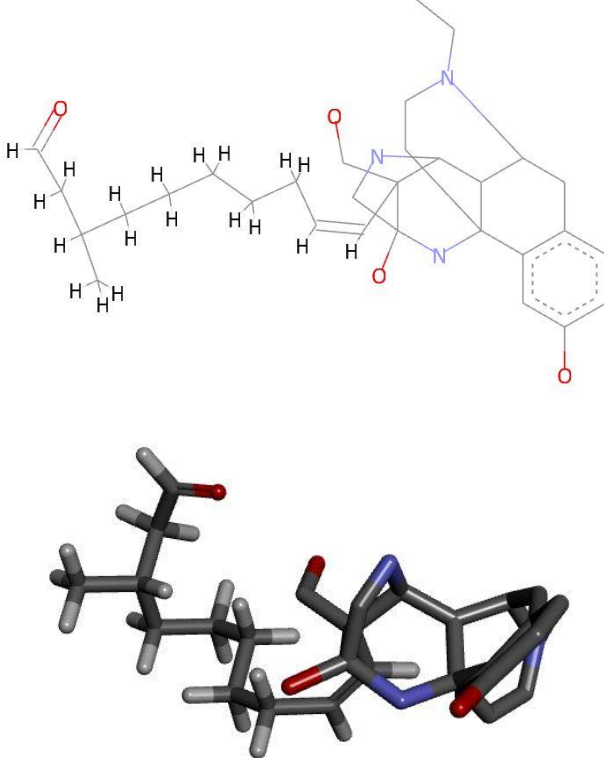
The top five molecules with the highest affinity and two molecules with the lowest affinity to the ligand binding pocket for each seed are presented in Table 3.4 on the next page.

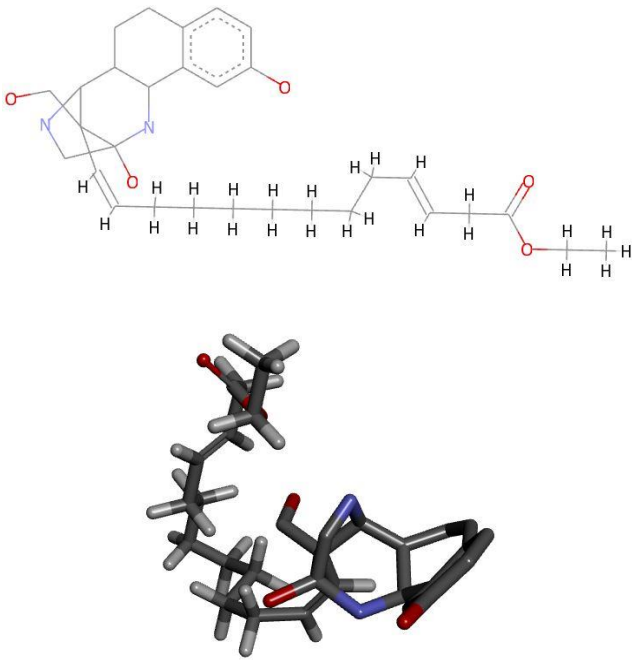
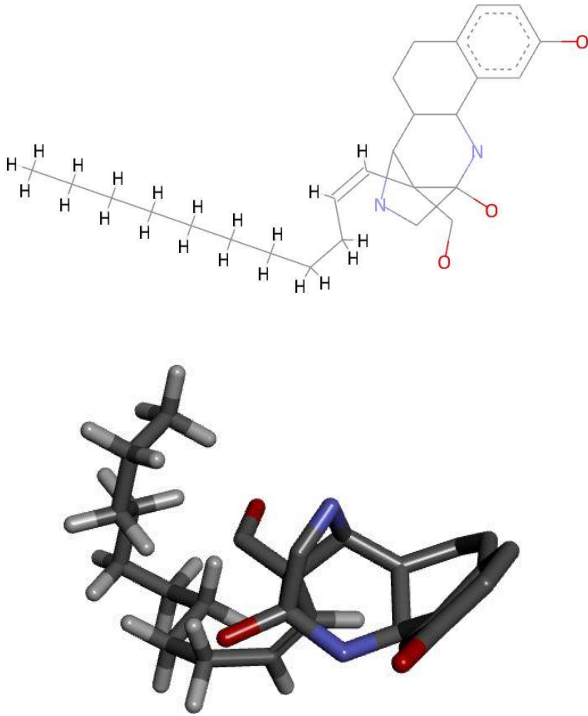
Table 3.4: Table showing the top five molecules with the highest affinity and two molecules with the lowest affinity to the ligand binding pocket of the kOR for each seed and their properties. Rendered using BIOVIA Discovery Studio® (Dassault Systèmes BIOVIA, 2015).

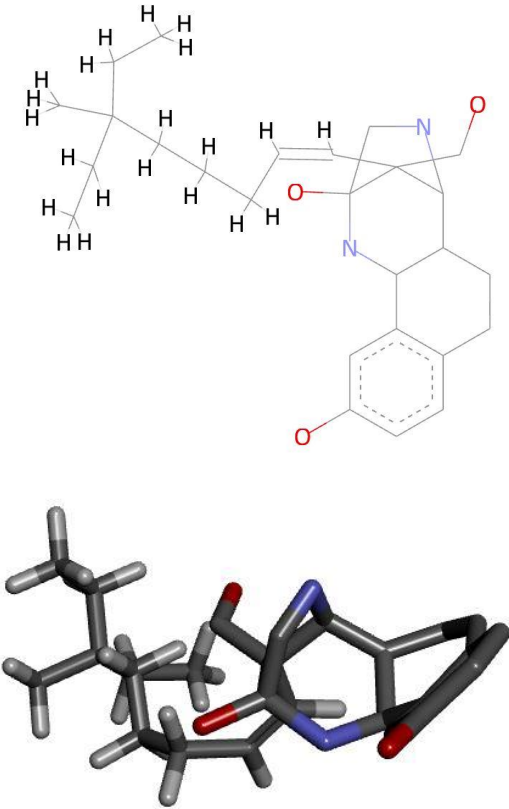
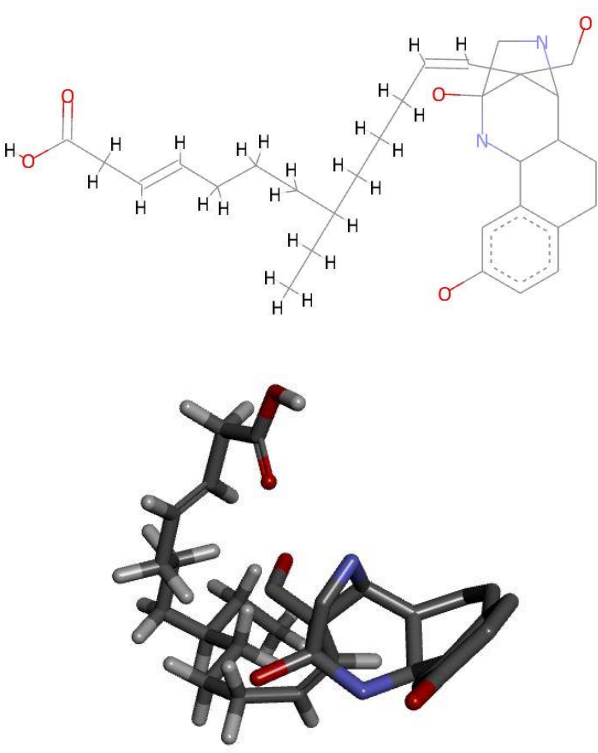
Seed Number	2-D and 3-D Structures	Properties
Seed 1	 <p data-bbox="683 1644 922 1675">Family 2 Molecule 7</p>	<p data-bbox="1206 1088 1426 1155">Molecular weight: 491</p> <p data-bbox="1254 1196 1378 1227">LogP: 3.88</p> <p data-bbox="1257 1263 1375 1294">pKd: 9.62</p> <p data-bbox="1276 1330 1356 1361">HBA: 6</p> <p data-bbox="1276 1397 1356 1429">HBD: 5</p>

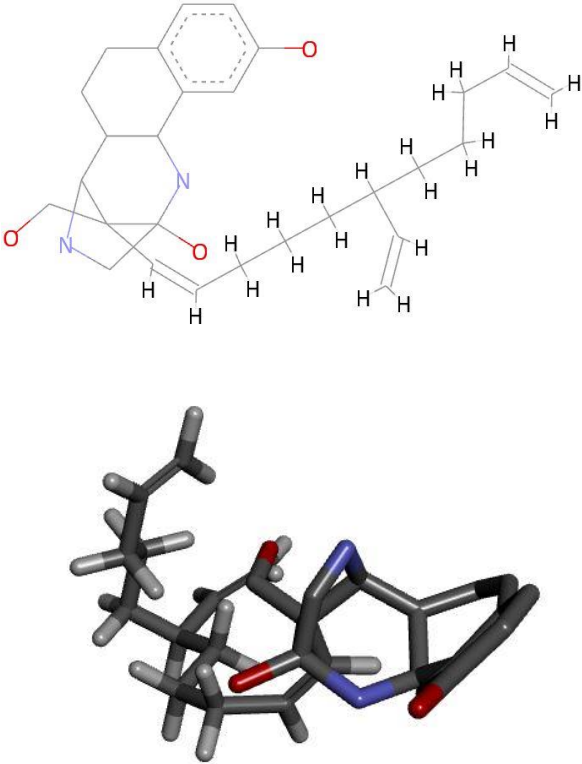
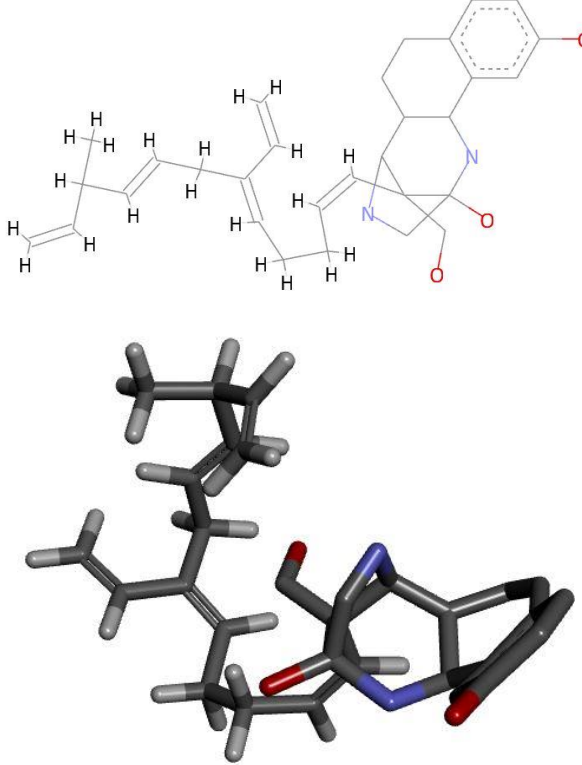
<p>Seed 1</p>	 <p>Family 4 Molecule 26</p>	<p>Molecular weight: 485</p> <p>LogP: 4.75</p> <p>pKd: 9.49</p> <p>HBA: 6</p> <p>HBD: 5</p>
<p>Seed 1</p>	 <p>Family 2 Molecule 10</p>	<p>Molecular weight: 497</p> <p>LogP: 4.95</p> <p>pKd: 9.23</p> <p>HBA: 6</p> <p>HBD: 5</p>

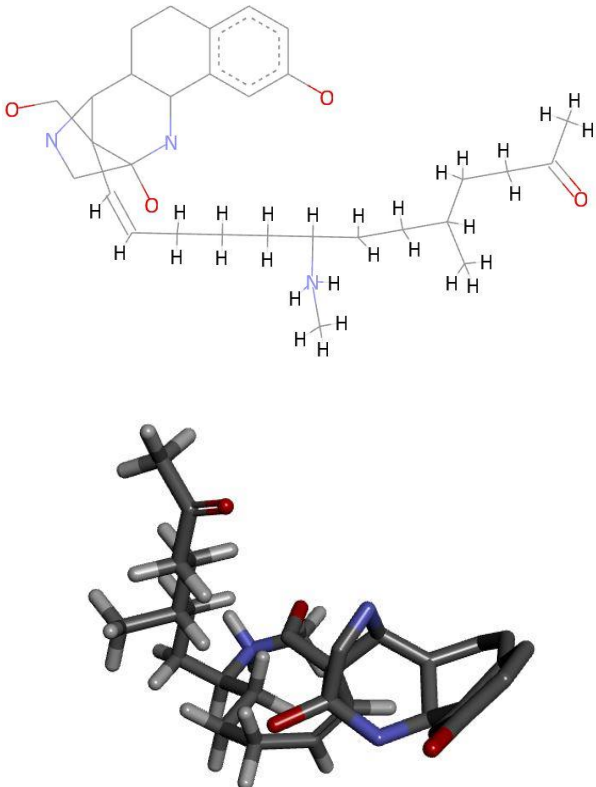
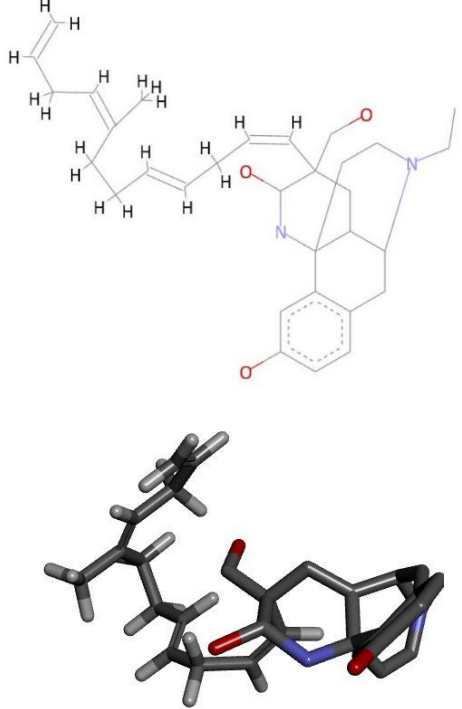
<p>Seed 1</p>	 <p>Family 2 Molecule 11</p> 	<p>Molecular weight: 467</p> <p>LogP: 3.77</p> <p>pKd: 9.23</p> <p>HBA: 6</p> <p>HBD: 5</p>
<p>Seed 1</p>	 <p>Family 4 Molecule 29</p> 	<p>Molecular weight: 457</p> <p>LogP: 4.9</p> <p>pKd: 8.51</p> <p>HBA: 6</p> <p>HBD: 5</p>

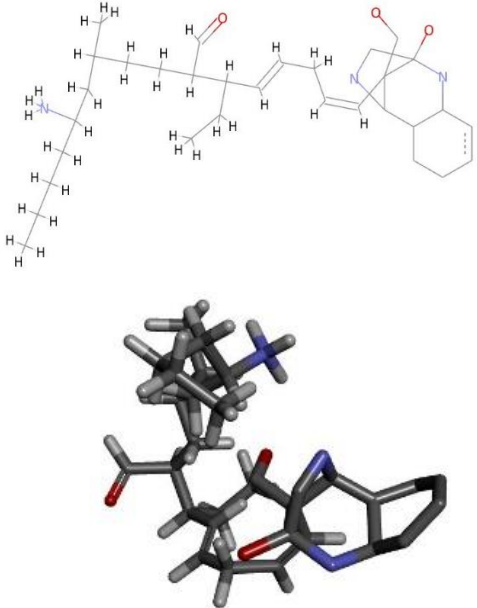
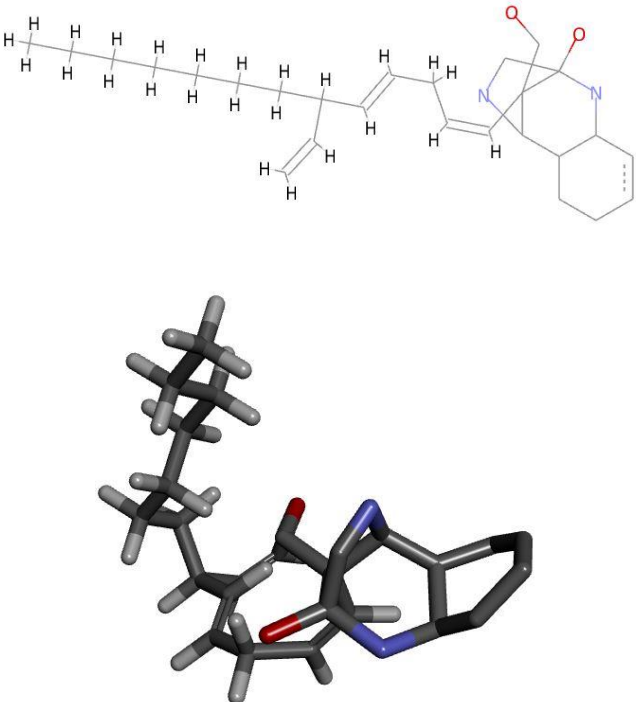
<p>Seed 1</p>	 <p>Family 2 Molecule 16</p>	<p>Molecular weight: 483</p> <p>LogP: 3.56</p> <p>pKd: 6.82</p> <p>HBA: 7</p> <p>HBD: 6</p>
<p>Seed 1</p>	 <p>Family 4 Molecule 33</p>	<p>Molecular weight: 485</p> <p>LogP: 3.95</p> <p>pKd: 6.38</p> <p>HBA: 7</p> <p>HBD: 5</p>

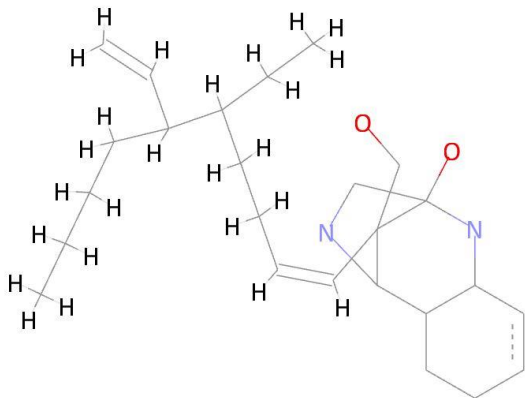
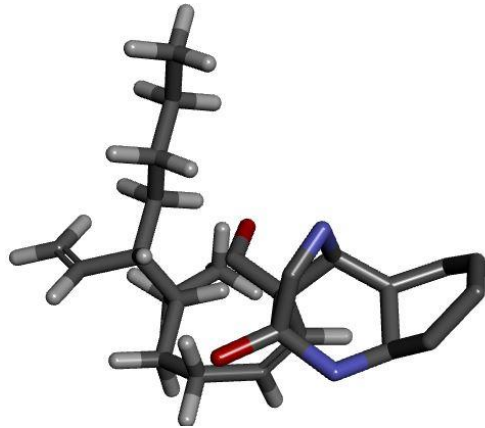
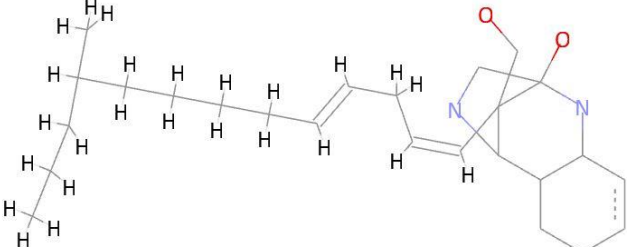
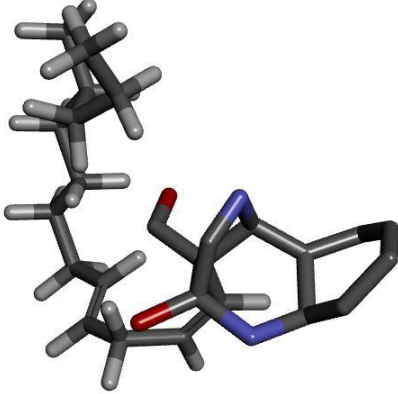
Seed Number	2-D and 3-D Structures	Properties
Seed 2	 <p>The 2-D structure shows a complex polycyclic system with a benzene ring substituted with a hydroxyl group, fused to a six-membered ring, which is further fused to a bicyclic nitrogen-containing system. A long alkyl chain is attached to the nitrogen-containing system, ending in a methyl group. The 3-D ball-and-stick model shows the spatial arrangement of atoms, with carbon in grey, hydrogen in white, oxygen in red, and nitrogen in blue.</p> <p>Family 2 Molecule 29</p>	<p>Molecular weight: 493</p> <p>LogP: 4.52</p> <p>pKd: 9.99</p> <p>HBA: 7</p> <p>HBD: 5</p>
Seed 2	 <p>The 2-D structure shows a complex polycyclic system similar to Molecule 29, but with a different ring fusion pattern. It features a benzene ring with a hydroxyl group, fused to a six-membered ring, which is further fused to a bicyclic nitrogen-containing system. A long alkyl chain is attached to the nitrogen-containing system, ending in a methyl group. The 3-D ball-and-stick model shows the spatial arrangement of atoms, with carbon in grey, hydrogen in white, oxygen in red, and nitrogen in blue.</p> <p>Family 2 Molecule 30</p>	<p>Molecular weight: 409</p> <p>LogP: 4.62</p> <p>pKd: 9.99</p> <p>HBA: 5</p> <p>HBD: 5</p>

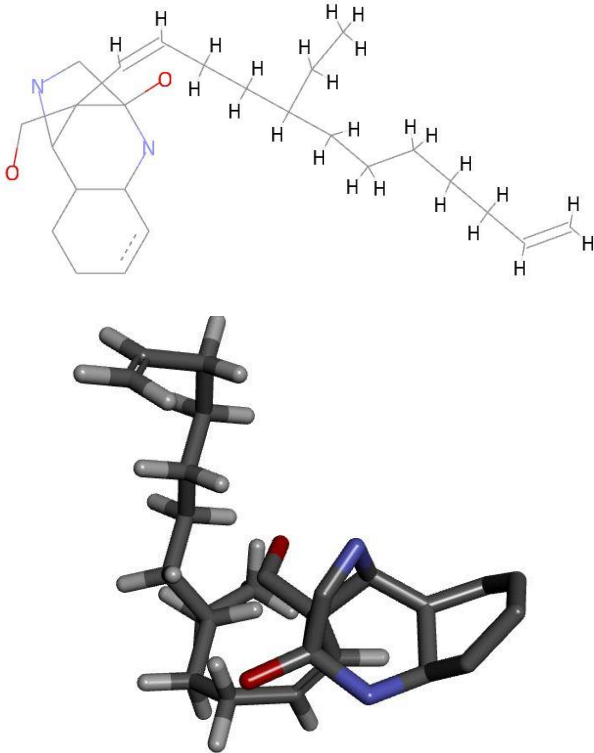
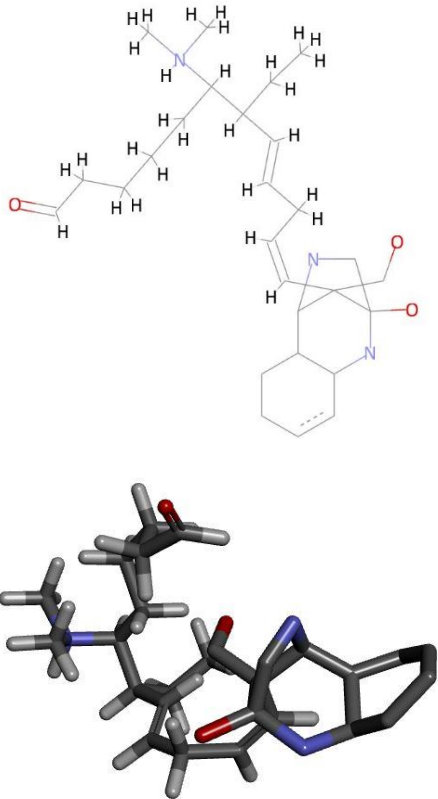
Seed 2	 <p>The image shows two representations of Family 3 Molecule 79. The top representation is a 2D skeletal structure with a complex polycyclic core, including a benzene ring with a chlorine atom at the para position, a fused six-membered ring, and a bicyclic nitrogen-containing system. A long aliphatic chain is attached to the nitrogen-containing system. The bottom representation is a 3D ball-and-stick model of the same molecule, showing the spatial arrangement of atoms.</p> <p>Family 3 Molecule 79</p>	<p>Molecular weight: 409</p> <p>LogP: 4.6</p> <p>pKd: 9.96</p> <p>HBA: 5</p> <p>HBD: 5</p>
Seed 2	 <p>The image shows two representations of Family 2 Molecule 35. The top representation is a 2D skeletal structure, similar to Family 3 Molecule 79 but with a different aliphatic chain. The bottom representation is a 3D ball-and-stick model of the same molecule.</p> <p>Family 2 Molecule 35</p>	<p>Molecular weight: 493</p> <p>LogP: 4.64</p> <p>pKd: 9.95</p> <p>HBA: 7</p> <p>HBD: 6</p>

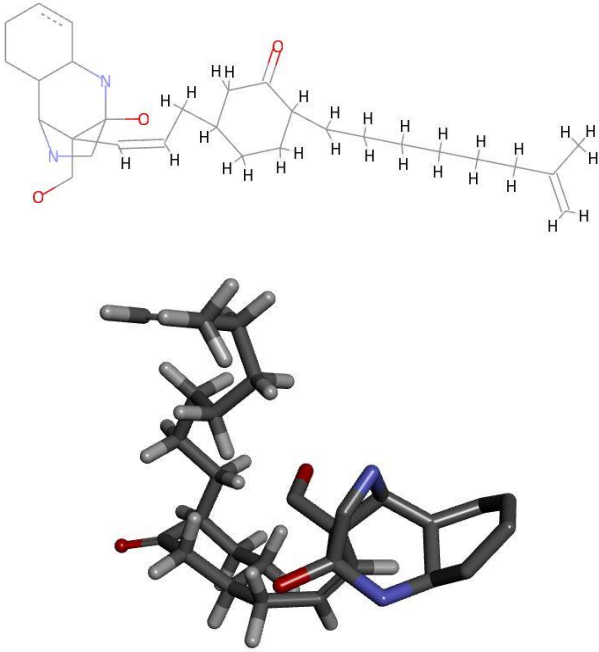
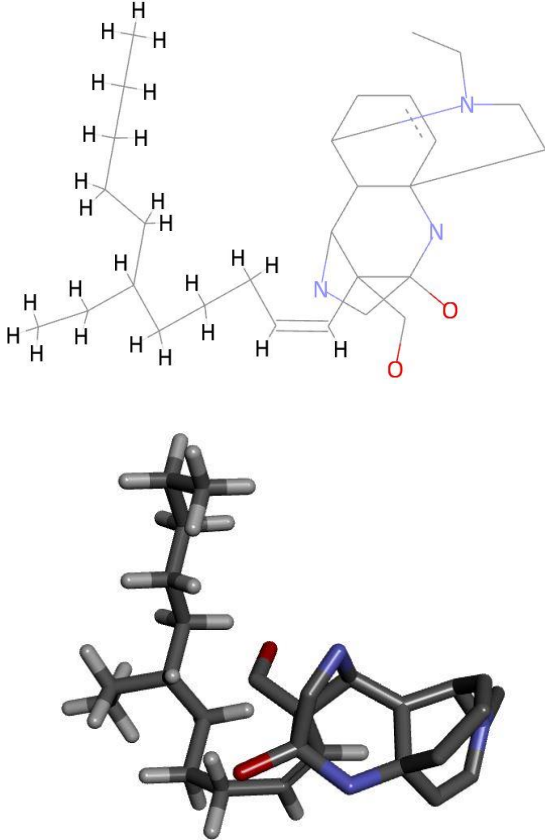
Seed 2	 <p>The image shows two representations of Family 2 Molecule 39. The top representation is a 2D chemical structure with a complex polycyclic core containing a nitrogen atom (blue) and two oxygen atoms (red). It features a benzene ring with a dashed circle and a hydroxyl group (-OH) at the para position. A long, branched aliphatic chain with multiple double bonds is attached to the core. The bottom representation is a 3D ball-and-stick model of the same molecule, showing the spatial arrangement of atoms.</p> <p>Family 2 Molecule 39</p>	<p>Molecular weight: 433</p> <p>LogP: 4.76</p> <p>pKd: 9.75</p> <p>HBA: 6</p> <p>HBD: 6</p>
Seed 2	 <p>The image shows two representations of Family 2 Molecule 76. The top representation is a 2D chemical structure similar to Molecule 39, but with a different aliphatic chain. The bottom representation is a 3D ball-and-stick model.</p> <p>Family 2 Molecule 76</p>	<p>Molecular weight: 481</p> <p>LogP: 3.09</p> <p>pKd: 6</p> <p>HBA: 7</p> <p>HBD: 5</p>

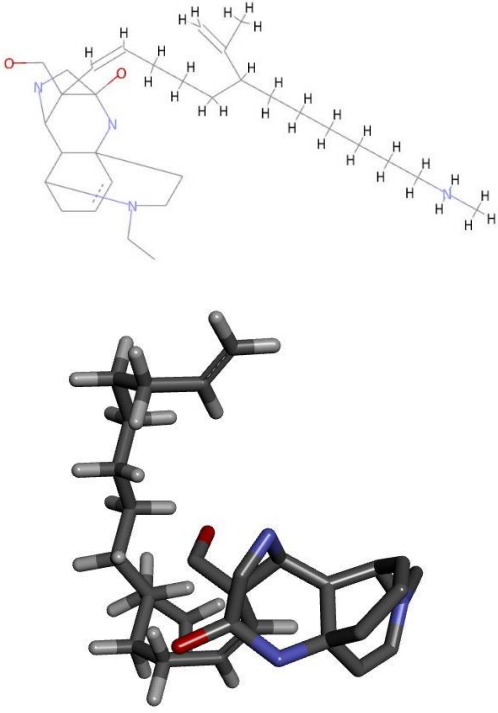
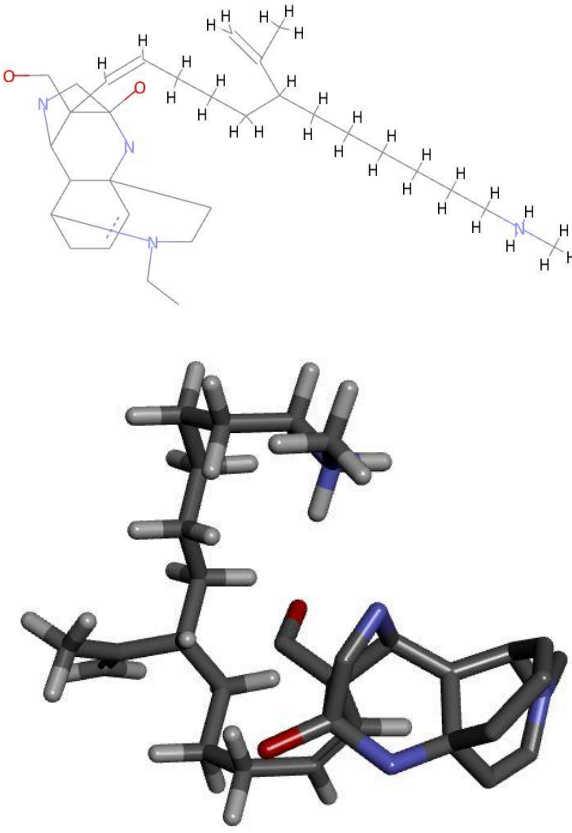
Seed 2	 <p>Family 2 Molecule 78</p>	<p>Molecular weight: 495</p> <p>LogP: 3.6</p> <p>pKd: 5.42</p> <p>HBA: 6</p> <p>HBD: 6</p>
Seed Number	2-D and 3-D Structures	Properties
Seed 3	 <p>Family 1 Molecule 20</p>	<p>Molecular weight: 467</p> <p>LogP: 4.74</p> <p>pKd: 8.11</p> <p>HBA: 5</p> <p>HBD: 4</p>

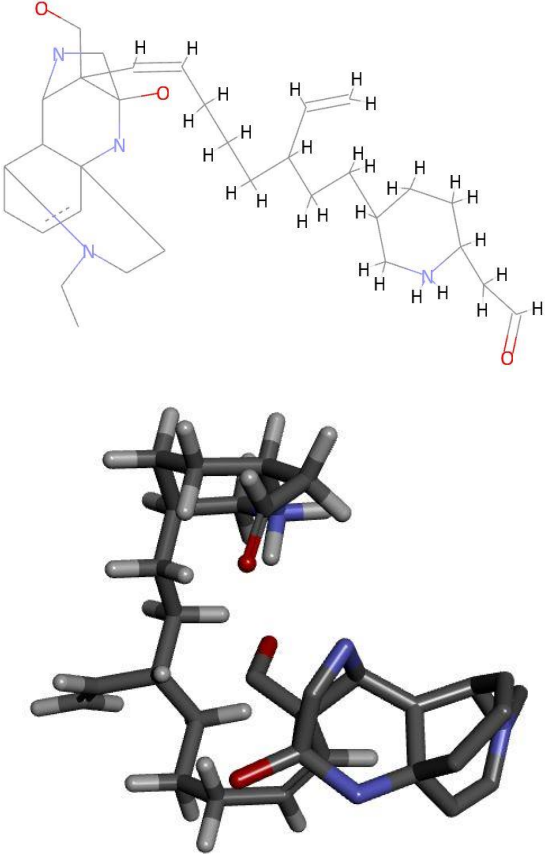
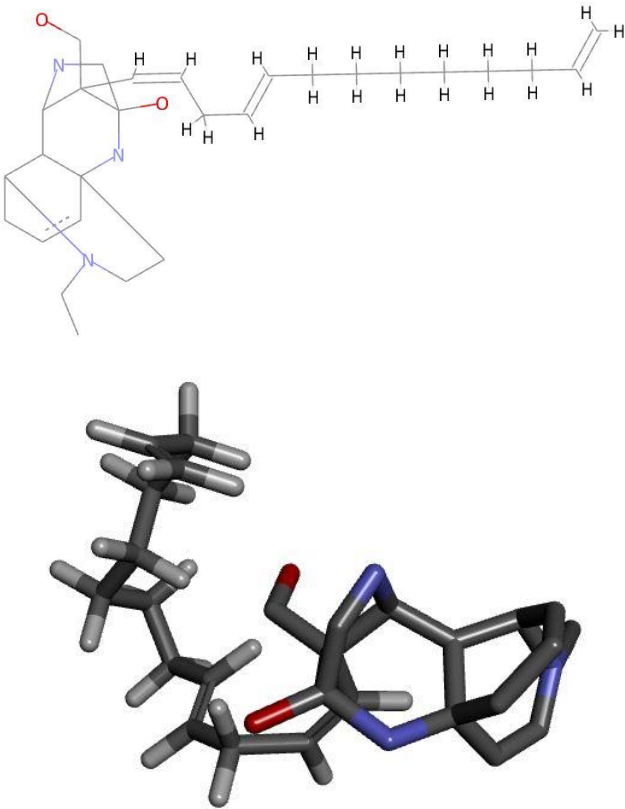
Seed Number	2-D and 3-D Structures	Properties
Seed 4	 <p data-bbox="670 952 925 985">Family 2 Molecule 34</p>	<p data-bbox="1173 504 1444 537">Molecular weight: 499</p> <p data-bbox="1244 571 1372 604">LogP: 4.55</p> <p data-bbox="1252 638 1364 672">pKd: 9.98</p> <p data-bbox="1268 705 1348 739">HBA: 5</p> <p data-bbox="1268 772 1348 806">HBD: 5</p>
Seed 4	 <p data-bbox="662 1780 933 1814">Family 3 Molecule 108</p>	<p data-bbox="1173 1276 1444 1310">Molecular weight: 397</p> <p data-bbox="1244 1344 1372 1377">LogP: 4.97</p> <p data-bbox="1252 1411 1364 1444">pKd: 9.95</p> <p data-bbox="1268 1467 1348 1500">HBA: 4</p> <p data-bbox="1268 1534 1348 1568">HBD: 4</p>

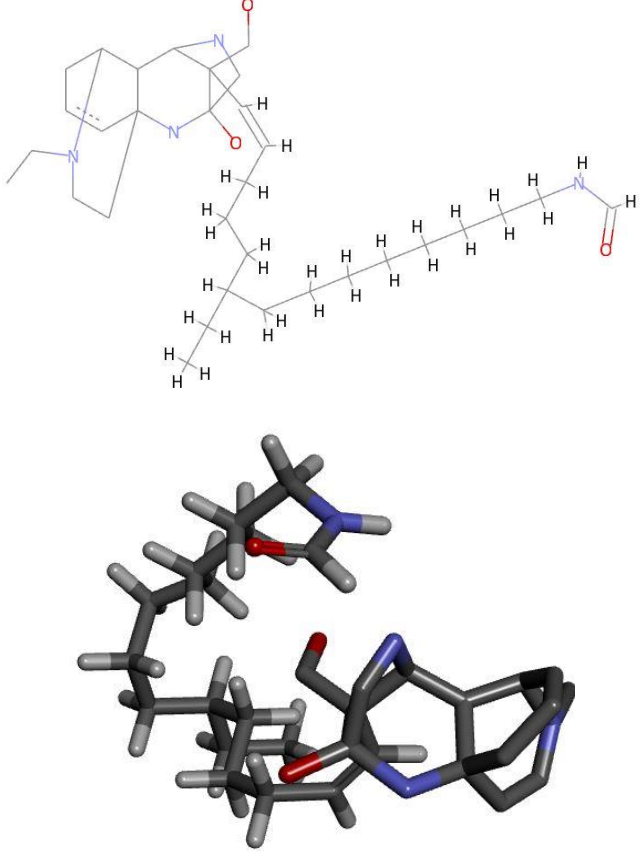
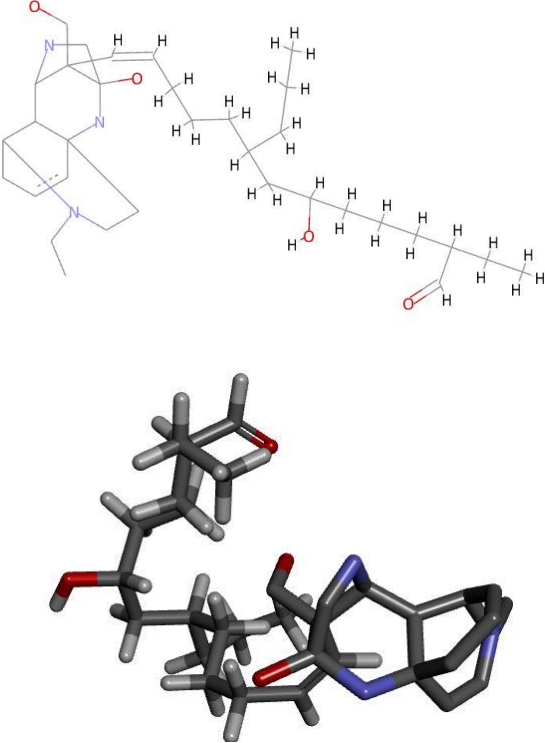
<p>Seed 4</p>	 <p>Family 1 Molecule 3</p> 	<p>Molecular weight: 385</p> <p>LogP: 4.77</p> <p>pKd: 9.87</p> <p>HBA: 4</p> <p>HBD: 4</p>
<p>Seed 4</p>	 <p>Family 2 Molecule 42</p> 	<p>Molecular weight: 385</p> <p>LogP: 4.87</p> <p>pKd: 9.75</p> <p>HBA: 6</p> <p>HBD: 4</p>

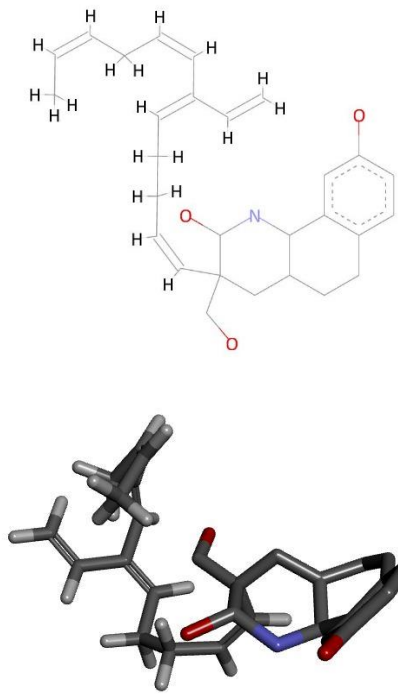
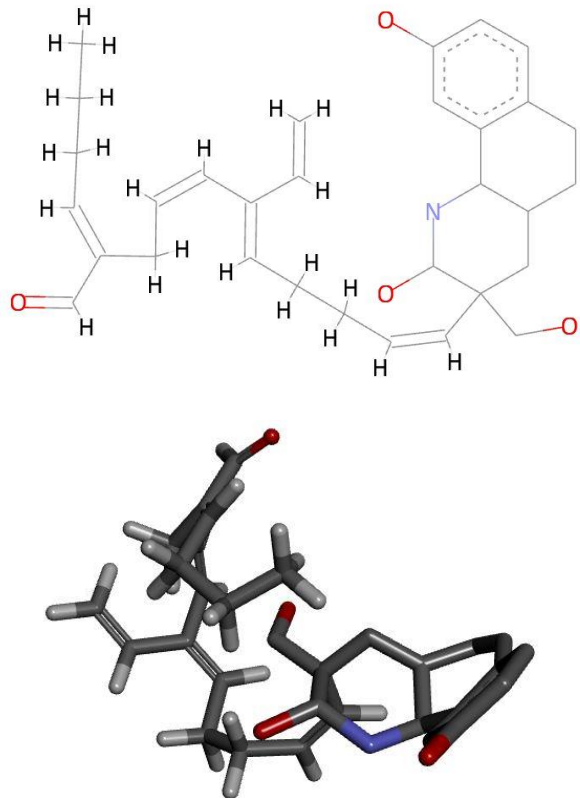
<p>Seed 4</p>	 <p>Family 1 Molecule 4</p>	<p>Molecular weight: 385</p> <p>LogP: 4.83</p> <p>pKd: 9.73</p> <p>HBA: 4</p> <p>HBD: 4</p>
<p>Seed 4</p>	 <p>Family 2 Molecule 106</p>	<p>Molecular weight: 443</p> <p>LogP: 3.15</p> <p>pKd: 5.37</p> <p>HBA: 5</p> <p>HBD: 5</p>

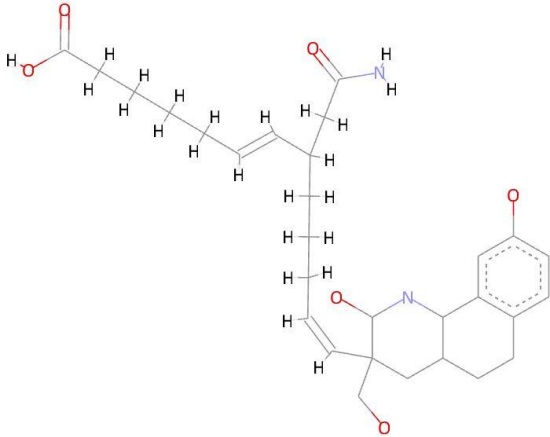
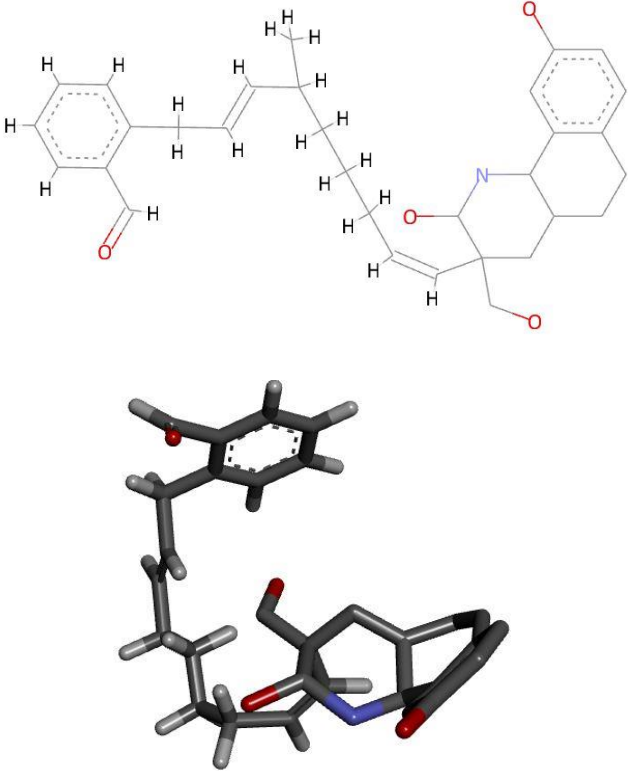
Seed 4	 <p style="text-align: center;">Family 5 Molecule 153</p>	<p>Molecular weight: 453</p> <p>LogP: 3.7</p> <p>pKd: 5.18</p> <p>HBA: 5</p> <p>HBD: 4</p>
Seed Number	2-D and 3-D Structures	Properties
Seed 5	 <p style="text-align: center;">Family 4 Molecule 39</p>	<p>Molecular weight: 457</p> <p>LogP: 4.13</p> <p>pKd: 8.77</p> <p>HBA: 5</p> <p>HBD: 4</p>

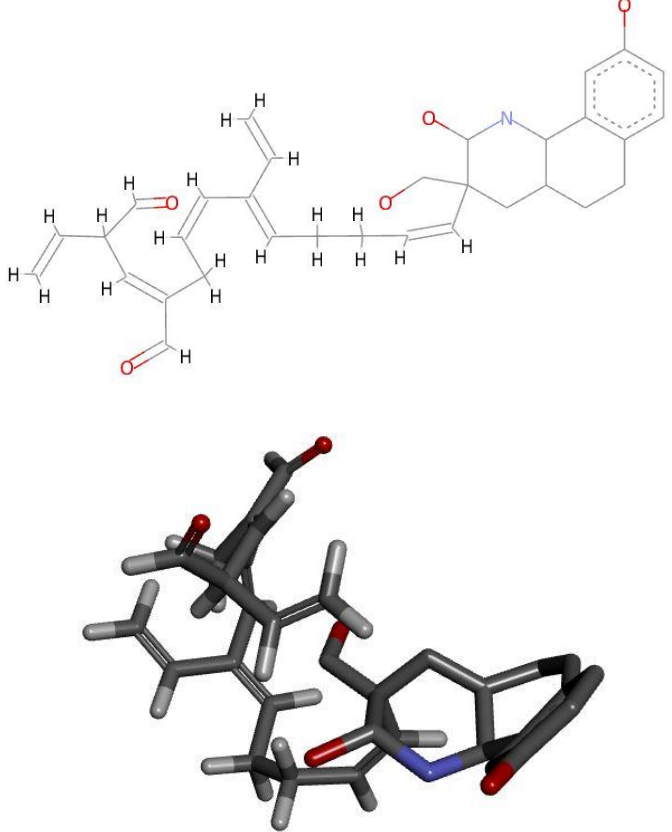
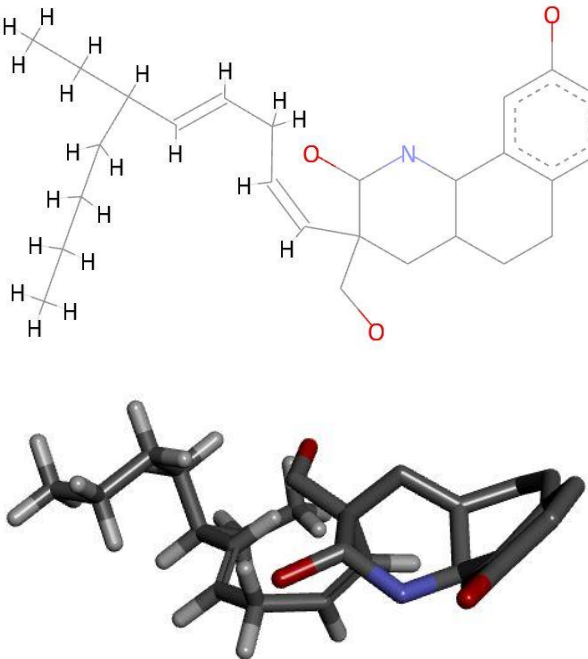
<p>Seed 5</p>	 <p>Family 4 Molecule 40</p>	<p>Molecular weight: 479</p> <p>LogP: 3.65</p> <p>pKd: 8.7</p> <p>HBA: 5</p> <p>HBD: 4</p>
<p>Seed 5</p>	 <p>Family 4 Molecule 41</p>	<p>Molecular weight: 453</p> <p>LogP: 3.36</p> <p>pKd: 8.64</p> <p>HBA: 5</p> <p>HBD: 5</p>

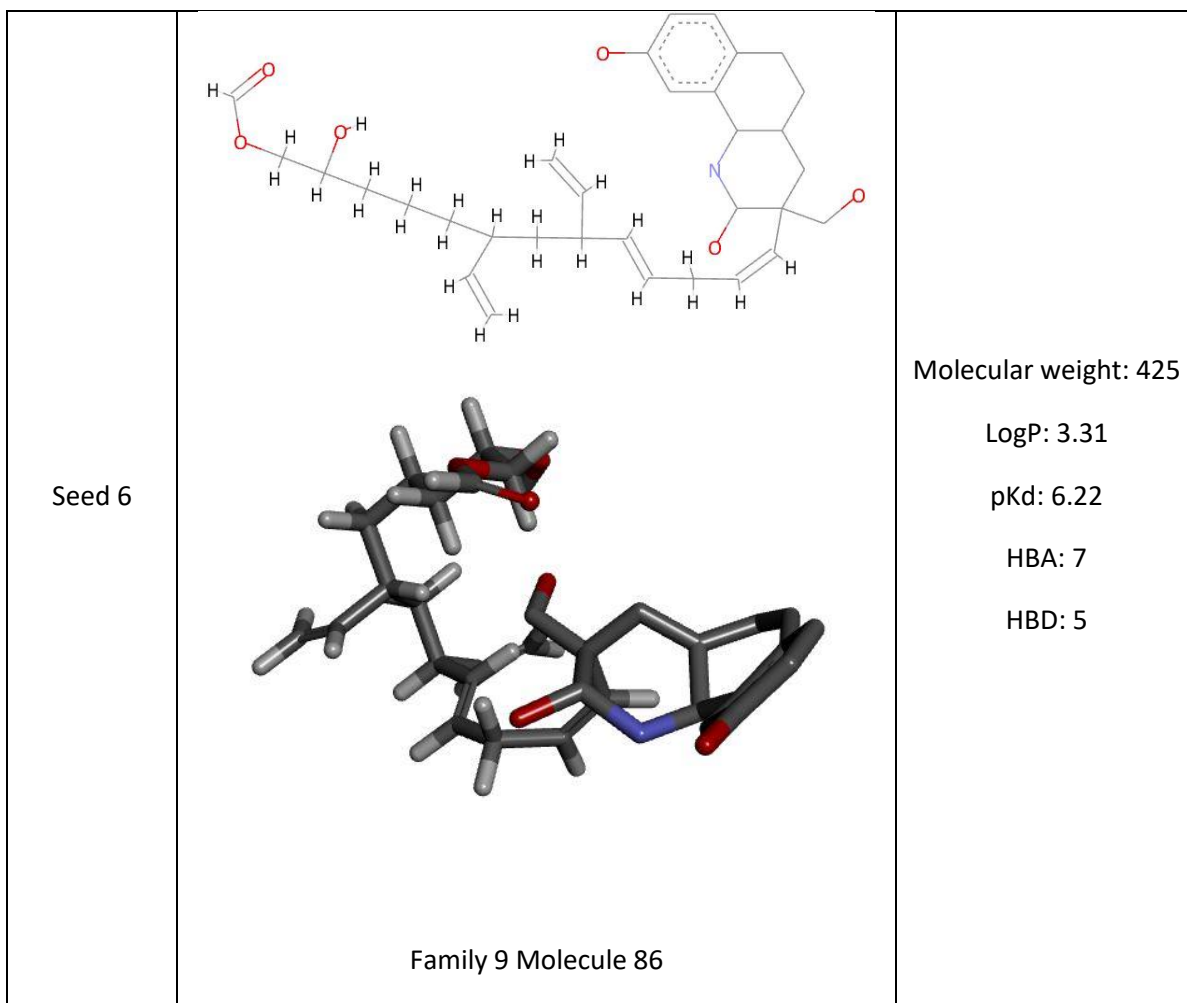
<p>Seed 5</p>	 <p>Family 4 Molecule 42</p>	<p>Molecular weight: 467</p> <p>LogP: 4.39</p> <p>pKd: 8.37</p> <p>HBA: 6</p> <p>HBD: 5</p>
<p>Seed 5</p>	 <p>Family 1 Molecule 12</p>	<p>Molecular weight: 485</p> <p>LogP: 4.26</p> <p>pKd: 8.34</p> <p>HBA: 4</p> <p>HBD: 3</p>

<p>Seed 5</p>	 <p>Family 4 Molecule 51</p>	<p>Molecular weight: 473</p> <p>LogP: 3.45</p> <p>pKd: 6.65</p> <p>HBA: 6</p> <p>HBD: 5</p>
<p>Seed 5</p>	 <p>Family 4 Molecule 53</p>	<p>Molecular weight: 475</p> <p>LogP: 3.42</p> <p>pKd: 5.71</p> <p>HBA: 7</p> <p>HBD: 5</p>

Seed Number	2-D and 3-D Structures	Properties
Seed 6	 <p>The 2-D structure shows a complex polycyclic molecule with a central nitrogen atom, a benzene ring, and several oxygen atoms. The 3-D structure is a ball-and-stick model showing the spatial arrangement of atoms, with carbon in grey, hydrogen in white, oxygen in red, and nitrogen in blue.</p> <p>Family 1 Molecule 3</p>	<p>Molecular weight: 487</p> <p>LogP: 4.93</p> <p>pKd: 9.42</p> <p>HBA: 4</p> <p>HBD: 4</p>
Seed 6	 <p>The 2-D structure shows a complex polycyclic molecule with a central nitrogen atom, a benzene ring, and several oxygen atoms. The 3-D structure is a ball-and-stick model showing the spatial arrangement of atoms, with carbon in grey, hydrogen in white, oxygen in red, and nitrogen in blue.</p> <p>Family 1 Molecule 4</p>	<p>Molecular weight: 475</p> <p>LogP: 4.87</p> <p>pKd: 9.35</p> <p>HBA: 5</p> <p>HBD: 4</p>

<p>Seed 6</p>	 <p>Family 4 Molecule 50</p>	<p>Molecular weight: 492</p> <p>LogP: 4.78</p> <p>pKd: 9.01</p> <p>HBA: 7</p> <p>HBD: 6</p>
<p>Seed 6</p>	 <p>Family 5 Molecule 62</p>	<p>Molecular weight: 437</p> <p>LogP: 4.81</p> <p>pKd: 8.99</p> <p>HBA: 5</p> <p>HBD: 4</p>

<p>Seed 6</p>	 <p>Family 1 Molecule 7</p>	<p>Molecular weight: 487</p> <p>LogP: 4.93</p> <p>pKd: 8.86</p> <p>HBA: 6</p> <p>HBD: 4</p>
<p>Seed 6</p>	 <p>Family 9 Molecule 85</p>	<p>Molecular weight: 511</p> <p>LogP: 4.02</p> <p>pKd: 6.3</p> <p>HBA: 4</p> <p>HBD: 4</p>



Chapter 4

Discussion

Chapter 4: Discussion

The role of κ OR and μ OR antagonism in the treatment of disorders such as anxiety and depression has been highly researched (Carlezon & Krystal, 2016). A study from Pfeiffer *et. al.* (1986) showed that κ OR agonists result in depressive effects.

A combination treatment of the κ OR antagonist Buprenorphine and the μ OR antagonist Naltrexone were studied and showed promising antidepressant results without the expected adverse effects such as addiction or sedation. BU10119 is a molecule created to incorporate the critical binding sites of both these molecules to aid in drug dosing and administration, and eliminate abuse potential (Cueva *et. al.*, 2015).

The aim of this project was to use the dual κ OR and μ OR antagonist, BU10119, as a lead to identify analogous hits capable of dual receptor antagonism for the treatment of SSRI Refractory Depression. The thesis presented by Cueva *et. al.* in 2015 stated that buprenorphine-like pharmacological compounds, such as the molecule BU10119 studied in this project, showed a lower efficacy at the μ OR. However, these molecules showed positive results in clinical tests for depression such as the FST and NIH.

Two different approaches were used in this project, Structure-Based Drug Design and Ligand-Based Drug Design.

Structure Based Drug Design uses information about the Ligand Binding Pocket of the target receptor obtained from the PDB. PDB 4DJH (Wu *et. al.*, 2012) was used for the KOR which described the structure of the human KOR in complex with the KOR antagonist JDC1300 (JDTiC). PDB 4DKL (Manglik *et. al.*, 2012) was used to obtain information for the μ OR as it described the crystal structure of the μ OR bound to the morphinan antagonist BF0601.

This drug design study utilised two different methods, the Virtual Screening Approach, and the *de novo* Approach. These are complementary approaches, each having their inherent strengths and weaknesses. The parallel combination of both approaches in one study may consequently be considered as more holistic, and ensuring that the explored pharmacophoric space is as broad as possible. The strengths and weaknesses associated with each rational drug design approach are summarised in Table 4.1

Table 4.1: Table comparing the strengths and weaknesses of Virtual Screening

Approach and *de novo* Design.

Virtual Screening Approach	<i>de novo</i> approach
Highly innovative- given that the query structure is a general pharmacophore, there is significant structural diversity in the hit molecules obtained	Less innovative- there is limited structural diversity in the designed molecular cohorts
Larger pharmacophoric space (protomol) which while representing the interior vacant space in its entirety is not necessarily bioactive.	Smaller (bioactive) ligand binding pocket utilised therefore more limitations
Most of the molecules on commercial databases have already been synthesised and are purchasable. This therefore reduces costs and time from the drug development process	Since the molecules are designed <i>de novo</i> , there is almost always the need to identify a synthetic pathway prior to <i>in vitro</i> studies
Lower propensity to bioactivity	Greater propensity to bioactivity

In the Virtual Screening Approach, the application of filters that ensured not only Lipinski Rule Compliance (REF), but also lead likeness ascertained that the hit structures obtained when the JDC1300/BU10119 consensus pharmacophore for the κ OR and the BF0601/BU10119 consensus pharmacophore for the μ OR were sequentially submitted to the ZincPharmer[®] database would leave space for optimisation in later stages of the study.

The 2 filtered hit structure cohorts derived from the two pharmacophores were assessed for affinity for the modelled κ OR and μ OR protomols respectively. Reference is made to Table 4.1 previously. The protomol represents the energetically unsatisfied area at the interior of a receptor. The use of this modelled space was advantageous from the point of view of exploration of all the possible pharmacophoric space at the interior of the targeted receptors but provided a much lower guarantee of ultimate bioactivity.

The 3 optimally binding molecules were identified for each receptor (κ OR and μ OR) protomols. These structures, identified through Virtual Screening as optimally binding, have the advantage of structural innovation, incorporate moieties that were significantly diverse from the lead molecules and from those obtained through *de novo* design. For example, the consensus pharmacophore created between the κ OR antagonist JDC1300 and BU10119 presented solely 3 hydrophobic interactions. On the other hand, the consensus pharmacophore created between the μ OR antagonist BF0601 and BU10119 resulted in two hydrophobic interactions, two hydrogen bond acceptors and one positive ionisable area.

In this study, it was not possible to obtain an overall consensus pharmacophore due to the significant structural dissimilarities of the two different pharmacophores for each receptor. In fact, the Virtual Screening exercise was performed using the pharmacophores derived from the JDC1300/BU10119 for the KOR and the BF0601/BU10119 for the μ OR in isolation. The modelling of a consensus pharmacophore would have added robustness to this Virtual Screening process.

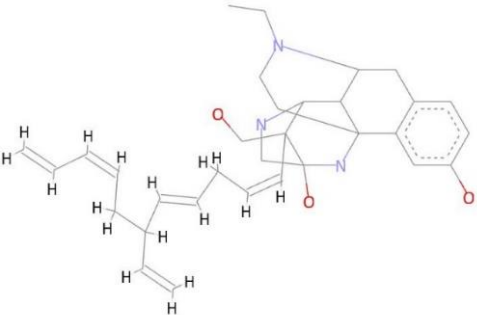
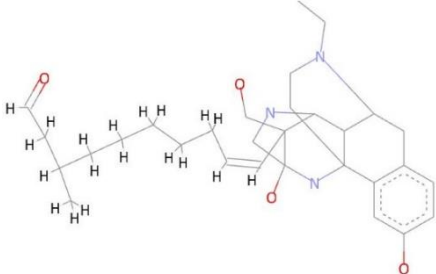
Each of the 6 modelled seed structures described in Section 3.2.2 of the Methodology yielded *de novo* designed Lipinski Rule Compliant molecular cohorts as follows in Table 4.2.

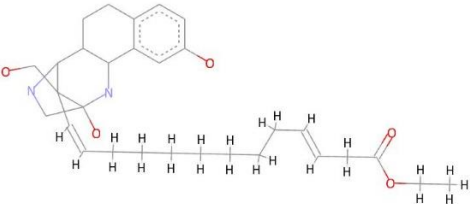
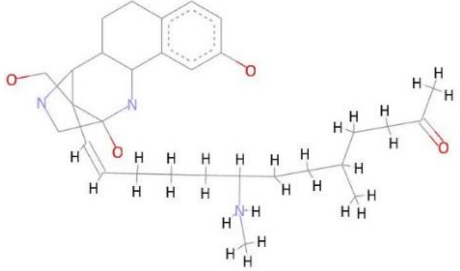
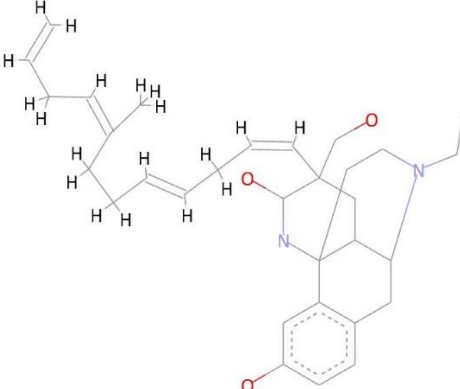
Table 4.2: Table showing the number of molecular cohorts obtained through the *de novo* Design.

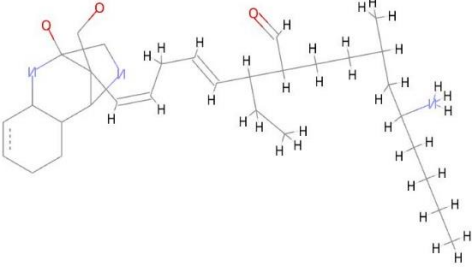
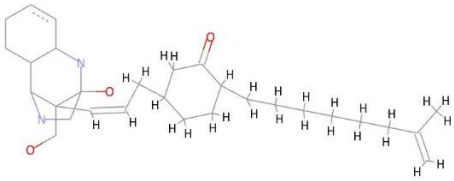
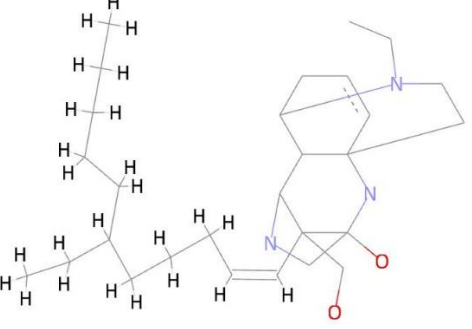
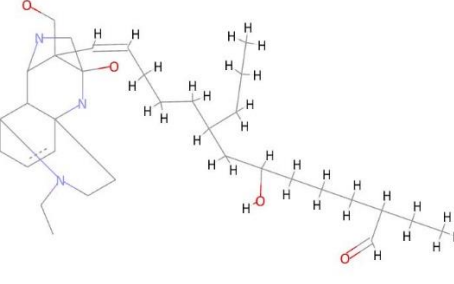
Seed Number	Families obtained	Total number of cohorts created
1	5 families	11 molecular cohorts
2	4 families	29 molecular cohorts
3	1 family	1 molecular cohort
4	9 families	122 molecular cohorts
5	6 families	21 molecular cohorts
6	9 families	20 molecular cohorts

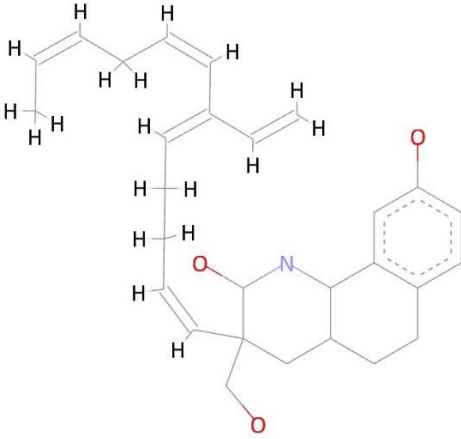
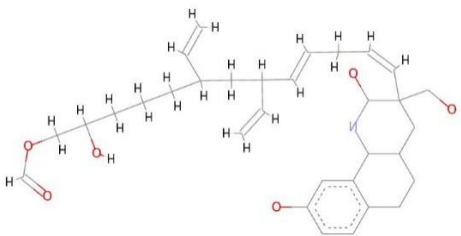
The optimally binding structure for each family was compared to the lowest affinity molecule in the same family in order to understand which structural molecules contributed most to affinity.

Table 4.3: Table comparing the P2 molecules with the highest and lowest affinity to the ligand binding pocket for each seed structure. Rendered using BIOVIA Discovery Studio (Dassault Systèmes BIOVIA, 2015).

Seed Number	Highest Affinity P2	Lowest Affinity P2
Seed 1	 <p data-bbox="596 1541 858 1570">Molecule 7 Family 2</p> <p data-bbox="643 1603 812 1632">Affinity: 9.62</p>	 <p data-bbox="1086 1541 1369 1570">Molecule 33 Family 4</p> <p data-bbox="1142 1603 1311 1632">Affinity: 6.38</p>
Comparison for Seed 1	<p data-bbox="568 1671 1378 1778">The higher number of covalent bonds available on Molecule 7 contributes to a higher affinity.</p>	

Seed 2	 <p>Molecule 29 Family 2 Affinity: 9.99</p>	 <p>Molecule 78 Family 2 Affinity: 5.42</p>
Comparison for Seed 2	<p>The carboxylic acid group on Molecule 29 contrasts with the ketone group on Molecule 78 as it presents more hydrogen bond acceptors.</p> <p>The straight chain on Molecule 29 also allows for a higher affinity.</p>	
Seed 3	 <p>Molecule 20 Family 1 Affinity: 8.11</p>	<p>No other molecules left over after the Filtering Process.</p>
Comparison for Seed 3	<p>A comparison between Seed 3 molecules could not be performed as only 1 molecule was left over after filtering for Lipinski Compliant Molecules.</p>	

<p>Seed 4</p>	 <p>Molecule 34 Family 2 Affinity: 9.98</p>	 <p>Molecule 153 Family 5 Affinity: 5.18</p>
<p>Comparison for Seed 4</p>	<p>Both molecules have ketone groups representing a hydrogen bond acceptor group. The presence of the amine group on Molecule 34 provides a better balance between the hydrogen bond acceptor and hydrogen bond donor groups present. This allows the molecule to have a higher affinity. The higher amount of covalent bonds on Molecule 34 also helps to increase the molecule's affinity.</p>	
<p>Seed 5</p>	 <p>Molecule 39 Family 4 Affinity: 8.77</p>	 <p>Molecule 53 Family 4 Affinity: 5.71</p>
<p>Comparison for Seed 5</p>	<p>The increased amount of ketone groups and hydroxyl groups present on Molecule 53 may contribute to the lower affinity when compared to Molecule 39. Thus, Molecule 39 has a higher affinity.</p>	

<p>Seed 6</p>	 <p>Molecule 3 Family 1 Affinity: 9.42</p>	 <p>Molecule 86 Family 9 Affinity: 6.22</p>
<p>Comparison for Seed 6</p>	<p>Molecule 86 has a higher number of carboxylic acid and hydroxyl groups which increase the number of hydrogen bond acceptor groups. There is also an increased number of covalent bonds on Molecule 3. These two together explain the increased affinity of Molecule 3.</p>	

The molecular cohort with the highest affinity to the KOR obtained through the *de novo* design phase was identified to be Molecule 39 from Seed 2 with a pKd of 9.99. This molecule was docked into the KOR Ligand Binding Pocket, and a 2-Dimensional Map was created to view the critical ligand interactions available. This 2-Dimensional Map can be seen in Figure 4.1 on the next page.

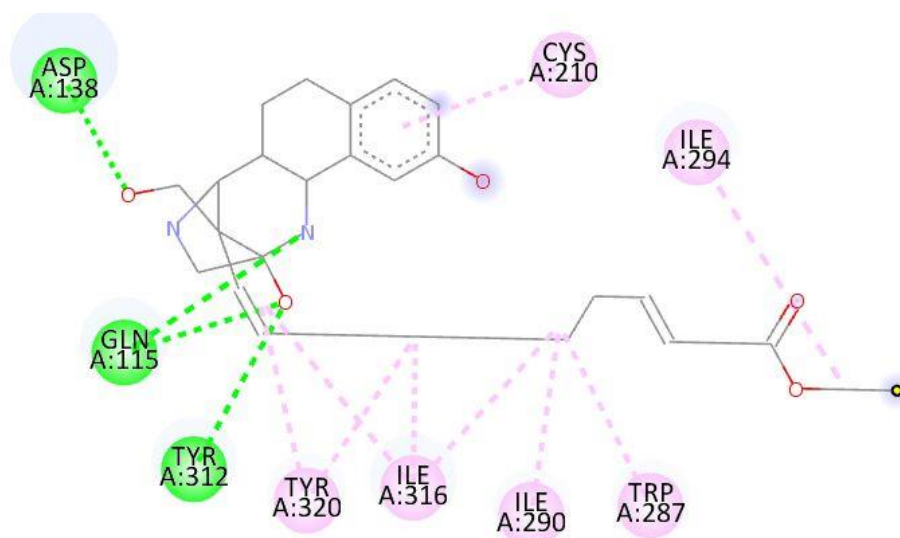


Figure 4.1: Figure showing the critical ligand interactions between the P2 molecule 39 obtained from Seed 2 after docking into the Kappa Opioid Receptor. Rendered using Biovia Discovery Studio® (Dassault Systèmes BIOVIA, 2015).

This 2-Dimensional Topology Map can be contrasted to the 2-Dimensional Topology Map of the initial JDC1300/BU10119 pharmacophore initially docked into the kOR, whereby the unfavourable interactions present in Figure 3.5 in the Methodology have been removed and are no longer present on the Topology Map for Molecule 39. This explains the increased affinity of the molecule to the kOR Ligand Binding Pocket. The interactions marked in green in Figure 4.1 above are favourable conventional hydrogen bonds, while the interactions marked in pink represent favourable alkyl and pi-alkyl interactions with their respective amino-acids.

Conclusion

This project sought to obtain different pharmacophores of the novel molecule BU10119 capable of binding to the κ OR and μ OR for its possible use in SSRI Refractory Depression. The Virtual Screening Approach and the *de novo* Approach used in this project ensured that an exhaustive result was obtained.

The lack of activity of BU10119 at the μ OR Ligand Binding pocket, despite the production of various pharmacophores at the κ OR Ligand Binding Pocket proves that the novel molecule showed high κ OR activity, and little to none μ OR activity. This result goes in tandem with the findings presented by Cueva *et. al.* (2015) in his thesis.

The optimal ligands obtained through both the approaches mentioned above could be further studied to properly analyse their efficacy, and whether or not they meet the clinical needs for potential SSRI Refractory Depression treatment. Although the Ligand Binding Affinity (pKd) of these molecules is usually an indicator for successful ligands, other pharmacological factors such as bioavailability, half-life and potential side effects are also considered during the clinical testing of these ligands to determine their potential efficacy.

References

ACD/ChemSketch Freeware. ChemSketch Version 11. Advanced Chemistry Development Inc. 2006. Available from: www.acdlabs.com

Akaka J, Bernstein CA, Crowley B, Everett AS, Geller J, Graff MD. Section II: Diagnostic Criteria and Codes: Depressive Disorders. In: American Psychiatric Association, editors. Diagnostic and Statistical Manual of Mental Disorders – 5th edition. London, Washington DC: American Psychiatric Publishing; 2013. p. 155-188.

Almatroudi A, Husbands SM, Bailey CP, Bailey SJ. Combined administration of buprenorphine and naltrexone produces antidepressant-like effects in mice. *J Psychopharmacol.* 2015; 29(7): 812-821.

Andrade L, Caraveo-Anduaga JJ, Berglund P, Bijl RV, De Graaf R, Vollebergh W, et al. The epidemiology of major depressive episodes: results from the International Consortium of Psychiatric Epidemiology (ICPE) Surveys. *Int J Methods Psychiatr. Res.* 2003; 12: 3–21.

Ash S, Cline MA, Homer RW, Hurst T, Smith GB. ChemInform Abstract: Sybyl[®] Line Notation (SLN): A versatile Language for Chemical Structure Representation. *ChemInform.* 2010;28(18):66-78.

Bals-Kubik R, Ableitner A, Herz A, Shippenberg TS. Neuroanatomical sites mediating the motivational effects of opioids as mapped by the conditioned place preference paradigm in rats. *J Pharmacol Exp Ther.* 1993; 264: 489–495.

Berman HM, Westbrook J, Feng Z, Gilliland G, Bhat TN, Weissig H et al. The Protein Data Bank. *Nucleic Acids Res.* 2000; 28(1): 235-242.

Bruijnzeel AW. Kappa-Opioid receptor signalling and brain reward function. *Brain Res Rev.* 2009; 62: 127-146

Britt J.P, McGehee D.S. Presynaptic opioid and nicotinic receptor modulation of dopamine overflow in the nucleus accumbens. *J Neurosci.* 2008; 28: 1672–1681.

Can A, Dao DT, Arad M, Terrillion CE, Piantadosi SC, Todd DG. The Mouse Forced Swim Test. *J Vis Exp.* 2012; 59: 3638.

Carr GV, Bangasser DA, Bethea T, Young M, Valentino RJ, Lucki I. Antidepressant-like Effects of κ -Opioid Receptor Antagonists in Wistar Kyoto Rats. *Neuropsychopharmacology.* 2010; 35: 752-763.

Carroll FI, Carlezon WA. Development of Kappa Opioid Receptor Antagonists. *J Med Chem.* 2013; 56(6): 2178-2195.

Chavkin C, James IF, Goldstein A. Dynorphin is a specific endogenous ligand of the kappa opioid receptor. *Science*. 1982; 215(4531): 413–5.

Chen Y, Mestek A, Liu J, Hurley JA, Yu L. Molecular cloning and functional expression of a μ -opioid receptor from rat brain. *Mol Pharmacol*. 1993; 44: 8–12.

Cueva JP, Roche C, Ostovar M, Kumar V, Clark MJ, Hillhouse TM, et al. C7 β -Methyl Analogues of the Orvinols: The Discovery of Kappa Opioid Antagonists with Nociceptin/Orphanin FQ Peptide (NOP) Receptor Partial Agonism and Low, or Zero, Efficacy at Mu Opioid Receptors. *J Med Chem*. 2015; 58(10): 4242-4249.

Dassault Systèmes BIOVIA, Accelrys BIOVIA Draw, San Diego: Dassault Systèmes, 2001.

Dassault Systèmes BIOVIA, BIOVIA Discovery Studio Visualizer, San Diego: Dassault Systèmes, 2015.

Dror O, Schneidman-Duhovny D, Inbar Y, Nussinov R & Wolfson HJ. A Novel Approach for Efficient Pharmacophore-based Virtual Screening: Method and Applications. *J Chem Inf Model*. 2010; 49(10): 2333-2343.

Evans CJ, Keith DE Jr, Morrison H, Magendzo, Edwards RH. Cloning of a delta opioid receptor by functional expression. *Science*. 1992; 258: 1952–1955.

Gelenberg AJ, Freeman MP, Markowitz JC, Rosenbaum JF, Thase ME, Trivedi MH. Part A: Treatment Recommendations: Section II. Formulation and Implementation of a Treatment Plan: Subsection B Acute Phase, C Continuous Phase, D Maintenance Phase, E Discontinuation of Treatment. In: American Psychiatric Association, editors. *Practice Guideline for the Treatment of Patients with Major Depressive Disorder, 3rd Edition*. London, Washington DC: American Psychiatric Press Inc, 2010. p. 30-58.

George SR, Zastawny RL, Briones-Urbina R, Cheng R, Nguyen T, Heiber M *et al*. Distinct distributions of mu, delta and kappa opioid receptor mRNA in rat brain. *Biochem Biophys Res Commun*. 1984; 205(2): 1438-1444.

Goldstein A, Fischli W, Lowney LI, Hunkapiller M, Hood L. Porcine pituitary dynorphin: complete amino acid sequence of the biologically active heptadecapeptide. *Proc Natl Acad Sci USA*. 1981; 78: 7219–7223.

Hilbig M, Rarey M. MONA 2: a light cheminformatics platform for interactive compound library processing. *J. Chem. Inf. Model*. 2015; 55(10): 2071-2078.

Hughes JP, Rees S, Kalindjian SB, Philpott KL. Principles of early drug discovery. *Br J Pharmacol.* 2011; 162(6): 1239-1249.

International Classification of Disease 10th edition (2010): Chapter V Mental and Behavioural Disorders: F32 Depressive Episode - F33 Recurrent Depressive Disorder. (ICD-10 Version 2010) Available at: <http://apps.who.int/classifications/icd10/browse/2010/en#/F30-F39> [Accessed 28.04.2018]

Keller MB, Hirschfeld RM, Demyttenaere K, Baldwin DS. Optimizing outcomes in depression: focus on antidepressant compliance. *Int Clin Psychopharmacol.* 2002; 17: 265–271.

Kieffer BL, Befort K, Gaveriaux-Ruff C, Hirth CG. The δ -opioid receptor: Isolation of a cDNA by expression cloning and pharmacological characterization. *Proc Natl Acad Sci USA.* 1992; 89: 12048–12052.

Knoll AT, Carlezon WA Jr. Dynorphin, stress, and depression. *Brain Res.* 2010; 1314: 56–73.

Koes D, Camacho C. ZINCPharmer: pharmacophore search of the ZINC database. *Nucleic Acids*

Research. 2012; 40(W1): W409-W414.

Kronish IM, Rieckmann N, Halm EA, Shimbo D, Vorchheimer D, Haas DC et al. Persistent depression affects adherence to secondary prevention behaviors after acute coronary syndromes. *J Gen Intern Med.* 2006; 21(11): 1178–1183.

Lalanne L, Ayranci G, Kieffer BL, Lutz PE. The kappa opioid receptor: from addiction to depression, and back. *Frontiers in Psychiatry.* 2014; 5(170): 1-17.

Law PY, Wong YH, Loh HH. Molecular mechanisms and regulation of opioid receptor signaling. *Ann Rev Pharmacol Toxicol.* 2000; 40: 389–430.

Le Merrer J, Becker JA, Befort K, Kieffer BL. Reward processing by the opioid system in the brain. *PhysiolRev.* 2009; 89(4): 1379–1412.

Lipinski CA, Lombardo F, Dominy BW, Feeney Pj. Experimental and computational approaches to estimate solubility and permeability in drug discovery and development settings. *Advanced Drug Delivery Reviews* 2015; 46(1-3):3-26.

Lutz PE, Kieffer BL. Opioid receptors: distinct roles in mood disorders. *Trends Neurosci.* 2013; 36(3): 195–206.

Mandal S, Moudgil M, Mandal SK. Rational drug design. *Eur J Pharmacol.* 2009; 625(1-3): 90-100.

Mague SD, Pliakas AM, Todtenkopf MS, Tomaiewicz HC, Zhang Y, Stevens Jr WC et al. Antidepressant-like effects of κ -opioid Receptor Antagonists in the Forced Swim Test in Rats. *J Pharmacol Exp Ther.* 2003; 305(1): 323-330.

Manglik A, Kruse AC, Kobilka TS, Thian FS, Mathiesen JM, Sunahara RK et al. Crystal Structure of the mu-opioid receptor bound to a morphinan antagonist. 2012. Doi: 10.2210/pdb4DKL/pdb. Available from: <https://www.rcsb.org/structure/4DKL>

Mansour A, Fox CA, Akil H, Watson SJ. Opioid-receptor mRNA expression in the rat CNS: anatomical and functional implications. *Trends Neurosci.* 1995; 18: 22–29.

Margolis EB, Hjelmstad GO, Bonci A, Fields HL. Kappa-opioid agonists directly inhibit midbrain dopaminergic neurons. *J Neurosci.* 2003; 23(31): 9981–9986.

Margolis EB, Lock H, Chefer VI, Shippenberg TS, Hjelmstad GO, Fields HL. Kappa opioids selectively control dopaminergic neurons projecting to the prefrontal cortex. *Proc Natl Acad Sci USA.* 2006; 103(8): 2938–2942.

McLaughlin JP, Marton-Popovici M, Chavkin C. K Opioid Receptor Antagonism and Prodynorphin Gene Disruption Block Stress-Induced Behavioural Response. *J Neurosci.* 2003; 23(13): 5674-5683.

Murray CJ, Lopez AD. Evidence-based health policy--lessons from the Global Burden of Disease Study. *Science.* 1996a; 274: 740–743.

Murray CJL, Lopez AD. The Global Burden of Disease: A Comprehensive Assessment of Mortality and Disability from Diseases, Injuries, and Risk Factors in 1990 and Projected to 2020. World Health Organisation: World Bank: Harvard School of Public Health. 1996b. Available from: <http://apps.who.int/iris/handle/10665/41864>. [Accessed on: 29.05.2018].

National Institute for Clinical Excellence (2009) Depression in adults: recognition and management. (NICE Guideline 90). Available at: <https://www.nice.org.uk/guidance/cg90>. [Accessed 28.04.2018]

Nestler EJ, Carlezon WA Jr. The mesolimbic dopamine reward circuit in depression. *Biol Psychiatry.* 2006; 59(12): 1151–1159.

O'Connor C, White K, Doncescu N, Didenko T, Roth BL, Czaplicki G et al., Solution NMR Structure of Dynorphin 1-13 bound to Kappa Opioid Receptor. 2015. DOI: 10.2210/pdb2N2F/pdb. Available from: <http://www.rcsb.org/structure/2N2F>

Parenti MD, Rastelli G. Advances and applications of binding affinity prediction methods in drug discovery. *Biotechnol Adv.* 2012; 30: 244-250.

Pert CB, Snyder SH. Opiate receptor: Demonstration in nervous tissue. *Science.* 1973; 179: 1011–1014.

Pettersen EF, Goddard TD, Huang CC, Couch GS, Greenblatt DM, Meng EC et al. UCSF Chimera--a visualization system for exploratory research and analysis. *J Comput Chem.* 2004; 25(13): 1605-1612.

Pfeiffer A, Brantl V, Herz A, Emrich HM. Psychotomimesis mediated by kappa opiate receptors. *Science.* 1986; 233: 774–776.

Piros ET, Hales TG, Evans CJ. Functional analysis of cloned opioid receptors in transfected cell lines. *Neurochem Res.* 1996; 21: 1277–1285.

Pliakas AM, Carlson RR, Neve RL, Konradi C, Nestler EJ, Carlezon WA Jr. Altered responsiveness to cocaine and increased immobility in the forced swim test associated with elevated cAMP response element-binding protein expression in nucleus accumbens. *J Neurosci.* 2001; 21: 7397–7403.

Rimoy GH, Wright DM, Bhaskar NK, Rubin PC. The cardiovascular and central nervous system effects in the human of U-62066E. A selective opioid receptor agonist. *Eur J Clin Pharmacol.* 1994; 46: 203–220.

Sansone RA, Sansone LA. 2012. Antidepressant Adherence: Are patients taking their medications? *Innov Clin Neurosci* 2012; 9(4-5): 41-46

Stierand K, Rarey M. From Modelling to Medicinal Chemistry: Automatic Generation of Two-Dimensional Complex Diagrams. *Chem Med Chem.* 2007; 2(6): 853-860.

Stierand K, Rarey M. PoseView -- molecular interaction patterns at a glance. *Journal of Cheminformatics.* 2010; 2(1): 50.

Stierand K, Rarey M. Drawing the PDB: Protein-Ligand Complexes in Two Dimensions. *ACS Med Chem Lett.* 2010; 1(9): 540-545.

Spanagel R, Herz A, Shippenberg TS. Opposing tonically active endogenous opioid systems modulate the mesolimbic dopaminergic pathway. *Proc Natl Acad Sci USA.* 1992; 89(6): 2046–2050.

Trivedi MH, Lin EH, Katon WJ. Consensus recommendations for improving adherence, self-management, and outcomes in patients with depression. *CNS Spectr.* 2007; 12: S1–27.

Wang R, Lai L, Wang S. Further Development and Validation of Empirical Scoring Functions for Structure-Based Binding Affinity Prediction. *J Comput Aided Mol Des.* 2002; 16: 11-26.

Wolber G, Langer T. LigandScout: 3-D Pharmacophores Derived from Protein-Bound Ligands and Their Use as Virtual Screening Filters. *ChemInform.* 2005; 36(16).

Wu H, Wacker D, Katritch V, Mileni M, Han GW, Vardy E et al., Structure of the human kappa opioid receptor in complex with JD1c. Doi: 10.2210/pdb4DJH/pdb. Available from: <https://www.rcsb.org/structure/4DJH>.


Yuan Y, Jianfeng P, Luhua L. LigBuilder 2: A Practical de Novo Drug Design Approach. *J Chem Inf Model.* 2011; 51(5): 1083–1091.

Vijaykrishnan R. Structure-based drug design and modern medicine. *J Postgrad Med.* 2009; 55(4): 301-304.

List of Publications

The abstract above has been submitted to the below Journals:

- Current Medicinal Chemistry
- Journal of Biochemistry

 **cmc@benthamsience.net** <admin@bentham.manuscriptpoint.com> Wed, 25 Aug, 21:44 (4 days ago) ☆ ↶ ⋮
to me, cmc ▾

Dear Dr. Matthew Grech

I am pleased to inform you that the abstract entitled "Rational Design and Preliminary Validation of Novel BU10119 Analogs for the Management of SSRI Refractory Depression" has initially been approved for publication in "Current Medicinal Chemistry" journal. You are kindly requested to submit the complete manuscript.






Draft Manuscript For Review

Rational Design and Preliminary Validation of Novel BU10119 Analogs for the Management of SSRI Refractory Depression

Journal:	<i>The Journal of Biochemistry</i>
Manuscript ID	Draft
Manuscript Type:	Rapid Communication
Date Submitted by the Author:	n/a
Complete List of Authors:	Grech, Matthew; University of Malta, Department of Pharmacy
Keywords:	Drug < Metabolism, Drugs < Pharmacology, Pharmacology, depression, SSRIs
Topics:	18 Biochemical Pharmacology < BIOCHEMISTRY, 15 Neurochemistry < BIOCHEMISTRY

SCHOLARONE™
Manuscripts

The Journal of Biochemistry - Manuscript ID JB-21-08-0271 (mail:007) External ⓘ Inbox x  

 **The Journal of Biochemistry** <onbehalf@manuscriptcentral.com> Wed, 25 Aug, 11:57 (4 days ago) ☆ ↶ ⋮
to me, matthew.grech.31, jb.editorialoffice ▾

25-Aug-2021
(mail:007)

Dear Mr. Grech and the Co-Authors:

Your manuscript entitled "Rational Design and Preliminary Validation of Novel BU10119 Analogs for the Management of SSRI Refractory Depression" has been successfully submitted online and is presently being given full consideration for publication in the The Journal of Biochemistry.

Appendices

Appendix A: FREC Ethics Approval



Dr. Claire Shoemake
to Claire, FACULTY, me ▾

Fri, 27 Aug, 13:27 (4 days ago)



I endorse Matthew Grech's study.

Best Regards,

Dr. C. Shoemake



FACULTY RESEARCH ETHICS COMMITTEE
to Claire, me ▾

Mon, 30 Aug, 11:39 (21 hours ago)



Dear Mr Grech,

Since your self-assessment resulted in no issues being identified, FREC will file your application for record and audit purposes but will not review it.

Any ethical and legal issues including data protection issues are your responsibility and that of the supervisor.

Good luck with your project!

Regards,
Annalise



Addendum

A CD containing the relevant raw data in this project is added to include:

- Six files containing the raw data obtained for each of the six seeds obtained through the *de novo* Approach